Published in "Fundamentals of Cosmic Physics", Vol. 19, pp. 1-89, 1997.

Observations of the Magnetic Fields inside and outside the Milky Way, starting with Globules (~ 1 parsec), Filaments, Clouds, SuperBubbles, Spiral Arms, Galaxies, Superclusters, and ending with the Cosmological Universe's Background Surface (at ~ 8 Teraparsecs)

Jacques P. Vallée

Herzberg Institute of Astrophysics, National Research Council of Canada,
5071 West Saanich Road, Victoria, B.C., Canada V8X 4M6

Abstract. The observational study of galactic magnetic fields dates back to 1949; an excellent review of the early 30 years has been made by Verschuur (1979). I review here the developments since then and the current state of our *observational* knowledge on the magnetic fields inside and outside the Milky Way galaxy, for objects with sizes greater than 1 parsec (= 3.2 light-years; = 3.1 × 10^{16} m). Included are the medium-scale magnetic fields in the isolated globules, dusty elongated clouds and narrow filaments, large interstellar superbubbles, and in large-scale magnetic fields in the spiral arms in our Galaxy and in objects outside our Galaxy out to cosmological distances. The large-scale magnetic fields can act as guides to the low density gas in its motion in the rarefied areas of the interstellar medium, and as tracers of the past dynamical histories of galaxies in motion, linking galactic dynamic with galactic dynamos. Medium-scale magnetic fields can play a support role, supporting clouds against outside pressures or against collapse due to self-gravity. Small-scale magnetic fields play a significant role on smaller-scale phenomena: propagation of cosmic-rays, shock waves, cosmic dust orientation, star formation (although there is little detailed discussion here of magnetic fields on star formation and objects with sizes < 1 parsec).

Key words: Magnetic fields - Milky Way magnetism - Magnetized molecular clouds - Magnetized Superbubbles - Magnetic field and star formation - Dynamo magnetism - Magnetized galaxies - Cosmological magnetism

Table of Contents

1. INTRODUCTION

1.1. Review Scope and Type

Strong magnetic fields are encountered on pulsar surfaces (10^{12} Gauss), on white dwarf surfaces (10^{6} Gauss), on the solar chromosphere and Sunspots (10^{3} Gauss), and on the Earth's surface (1 Gauss), but are limited to a small linear size (10^{4} - 10^{6} km). Weak magnetic fields are found in the interstellar and galactic spaces (a few 10^{-6} Gauss), but they are enormous in scale lengths (parsecs to Megaparsecs). The magnetic fields in spiral galaxies are related to the motions of interstellar gas in the spiral arms in the galactic disk and in the galactic halo; they still can significantly affect interstellar gas dynamics in the galactic disk and in the dense cores of molecular clouds within a galaxy.

Two salient points found in this review are the inclusion of medium-scale magnetic fields, and the choice of a fact-driven observational approach.

This review here includes the *medium scale* magnetic fields, on the scales of 1 pc to 1 kpc; these magnetic fields are not often found in galactic magnetic field reviews (e.g., Beck et al. 1996; Kronberg 1994; Sofue et al. 1986). Yet these medium-scale magnetic fields are necessary (i) for the study of molecular clouds (1-50 pc) and of magnetized superbubbles (50-500 pc), and (ii) for magnetic field reconnections used as energy input for the large-scale (> 1 kpc) magnetic fields (e.g., Parker 1992; Kahn 1992; Kahn and Brett 1993; Ferrière 1993a; Ferrière 1993b).

Many reviews have emphasized a predominently 'physical approach', being 'concept-driven', employing known physical laws to explain new discoveries in a 'theory-to-nature' type emphasizing the explanatory aspect. A few earlier reviews used a 'morphological approach', being 'fact-driven', employing empirical discoveries to spur new links with known physical laws in a 'nature-to-theory' type emphasizing the discovery aspect. This review uses the latter type, emphasizing the *discovery aspect* through its morphological, fact-driven, observational approach, with a larger emphasis on medium-scale areas of the Milky Way: interstellar objects, molecular clouds, superbubbles, nearby spiral arms, and the interstellar matter medium as a whole.

Fact-driven reviews on the subject of magnetism, covering the beginning of polarization observations since 1949, have been given elsewhere for the Milky Way (e.g., Verschuur 1970; Verschuur 1979; Vallée 1983a; Vallée 1997a) and for nearby spiral galaxies and cosmology (e.g., Vallée 1984a,; Sofue et al. 1986; Vallée 1997b). More recent discussions have been made on the Milky Way (e.g., Asseo & Sol 1987; Heiles 1987; Wielebinski 1995; Heiles 1996). Recent concept-driven reviews have been made on nearby galaxies and cosmology (e.g., Asseo & Sol 1987; Kronberg 1994; Beck et al. 1996; Lesch & Chiba 1997).

1.2. Polarimetry

The large majority of recent observations of medium-scale and large-scale magnetic fields were in radio astronomy (e.g., cm, mm, submm/extreme-infrared wavelengths), with some additional observations from optical astronomy (e.g., μm wavelengths).

The methods employed to study the magnetic fields in Milky Way objects are similar to the ones used to study the magnetic fields in other galaxies. The methods of Faraday rotation, synchrotron equipartition, and cosmic-ray collisions as discussed at length in Section 4.1, while the methods of dust grain emission and absorption and of Zeeman splitting are discussed more fully in Section 2.1. The two main methods largely used (Faraday rotation, grain emission) are briefly outlined below.

Rotatable polarimeters give the position angle of the electric vector at maximum intensity for the incoming radiation, as well as the percentage of the incoming radiation that is linearly polarized. Observing wise, for detecting a source that is 4% linearly polarized, one requires more time by a factor $1 / (0.04)^2 = 625$ at the telescope for detecting the polarized signal than for detecting the total continuum emission.

One important physical phenomenon used to measure medium-scale magnetic fields is thermal dust emission. Thermal dust emission processes from dust particles aligned by the magnetic fields in interstellar clouds show linearly polarized continuum emission in the extreme infrared (mm and submm wavelengths) and far infrared (e.g., 100 μm), allowing the study and the mapping of the magnetic fields in large clouds. In emission, the position angle PA of the electric vector at maximum intensity is perpendicular to the magnetic field lines. To study magnetic fields at moderate thermal density, it is best to use telescope at submm wavelengths, because of the following. At cm and long mm wavelengths, there is often not enough signal from dust in many cases (poor signal to noise ratio). At far infrared wavelengths, there are costly airborne flights necessary. At near infrared and optical wavelengths one has to cope with several physical problems: (i) multiple scatterings that induce polarization, independent of magnetic fields, (ii) the need to find bright background sources behind clouds, (iii) the ambiguity between one magnetic field direction and its opposite, and (iv) there is no secure method to get the magnetic field strength. Scarrott (1996) reviews the limited data obtained by optical observations, while Scarrott et al. (1996) argue for a mixture of two mechanisms to explain optical polarization data in the galaxy NGC 5128.

One important physical phenomenon used to deduce the large-scale galactic magnetic field is the Faraday rotation effect. Large scale magnetic fields in spiral galaxies are studied primarily through Faraday rotation of nearby pulsars and of distant galaxies and quasars. Due to the well known Faraday rotation observable at centimeter wavelengths, the change of the position angle PA of the electric vector at maximum intensity ΔPA with wavelength λ, follows the Faraday formula: $\Delta PA = (\mathrm{RM}) \cdot \lambda^2$, where ΔPA is in radians, λ is in m, and RM is the rotation measure (rad./m^2). One has: $\mathrm{RM} = \oint 0.8 n_e \cdot B_{\mathrm{l}} \cdot dL$ where n_e is the free electron density (cm^{-3}), B_{l} is the magnetic field (μgauss) component parallel to the line of sight, and L is the length (pc) along the line of sight. The RM is the linear sum of the individual contributions from the radio emitter (a galaxy or a quasar, say), from the intracluster medium around the source, the intergalactic medium between clusters of galaxies (quite negligible), and from the interstellar medium in our Galaxy (in spiral arms and in large interstellar bubbles). A catalogue of unambiguous rotation measure for 674 galaxies and quasars was published by Broten et al. (1988). It contains sources whose data had been selected in one physical wavelength range only, to cover a single physical régime, that of a Faraday-thin, one-component, spectrum-limited source.

Galactic magnetic fields can be split into a random component B_{ran} and a uniform (ie regular) component B_{reg}, and these components can be added in the usual quadratic way: $B_{\mathrm{tot}}^2 = B_{\mathrm{reg}}^2 + B_{\mathrm{ran}}^2$. The random component is on average twice as strong as the uniform component ($B_{\mathrm{reg}} \approx 0.5 B_{\mathrm{ran}}$, e.g., Table 2 in Vallée 1984a). In the Milky Way, the uniform component was found to be oriented nearly azimuthally, i.e., locally towards galactic longitude $l \approx 90°$ (e.g., equation 5 in Vallée 1983a).

Important subtleties involved in deducing polarization and in interpreting them, to alert the theoretical reader to the pitfalls in interpreting the data, can be found in Sections 3 and 4 here, as well as elsewhere (e.g., Vallée 1980; Heiles 1987; Kronberg 1994; Vallée 1995a; Vallée 1996a; Vallée 1996b).

The aim of the present review is to highlight the salient discoveries, on the subject of magnetic fields on mid scales and large scales. Section 2 deals with medium and large objects within our Milky Way, while Section 3 deals with the Milky Way as a whole. Sections 4 and 5 study the nearby galaxies and the more distant objects.

2. SELECTED CELESTIAL ZONES IN OUR GALAXY

2.1. Methodology and Techniques

2.1.1. *Optical dust absorption*

The optical polarization observed on Earth of stars located behind dusty molecular clouds is due to dichroic extinction by dust grains aligned by a cloud magnetic field (e.g., Johnson 1982). But the dense cores within a cloud are opaque at optical wavelengths, prohibiting optical polarization observations of background stars, restricting optical polarimetry to the tenuous parts of cloud halos. At optical and near infrared wavelengths, the observed polarization from stars through a cloud halo could be due to various mechanisms. It could be due to a magnetic field via dust absorption, but Goodman (1995) and Goodman et al. (1995) warn that a lack of polarizing grains for optical and near infrared photons in a dark cloud could prevent measurement of the cloud's own magnetic field, when observing background starlight through a cloud. It could be due also to multiple scattering via dust without any effect from a magnetic field (e.g., Bastien and Ménard 1988; 1990) - thus the typical centro-symmetric pattern for the polarization position angle around a bright star gives no information at all about the magnetic field there.

Looking at dust absorption at optical and near infrared wavelengths, one finds that the ratio of the polarization amplitude at 2 different wavelengths varies according to the Serkowski relation with 2 parameters: $\lambda_{max} \sim 0.55\ \mu$m which is related to the mean size of the polarizing grain, and pmax which is directly related to the extinction along the line of sight, and thus indirectly related to the distance to the star being looked at. In dark clouds, $\lambda_{max} \sim 0.75\ \mu$m (e.g., Breger et al. 1981).

2.1.2. *Infrared Dust Emission*

The presence of magnetic fields in molecular clouds can be revealed by dust grains aligned by the magnetic fields. Elongated dust grains are aligned with their long axis perpendicular to the magnetic field lines. These needle-like grains rotate primarily around one of the short axes (i.e., end-over-end). The rotation axis is parallel to the magnetic field lines. As such, original unpolarized background stellar light at optical wavelengths is mostly transmitted (not absorbed) if the photon's electric vector is in the plane of the grain's short axis, so we observe at optical wavelengths the transmitted photons to be polarized at a position angle parallel to the ambient magnetic field lines. The dust's own *emission* in the far infrared, mm and submm wavelengths is primarily in the plane of rotation of the long axis of the needle, so we observe at far infrared, mm and submm wavelengths the emitted photons to be polarized at a position angle perpendicular to the ambient magnetic field lines. The first successful polarimetry at submillimeter wavelengths was done by Flett and Murray (1991), using the James Clerk Maxwell Telescope (JCMT). The first successful polarimetry at millimeter wavelengths was done by Barvainis et al (1988). For an early review, see Heiles et al. (1991)

Dust grains are in an active, dynamic environment, so to keep them aligned with a magnetic field would require a sufficient magnetic field strength (e.g., Hildebrand 1987, 1988, 1989). Looking at dust emission at far infrared and extreme infrared wavelengths, one finds that the ratio of the polarization amplitude at 2 different wavelengths varies with wavelength according to grain composition, i.e., silicate grains give a nearly constant ratio of polarization percentage, while graphite grains give an increasing polarization percentage at longer wavelengths (e.g., Hildebrand 1988; Minchin & Murray 1994; Leach et al. 1991; Clayton 1996).

2.1.3. *Radio Zeeman Effect*

Another method to determine the magnetic field strengths uses the Zeeman effect. It involves the separation of two opposite circularly polarized components of the radiation (Stokes parameter V). This separation is proportional to the strength of the component of the magnetic field parallel to the line-of-sight. Zeeman splitting at centimeter and millimeter wavelengths, acting on circularly polarized radiation emitted by neutral atoms (HI) or molecules (OH, SiO, H_2O, CN), allows the study of magnetic fields in large HI filaments in low density gas outside clouds, and in substellar hot spots at high thermal gas densities and small object sizes. The instruments most employed are located at Green Bank, Hat Creek, Very Large Array, and Effelsberg. A recent review can be found in Heiles (1987) and Crutcher (1994). Zeeman splitting provides a component of the magnetic field strength in some individual clouds, but there are not enough such data to shed light on the mid-scale and large-scale magnetic fields in the Milky Way galaxy (e.g., Heiles et al. 1993; Heiles 1996b).

At low magnetic field values near 10 μGauss, many Zeeman detection claims by Heiles & Troland (1982), Heiles (1988), Goodman & Heiles (1994), and others, have been followed by several *counter-claims* that deny many previous Zeeman detection claims in nearby HI clouds, based on instrumental problems having to do with the 'squint' effect of single-dish telescopes, or the *polarized sidelobes* of the telescopes used, creating spurious signals capable of mimicking magnetic fields (e.g., Verschuur 1995a, 1995b; Wielebinski 1995; Kazès and Crutcher 1986).

At magnetic field levels near 100 μGauss, claims of detections of the Zeeman effect near a few star-forming regions were made (e.g., Roberts et al. 1996). Some *counter-claims* have appeared (e.g., Crutcher et al. 1996b) could not detect the Zeeman effect above the *detector noise* in molecular cloud cores with gas densities of 10^6 cm^{-3}, putting upper limits of around 200 μGauss, which is well below the expected virial values of about 600 μGauss. A 100 μGauss detection (Güsten and Fiebig, 1990) has been withdrawn (Troland & Heiles, 1996).

At magnetic field levels near 500 μGauss, detections by Zeeman effect of a magnetic field of about 500 μGauss in Sagittarius B2 near the Galactic center were made (e.g., Crutcher et al. 1996a). A *counter-claim* has appeared, i.e., no Zeeman detections leading to an upper limit of 500 μGauss toward objects within 3 parsecs of the Galactic Center (e.g., Marshall et al. 1995; see also Section 2.5 here). Values near 500 μGauss claimed in Si06 (Roberts et al., 1995; Kazès et al., 1988) have been reduced to 140 μGauss (Verschuur, 1996).

At magnetic field values near 1000 μGauss and above, Zeeman detections of magnetic field are toward objects that are dense (> 10^6 cm^{-3}) and small (< 0.1 parsec). Whereas some Zeeman information have been obtained so far in some atomic or molecular clouds, still no global Zeeman information has been obtained on the Milky Way's galactic magnetic fields. And no extragalactic Zeeman detection has been possible so far. Thus at the moment, the Zeeman method is limited by sensitivity and instrumental problems to small-scale objects with high-strength magnetic fields in our own Milky Way galaxy, and a significant improvement in detector sensitivity and in telescope structure is necessary to help advance further.

2.1.4. *Radio Faraday Rotation*

Using the Faraday Rotation method, a novel technique to study the magnetic field in our Galaxy was proposed by Vallée (1983b), consisting of measuring the linear polarization (Stokes Q and U) of extragalactic radio sources located in a selected celestial zone of a few dozens of degrees of angular extent at a time. Radio observations were done between λ2 cm and λ21 cm, using such telescopes as the 27 km Very Large Array in New Mexico, USA, the 46m Algonquin Radio Observatory in Ontario, Canada, the 100m Effelsberg Radio Telescope near Bonn in Germany, and the 3 km Westerbork Synthesis Radio Telescope in the Netherlands,

Selected celestial zones are often centered on specific large-scale features, such as a ring. Polarization observations were made of quasars and compact galaxies shining through the ring, to compare with polarization observations of other quasars and compact galaxies adjacent to the ring, in order to study the variation in RM with respect to angular distance from the ring center.

The first region thus chosen was the galactic anticenter (Vallée, 1983b); the next was the celestial zone encompassing the Gum nebula (Bignell & Vallée, 1983); the third was the Gemini area (MacLeod et al., 1984). The fourth was the area around the cluster of galaxies Abell 2319 (Broten et al., 1986), the fifth area encompassed the central nucleus of our galaxy (Bignell et al., 1988), and the sixth area enclosed the Orion-Eridanus region (MacLeod et al., 1988; Vallée et al., 1988a). This technique has facilitated the investigation of localized effects or RM contributions from a given celestial zone on the passage of the radiation through our Galaxy.

2.2. Interstellar objects (~ 1 to 50 pc)

2.2.1. *Excess line width W_{excess} relationship with Object size R*

There is a relationship between an object size (R) and a parameter of the emitted spectral line from an object, namely the line width (= W_{excess}) in excess of (i) the usual thermal width and in excess of (ii) the width due to large scale motion . Statistics for objects with sizes R from 1 pc up to 1000 pc, including globules, molecular clouds, HII regions in our Galaxy and extragalactic HII regions, suggest a law of the form $W_{excess} \sim R^q$.

An observed general law with $q = 0.5 \pm 0.1$ is indicated for objects with $R > 1$ pc (e.g., Larson 1979; Vallée 1994e).

Several theoretical models which predicted values of $q >> 0.5$ or $q << 0.5$ could be eliminated, due to the small error bars (± 0.1). The remaining models with $q \approx 0.5$ use (i) turbulences, or else (ii) virial balance for gravitationally-bound clouds. (i) Models with small scale turbulence often employ non-magnetic turbulence (e.g., stellar winds, outflows embedded in gaseous clouds, thermal instabilities around cloud edges, clump collisions in clouds (e.g., Miesch & Bally 1994), although later on in the presence of a magnetic field these non-magnetic turbulences can be theoretically converted into weak MHD waves (e.g., Arons & Max 1975). Heithausen (1996) has shown that high-latitude molecular clouds, with low gas density $n \approx 10$ cm^{-3} and small sizes $\approx$ 2 pc, are not in virial balance with self-gravity; these clouds are compressed by the external rarefied HI gas, implying that the cloud relation $W_{excess} \sim r^q$ is due to internal turbulences needed to oppose the external compression. (ii) For larger density clouds, models using the virial balance with self-gravity also involve the internal magnetic field pressure. Questions to be addressed concern the strength of the cloud magnetic field. Future trends: can strong magnetic support be ruled out in most clouds ? Which *degree* of magnetic support of a cloud is reasonable, i.e. 1/5 of the overall energy due to magnetism, gravitation, kinetic/thermal motions, turbulent motions, and cloud rotation (e.g., Myers and Goodman 1990) ?

2.2.2. *Globules and Magnetic Fields*

An isolated Bok-type globule is the simplest dusty molecular cloud which can form one star. Little is known about its magnetic field. The distributions of gas and of dust inside the nearby globules are now becoming available, thanks to millimeter and submillimeter telescopes. In particular, the rotation axis of some globules are now known, and have been compared to the polarization angles (parallel to the magnetic field) obtained at optical wavelengths from stars around the globules (but not inside). Kane and Clemens (1996) found that in six globules, there was a trend for the globule's rotation axis to be roughly aligned with the external magnetic field.

As is well known, the distribution of the magnetic field in the densest core of a cloud or globule is unlikely to be an indicator of the magnetic field direction outside of the cloud or globule (e.g., Goodman 1996). The best way to get the direction of the magnetic field inside the globules would be through polarimetric observations of the dust's own emission at extreme infrared wavelengths. Such observations are under way at some telescopes, notably the JCMT.

It is possible that the evolution of a globule or cloud may force an evolution of its magnetic field (shape and strength), at least after a certain age. In this way, later observations may tell us whether a Bok globule is old enough to allow for an evolution of its magnetic fields.

2.2.3. Narrow Magnetized Features

2.2.3.1 NARROW MAGNETIZED ISOLATED FILAMENTS Nonthermal (synchrotron) emitting filaments have been found near a wavelength of 92 cm (Wieringa et al., 1993) in the interstellar medium, with the Westerbork Synthesis Radio Telescope in Holland. These filaments have a width $\approx$ 10% of their length, with sharp edges. They were found at a distance from Earth of ~ 0.2 kpc to 1 kpc, with length ~ 10 pc and width ~ 1 pc. There is virtually no change in the angle of linear polarization along the filaments. Some may come in systems of almost parallel filaments. These observations were interpreted as small clouds of gas with gas density ~ 0.2 cm^{-3}, concentrated along the local magnetic field lines.

An intriguing 'lens' or filament has been found near the W 5 complex HII region, in continuum emission at a wavelength of 21 cm (e.g., Gray et al. 1997) with the Dominion Radio Synthesis Telescope near Penticton, B.C., Canada, being apparently unrelated to the thermal emission (the boundary of the HII region coincides with the diaappearance of the polarization structure). This 'lens' has a remarkably smooth structure in which the position angle of the linear polarization swings continuously from the center to the edge, possibly due to line-of-sight dependent Faraday rotation effects in a foreground screen.

Thermal (free-free) emitting filaments have been found near large dust clouds. In the Auriga filament (e.g., Puget 1991) the gas velocity changes slowly along the major axis of the filament, suggestive of a physical link such as a magnetic field to maintain the spatial correlation over a length of 1 pc. In the long (12 pc) thin (1 pc) filament near L204 (e.g., Heiles 1988b), a magnetic field was measured by the Zeeman effect to be near 12 μGauss.

2.2.3.2 NARROW MAGNETIZED OUTFLOWS FROM CLOUDS When two high-velocity (~ 100 km/s) outflows emerge in opposite directions from a recently-formed protostellar disk, these outflows push out a shell of molecular gas and magnetic field, often extending to ~ 1 pc, with a lateral width of ~ 0.1 pc. Magnetic stresses at the cavity's surface may affect the evolution of the outflows. Observationally, Simonetti and Cordes (1986a) have determined the RM of background galaxies and QSO near and through the outflows in 2 cases, deriving a magnetic field of ~ 100 μGauss in the outflow walls. Crutcher (1991) used the Zeeman effect to derive a magnetic field near ~ 1000 μGauss (toward the observer) in the north lobe of S106 and ~ 600 μGauss (away from the observer) in the south lobe - thus the magnetic field reverses direction from one lobe to the other in S106. A recent theoretical review of outflows is given in Königl and Ruden (1993).

2.2.3.3 NARROW MAGNETIZED EDGES OF DUSTY MOLECULAR CLOUDS ($B \sim n^1$) A magnetized molecular cloud edge, near an adjacent HII region containing one or more O-type star(s), has been modeled as having successive compressed layers: first an atomic HI layer nearest the HII region, then a molecular H_2 layer further inside the cloud,

In these HI/H_2 layers, the carbon atoms are ionized into CII. Radio observations of CII recombination lines (e.g., near λ6cm) in cloud edges were compared with observations of CO lines (e.g., near λ3mm) deeper into the clouds, indicating a CII layer with the following parameters: depth ~ 0.1 pc, surface side ~ 1 pc, total gas density ~ 10^5 cm^{-3}, magnetic field ~ 100 μGauss, a *weak* compression factor between 2 and 10 due to the presence of magnetic fields; and these shocked molecular cloud edges display the $B \sim n^{1.0}$ behavior (e.g., Table 2 in Vallée 1989a).

Results were also obtained for the adjacent but deeper layer containing sulfur, by comparing the sulfur recombination lines SII with the CO lines from the cloud cores: depth ~ 1 pc, surface side ~ 1.5 pc, total gas density ~ 10^6 cm^{-3}, magnetic field ~ 180 μGauss (e.g., Table 3 in Vallée 1989a; Table 4 in Vallée 1989b).

The linear polarization of the 21 cm HI line from the molecular cloud edge of Orion *B* was studied closely by van der Werf et al. (1993), using the Very Large Array in its *D* configuration. They found 3 absorbing layers in front of the continuum HII region, with the outermost (A) layer having a total gas density $n \sim 10^3$ cm^{-3} and a magnetic field $B \sim 30$ μGauss, the next one having a total gas density $n \sim 10^4$ cm^{-3} and magnetic field $B \sim 40$ μGauss, and the innermost one having a total gas density $n \sim 10^5$ cm^{-3} and a magnetic field $B \sim 60$ μGauss.

2.2.4. *Magnetic field versus Gas density, on medium linear scales ($B \sim n^{0.5}$)*

Observational magnetic field values are often difficult to make in many instances, and come with some limitations due to detector sensitivity (e.g., Zeeman effect), or weighted by another physical parameter (e.g., Faraday rotation), or affected by projection effects, or by the tangling of magnetic field lines, etc. For many objects, this is nevertheless the best that can be had to date.

Table 1 gives a list of observational results for representative objects in the Milky Way (and beyond).

Table 1. Observed properties of various astronomical gas (non-degenerate, thermal gas)

Object type	Mean Density cm^{-3}	Mean Magn. field μG	Mean Size pc	Mean Temp. K	Reference
Gas in supercluster of gal.	10^{-6}	0.5	5×10^7	10^7	Vallée(1990b)
Gas in clusters of galaxies	10^{-4}	1	5×10^6	10^7	Vallée(199Ob)
Gas in galactic halos	10^{-3}	4	5×10^4	10^6	Vallee(199Ob)
Spiral arm interstellar gas	0.5	4	10^4	10^4	Vallée (199lb)
Large supershells-initial	0.8	3	300	1000	Vailee (1993d)
Large supershells-actual	2	8	20	1000	Vallée (1993d)
Hl gas in diffuse cl ds	3	5	10	100	Troland and Heiles (1986)
Large HII regions	5	10	30	104	Heiles and Chu (1980)
Hl gas in interclumps	90	15	10	100	Troland and Heiles (1986)
HI gas in abs.-initial	100	15	1	10	Troland and Heiles (1986)
HI gas in absorption-act.	300	50	1	50	Troland and Heiles (1986)
Gas from OH abs.-type 1	10^3	40	1	10	Troland and Heiles (1986)
Gas from OH abs.-type 2	10^4	120	1	10	Troland and Heiles (1986)
CII edges of clouds-initial	1.4×10^4	40	5	10	Vallée (1989a)
SII edges of clouds-initial	2.8×10^4	40	5	10	Vallée (1989a)
CII edges of clouds-actual	6×10^4	90	0.5	50	Vallee (1989a)
OH masertype l-initial	7×10^5	1500	10^{-2}	10	Draine and Roberge (1982)
OH maser type l-actual	10^6	4000	10^{-3}	-	Draine and Roberge (1982)
SII edges of clouds-actual	1.3×10^6	180	1	50	Vallée (1989a)
OH maser type 2-initial	2×10^6	3000	10^{-2}	10	Güsten et al. (1994)
OH maser type 2-actual	3×10^7	5000	10^{-3}	-	Bloemhof et al. (1982)
H_2O maser-initial	10^8	10^3	10^{-3}	10	Fiebig and Güsten (1989; $B / B_0 = n / n_0$)
SiO maser-initial	10^9	4×10^4	10^{-2}	10	Alcock and Ross (1986; $B / B_0 = n / n_0$)
H_2O maser-actual	10^{10}	10^5	10^{-4}	-	Fiebig and Güsten (1989)
SiO maser-actual	10^{12}	4×10^7	10^{-5}	-	Barvainis et al. (1987)

First break in behavior. Physically, one expects a different behavior of the magnetic field B at low gas densities than the behavior at medium gas densities. At low gas density n, the gas can stream along the magnetic field lines and can bunch up and increase its gas density, without the need to increase much the magnetic field, so one expects so $B \sim n^{0.0\text{-}0.3}$. At medium gas density n, the really bunched gas starts affecting the magnetic field, through turbulences and/or some virial equilibrium conditions, so one expects $B \sim n^{0.5}$. Where is the break between the 2 régimes ? Many observers have found it to be around $n \sim 100\ cm^{-3}$ (e.g.. Troland and Heiles 1986; Heiles 1987); Vallée 1990b; Vallée 1995d).

Figure 1 shows all the observed (B, n) data for $n > 100\ cm^{-3}$. A statistical least-squares-fit can be made, giving $B \approx 0.4\ \mu\text{Gauss} \cdot (n/cm^3)^{0.5}$, for $n > 100\ cm^{-3}$.

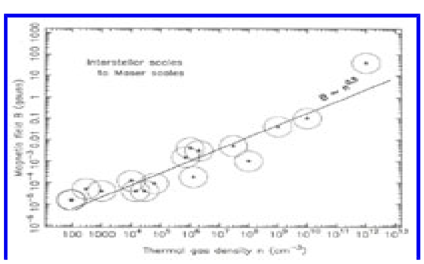

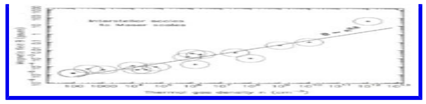

Figure 1. Observed behavior of the magnetic field B (in Gauss) as a function of the total gas density n (in cm^{-3}), for n > 100 cm^{-3}. The statistical results gave $B \approx 0.4$ μGauss $\cdot$ $n^{0.5}$. The most likely interpretation involves some turbulence and/or virial equilibrium between the main constituents. See Vallée (1995d) for more details.

On the theoretical side, a 'mechanical' equilibrium model was claimed by Fleck (1988, his Table 1), who used a fragmentation order from 0 to 3, leading to $B \sim n^{0.2}$. A model with vigorous injection of turbulent energy due to expanding HII regions, stellar winds, supernovae explosions, and stellar jets was employed by Whitworth (1991) to deduce a relation $B_{cloud} \sim 2.5$ μGauss $\cdot$ $(n$ / cm$^3)^{0.5}$. Bhatt and Jain (1992) also predicted a $B \sim 2.0$ μGauss $\cdot$ $n^{0.5}$ relation, using magnetic alignement of grains and collisional disorientation of grains, and specific grain parameters. A model of 'hierarchical' turbulences was proposed by Chaboyer and Henriksen (1990), with locally homogeneous, isotropic, and mirror symmetric turbulences, yielding a $B \sim n^{0.6}$ law. A model with 2 hierarchical sequences with different types of turbulences, by Dudorov (1991), yielded a $B \sim n^{0.5}$ law in one hierarchy and a $B \sim n^{2/3}$ law in the other hierarchy.

Second break in behavior. At even higher gas density n, another physical régime is predicted. The theoretical models predict a decoupling régime where the magnetic field massively decouples from the cloud cores and leaves the cloud cores, so the cloud cores own magnetic field decreases to low values $B \approx 0$ (e.g., Barker and Mestel 1996; etc). The models of Nakano and Tademaru (1972) and Nakano (1997) predict that the critical gas density for decoupling is around or above 10^{12} cm^{-3}. A third break is predicted at even higher gas density n approaching gas densities in stars, near 10^{24} cm^{-3}, where we can expect $B \sim 100$ Gauss due to a recoupling of B with n if the thermal ionization of alkaline metals can keep a high enough ionization fraction (e.g., Nakano 1997; Davies 1994).

Future trends: The observational data in Table 1 just about reaches gas densities near $10^{11\text{-}12}$ cm^{-3}. It would be interesting to observe clouds with higher gas densities and to detect or put an upper limit to B values, and thus to find the break from the $B \sim n^{0.5}$ régime, i.e. the onset for the decoupling régime, as soon as more sensitive detectors come on line.

2.2.5. Magnetic field shapes in Dusty Elongated Molecular Clouds

On the theoretical side, there has been many detailed models published for the behavior of gas density, temperature, turbulence, velocity, pressure, and of magnetic field in isolated or colliding molecular clouds, often involving ambipolar diffusion and energy equilibrium between some of these physical parameters (e.g., McLaughlin & Pudritz 1996; Ciolek and Mouschovias 1994; Morton et al. 1994; Crutcher et al. 1994; Just et al. 1994; Porro and Silvestro 1993; Elmegreen & Fiebig 1993; Ciolek & Mouschovias 1993; Elmegreen & Combes 1992; Elmegreen 1988; Mouschovias et al. 1985; etc).

While current limited observations cannot test many of the detailed physical parameters mentioned above, at least the distributions of thermal gas density and magnetic fields are amenable to observations, within the beamwidth limitations of the telescopes used. Various magnetic field theories have been published in the literature, predicting the magnetic field direction and amplitude in and near a molecular cloud. In this research area, there is a plethora of theories on magnetic field direction, yet few observations.

2.2.5.1 SUPERPOSITION OF CLOUDS A possible classification of observed magnetic fields in five 'spatial pattern types' has been suggested by Myers & Goodman (1991), involving chiefly a superposition of clouds or sub-clouds. The five 'spatial pattern types' found in typical clouds are as follows. (a) One cloud, with similar polarization PA values over its entire length (e.g., L1755, B216, etc). (b) One cloud, with randomly distributed polarization PA values over its entire length (e.g., L1689, N1333). A cloud with 2 distinct sub-clouds, each having a distinct polarization PA over its entire region, is classified as follow: (c) the 2 sub-clouds are seen across the line-of-sight (e.g., Lupus 3; L203; etc); or (d) the 2 sub-clouds are seen along the same line of sight (e.g., Perseus complex). (e) One cloud, with 2 distinct sub-clouds, one region with a distinct polarization PA and a small dispersion in polarization PA values, and another region across the line of sight with nearly random polarization PA values and a large dispersion in polarization PA values (e.g., Lupus 2; Ophiucus complex; etc).

The Myers and Goodman (1991) classification (a) - (e) uses two parameters, namely the number N of correlation lengths of the magnetic field in a cloud (i.e., the number of independent regions in a cloud), and the amount of the dispersion in polarization PA values. They concluded that N is small, perhaps 1 to 4, for a typical cloud size ~ 1 pc, from the spatial patterns of observed optical polarization vectors of background stars seen through a nearby cloud. Their classification, involving correlation lengths and angular dispersions between sub-clouds, has been used by Kobulnicky et al. (1994) and Jones et al. (1992).

2.2.5.2 MAGNETIC FIELD CLASSES A *new* classification has been proposed by Vallée & Bastien (1996, hereafter V&B) based on 11 'magnetic field classes', involving only one cloud (*no superposition* of sub-clouds). This classification has several bonuses. (i) It is *physically simple*, compared to the combinations of Myers &Goodman (1991). (ii) It can be later complexified by a *simple superposition* of any 2 of the 11 magnetic field classes here; thus one cloud in V&B class F seen along the same line of sight of one cloud in V&B class G can give the spatial pattern type *d* of Myers and Goodman (1991). (iii) These 11 magnetic field classes, when combined two by two along or across the line of sight, could of course allow more combinations than the five spatial pattern types of Myers and Goodman (1991) known so far.

The simple classification scheme of V&B uses 2 parameters: the magnetic field's shape and the magnetic field's distance scale. It has been used by V&B to compare with actual JCMT polarimetric observations in the extreme infrared.

Figure 2a-k shows several cartoon-style drawings with the main features for each magnetic class, as described further below.

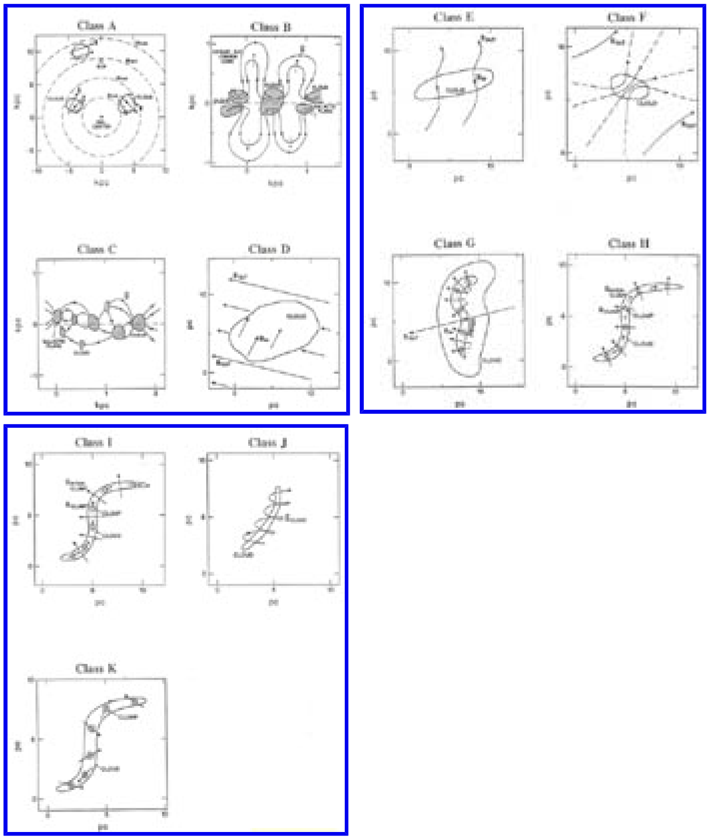

Figure 2. Cartoon-style drawings showing the main features of each 'magnetic class', described further in the text. *Class A.* Magnetized molecular clouds of varied shapes, with a spiral galactic magnetic field shape on 10 kpc scale. The *B* field shows a clockwise direction outside a 6 kpc radius from the galactic center, even inside molecular clouds (as shown). In this model, *B*-vectors are parallel to the galactic plane, and the magnetic field lines shown are going clockwise. In addition, a *B* reversal in the radial range 5.5 kpc < r_g < 7.5 kpc is known (magnetic field lines going counterclockwise), but not shown here. *Class B.* Magnetized molecular cloud, with a halo-disk magnetic field shape on 1 kpc scale. B-vectors follow a U-shaped bowl, coming from the galactic halo and being parallel to the galactic plane at the bottom of the bowl. *Class C.* Magnetized molecular cloud, with cloud-cloud magnetic field shape on 1 kpc scale. *B*-vectors follow the cloud elongation in a cloud, except near the edges of a cloud where *B*-vectors enter and leave in a Y-shape fashion (taken here at up to +40 or -40 degrees from the cloud elongation). *Class D.* Magnetized molecular cloud, with cloud magnetic field perpendicular to the regional magnetic field shape on 100 pc scale. *Class E.* Magnetized molecular cloud, with cloud magnetic field parallel to the regional magnetic field shape on 100 pc scale. *B*-vectors in a cloud are parallel to the regional magnetic field outside the cloud (~ 100 pc). *Class F.* Magnetized molecular cloud, with pinched magnetic field shape on 1 pc scale, and a local magnetic field on 10 pc scale. *B*-vectors in a clump show pinching effects of magnetic field lines in clump edges (X-shaped). *Class G.* Magnetized molecular cloud on 1 pc scale, with 1-dimensional collapse along localised magnetic field shape on 10 pc scale. B-vectors are perpendicular to the cloud elongation at each point, whatever the curvature of the cloud. *Class H.* Magnetized molecular cloud, with orthogonal-field in clumps and aligned-field in filament shape, 0.2 to 10 pc scale. *B*-vectors in clumps are perpendicular to cloud elongation, and *B*-vectors in-between clumps are aligned along cloud elongation. *Class I.* Magnetized molecular cloud, with aligned-field in clumps and orthogonal-field in cloud shape, 0.2 to 10 pc scale. *B*-vectors

in clumps are parallel to cloud elongation, and *B*-vectors in-between clumps are aligned perpendicular cloud elongation. *Class J.* Magnetized molecular cloud, with helically-wrapped field shape, 1 pc scale. Here *B*-vectors are skewed -20 degrees from the direction of cloud elongation. *Class K.* Magnetized molecular cloud, with magnetized independent-clump shape, 0.1 pc scale. *B*-vectors are randomly oriented in clumps. See Vallée & Bastien (1996) for more details.

Class A. The spiral-galactic magnetic field, with a galactic magnetic field on a scale of 10 kpc. In this first class of theoretical models, the *B*-vectors are parallel to the galactic plane, following the spiral arms, even in molecular clouds. A model in this class is supported by OH maser Zeeman observations (Reid and Silverstein, 1990), suggesting that the magnetic field direction is largely preserved during cloud contraction from low interstellar densities through the medium densities in giant molecular clouds up to the higher densities in star forming sites (e.g., Fig. 3 in Elitzur 1992).

Class B. The halo-disk magnetic field, with a galactic magnetic field on a scale of 1 kpc. In this second class of theoretical models, the *B*-vectors follow a *U*-shaped bowl, first coming from the galactic halo (perpendicular to $b = 0°$), then being parallel to the galactic plane at the bottom of the bowl (where the cloud sits). A model in this class employs cosmic-rays generated near the galactic plane to inflate magnetic arches between clouds, causing the magnetic field to expand upward at greater galactic latitudes (e.g., Fig. 3 in Parker 1976) and to drive the galactic dynamo (e.g., Parker 1992).

Class C. The linked cloud-cloud magnetic field, with a galactic magnetic field scale around 1 kpc. In this third class of models, the *B*-vectors are parallel to the cloud elongation, except near the two edges of the elongated cloud where the *B*-vectors enter and leave (as in a *Y*-shaped funnel). A model in this class employs galactic magnetic field lines connecting together several elongated molecular clouds (e.g., Fig. 4 in Beck et al. 1991). Here magnetic field lines are anchored in the clouds and influence cloud motions and cloud collisions (e.g., Clifford and Elmegreen 1983).

Class D. The cloud's magnetic field is perpendicular to the regional magnetic field, with a regional magnetic field on a scale of 100 pc, and a cloud magnetic field on a scale of 10 pc. In this fourth class of models, the *B*-vectors in the clumps are perpendicular to the magnetic field in the region on a scale of 100 pc surrounding the cloud and clumps. This 100 pc scale is the scale of the perturbation of the galactic magnetic field by interstellar magnetic superbubbles (100-125 pc in radius (e.g., Vallée 1993d). A model in that class was employed to explain the polarization around the stars HL Tau and Star #4 in L1551 by Vrba et al (1976), and to explain the arched filaments of the Galactic Center Arc by Morris et al. (1992), as well as to explain the polarization of the Taurus cloud by Nakajima & Hanawa (1996).

Class E. The cloud's magnetic field is parallel to the region's magnetic field, with a regional magnetic field on a scale of 100 pc, and a cloud magnetic field on a scale of 10 pc. In this fifth class of models, the *B*-vectors in clumps are parallel to the magnetic field in the region over a scale of 100 pc surrounding the cloud and clumps. This 100 pc scale is similar to that of the sizes of interstellar magnetic bubbles (100-125 pc in radius). Models in that class were employed by McDavid (1984) and Pudritz and Silk (1987), in which cloud fragmentation gives rise to cloudlets with *B*-vectors in cloudlets, and in between cloudlets, that are parallel to the original *B*-vector direction in the original cloud and in the 100-pc region.

Class F. The pinched galactic magnetic field in clumps, with a local magnetic field on a scale of 10 pc, and a collapsing core magnetic field on a scale of 1 pc. In this sixth class of models, the *B*-vectors in clumps and in-between clumps are parallel to the cloud elongation, with pinching effects of the magnetic field lines in clump edges (X-shaped). A model in this class was invoked for the clump W3-IRS5 (Greaves et al., 1992), and can be explained via a sudden collapse of gas to form a high-mass star, with pinching of the magnetic field lines at the stellar position.

Class G. The 1-dimensional collapse along localized magnetic field lines, with a local magnetic field on a scale of 10 pc, and a cloud magnetic field on a scale of 1 pc. In this seventh class of models, the *B*-vectors are roughly perpendicular to the cloud elongation, whatever the wavyness of the cloud. A model in this class employs a cloud originally spherical that collapses along the magnetic field lines in one dimension, becoming highly flattened in the process (e.g., Mestel 1965; Langer 1978). Another model in this class invokes the evolution of an elongated cloud by magnetic field control (50 μGauss) to minimise the disturbances which act on a cloud (McCutcheon et al., 1986). Whittet et al. (1994) showed evidence in Chamaeleon for such a magnetic class.

Class H. The orthogonal magnetic field in clumps plus aligned magnetic field in filament, with a cloud magnetic field on a scale of 0.2 pc to 10 pc. In this eighth class of models, the *B*-vectors in the clumps (within an elongated cloud) are perpendicular to the cloud elongation, whereas the *B*-vectors in-between clumps are parallel to the cloud elongation. A model in this class is employed to explain two dust filaments in the Ophiuchus cloud (optical data in Vrba et al., 1976; radio HI data in Heiles, 1987) and to explain a filament in R Coronae Australis (Vrba et al., 1981). McGregor et al. (1994) showed evidence in Chamaeleon for such a magnetic class.

Class I. The aligned magnetic field in clumps plus orthogonal magnetic field in cloud, with a cloud magnetic field on a scale of around 0.2 pc to 10 pc. In this ninth class, the *B*-vectors in clumps (within an elongated cloud) are parallel to the cloud elongation, whereas the *B*-vectors in-between clumps are perpendicular to the cloud elongation. A model in this class was employed to explain 3 elongated dense condensations in Taurus (DG Tau; Haro 6-13; Star no.1 in Fig. 1 of Moneti et al., 1984), and one in Serpens (Warren-Smith et al., 1987).

Class J. The helicoidally-wrapped magnetic field in a cloud, with a cloud magnetic field on a scale of 0.5 to 5 pc. In this tenth class of models, the *B*-vectors are helicoidally wrapped around the cloud elongation, but the magnetic field lines are skewed by about 20° from the cloud elongation. A model in this class is employed when there is a claim for a close connection between the cloud kinematics (the local-standard-of-rest velocities change gradually along the cloud elongation) and the magnetic fields (the polarization changes gradually along the cloud elongation), as in Bally (1989). A theoretical example is worked out in Hanawa et al. (1993) and in Shibata and Matsumoto (1991).

Class K. The magnetized independent, random clumps, with a clump magnetic field on a scale of 0.1 pc. In this eleventh class of models, the

B-vectors are randomly oriented in clumps. A model in this class is that of pressure-confined clumps in magnetized molecular clouds (e.g., Bertoldi and McKee 1992). Turbulent support inside a clump is provided by magnetic fields with an amplitude of about 10 to 40 μGauss for clump densities of 10^3 cm^{-3} and increasing as the square root of the clump density. In another model, it is postulated that the magnetic field lines thread both the clump and the interclump medium in a cloud (e.g., Blitz 1991, his Section 9). Because of thermal equilibrium between atomic gas in-between clumps and molecular gas in clumps, the deduced magnetic field amplitude is about 10μGauss in gas densities of 10^3 cm^{-3} (e.g., Blitz 1991).

2.2.5.3 COMPARISON The above classification system of V&B has been successfully compared with recent observations of the M17-SW molecular cloud at Extreme-Infrared wavelengths (λ800 μm) with the JCMT. Six positions of peak intensity (clumps) in the ridge of dust were observed with the Aberdeen-QMW polarimeter, and the observed linear polarization PA were converted to magnetic field PA (V&B, their Table 4). Also, the magnetic field PA predicted from each 'magnetic class' A to K was computed (V&B, their Table 5), and a comparison of observed minus predicted magnetic field PA was made (V&B, their Table 6) showing that 9 of the 11 'magnetic classes' could not explain M17-SW. Magnetic Class E and Class G could explain the magnetic field observed in M17-SW, and to separate them would require new observations to be made in the interclump medium, located between clumps (peak intensity positions) in the molecular cloud.

Figure 3 shows the proposed magnetic field map over the cloud M17-SW, with magnetic field lines going from bottom-left to the right (upper-right and lower-right). The dense dust and gas peaks/clumps were observed at the JCMT at λ800 μm (Vallée and Bastien, 1996), while the light dust and gas areas/halo data come from the KAO polarimeter at λ100 μm (Dotson, 1996a; Dotson, 1996b). Some problems inherent to Far Infrared Polarimetry near λ100 μm are discussed further in Hildebrand (1996).

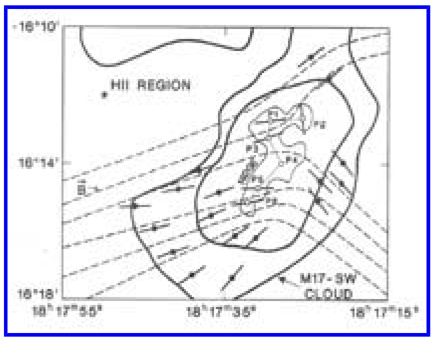

Figure 3. Observed magnetic field in the molecular cloud M17-SW. The ridge line (dots) links the 6 main dust peaks (P1 to P6) in the cloud core. The magnetic field vectors are shown by the bars. In the higher gas density core, the thick bars show the magnetic field derived from the JCMT λ800μ data (from Vallée & Bastien, 1996), and the thin contours show the total intensity continuum dust emission as well as the CO line emission. In the lower gas density envelope, the thick bars show the magnetic field direction as derived from the KAO λ100 μm data - only the locations where the KAO E-vector amplitude exceeded 2% are shown, as adapted here from Dotson (1996a).

A few other magnetic field maps of dusty molecular clouds observed at Extreme-Infrared (λ800 μm; λ450 μm) wavelengths have now been made for smaller clouds, mainly with the JCMT, i.e., W75N-IRS1 (Vallée and Bastien, 1995), Sagittarius B2 (Greaves et al., 1995a), MonR2 core (Greaves et al., 1995b), and Orion A (Schleuning et al., 1996). Preliminary results indicate that the medium-scale magnetic field lines do *bend a little* in MonR2 core in a similar way that they do in M17-SW, suggesting that there is some *evolution* of the magnetic field inside a molecular cloud, but without any excessive tangling of the magnetic field lines.

2.3. Interstellar Superbubbles and shells with $B \sim n^1$ (~ 50 to 500 pc)

Figure 4 shows the sky distribution of the 662 quasars (QSO) and galaxies with a measured Faraday Rotation Measure RM, done with the help of a Mercator projection of the galactic coordinates. Data from Broten et al. (1988). From such catalogues, one deduces the distribution (direction, strength) of the magnetic fields.

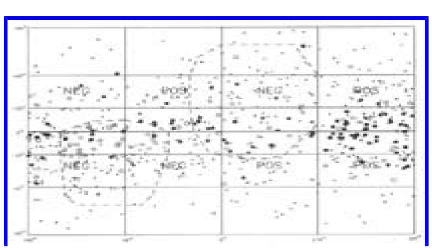

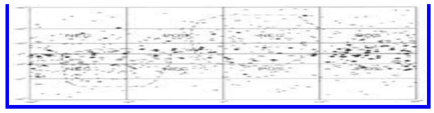

Figure 4. Sky distribution of quasars and galaxies with a known Faraday rotation measure (RM) value. A Mercator projection of galactic coordinates is used (galactic longitudes on horizontal axis; galactic latitudes on vertical axis). The Galactic Centre is at 0°, 0°. Zones of negative RM (empty circles - magnetic field going away from the Sun) alternate with zones of positive RM (filled circles - magnetic field coming toward the Sun). The two nearest and largest superbubbles are sketched (dashes), with Loop I/NPS centered near l = 330°, and Loop II/Cetus Arc centered near l = 110°.

We know that stellar winds from an association of OB stars can form a common superbubble, enclosed by a large supershell, through the combined effort of the winds from the stars at the center. Some authors have used the Zeeman effect in emission and others have used the Faraday effect to detect the magnetic field component $B_{\rm I}$ in some of these large superbubbles (e.g., Heiles 1989).

Some superbubbles are located close enough to the Sun that their large angular sizes can encompass the line of sights of many QSOs and galaxies, and their magnetic fields can be studied by the Faraday effect. Thus many authors have found the magnetic field component B2 in large superbubbles, as detected by radio RM observations of QSOs and galaxies. The magnetism of the "North Polar Spur" shell was first reported in Fig. 2 of Vallée & Kronberg (1973); the magnetism of the "Cetus Arc" shell was first reported in Fig. 3 of Simard-Normandin & Kronberg (1979); the magnetism of the "Gum Nebula" shell was first reported in Fig. 4 of Vallée and Bignell (1983); the magnetism of the 20° "Monogem Ring" shell was first reported in Fig. 3 of Vallée et al. (1984). Since then, magnetism has been found in other localized shells of superbubbles, e.g., Eridanus, G135-40-10, G062-23+13 (for a review, see Vallée, 1993d).

Averaging over four magnetized shells near the sun (North polar spur, Cetus arc, Gum nebula, and Monogem ring), it was found that a mean shell rotation measure of $\approx$ 90 radians/m^2 could be expected above the surrounding background (Table 1 in Vallée, 1984b). One could then not ignore the rotation measure contributions from these selected celestial zones in the total galactic contributions. These four interstellar shells, with a mean diameter $\approx$ 200 - 250 pc, are expanding at a mean speed of $\approx$ 23 km/s (e.g., Table 2 in Broten et al. 1985).

Broten et al. (1985) also found that the strength of the magnetic field in these shells increased with the relative shell compression, according to the empirical parabolic law: $B_{\rm shell} \approx 3\ \mu$Gauss + (9 μGauss).[inner shell radius/outer shell radius]^2 .

A more recent study (Vallée, 1993d) of nearby large interstellar magnetic bubbles (within 1 kpc of the Sun) showed an increase of the shell magnetic field with increasing shell thermal density, as a consequence of the narrowing of the shell width Δr, according to the law: $B_{\rm shell} = 3\ \mu{\rm Gauss} \cdot [1 - (1 - \Delta r / r_{\rm out})^3]^{-k}$ where $r_{\rm out}$ is the outer radius of the whole shell. Here Δr = (outer shell radius - inner shell radius), and k is the exponent in the well-known magnetic field versus gas density relation $B \sim n^k$. Vallée (1993d) thus found for several nearby interstellar magnetic bubbles with observed B and observed n that $B \sim n^k$ with observed $k = 1.0 \pm 0.1$, as expected for an expanding shocked medium (narrow shell width).

Figure 5 shows a plot of the shell magnetic field as a function of the relative thickness of a shell, for several nearby interstellar magnetic bubbles. Curves for $B \sim n^k$ are shown, with exponent values k = 0.0, 0.5, 1.0, 1.5, 2.0.

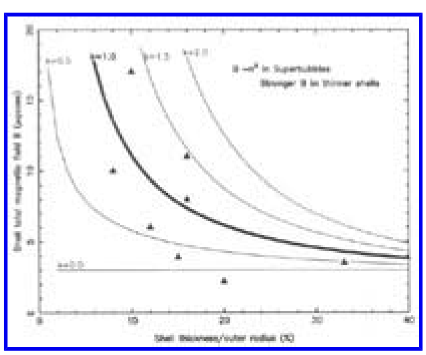

Figure 5. Plot of the magnetic field strength (B, in μgauss) in large supershells as a function of the relative shell thickness (shell thickness/outer shell radius, in %), for shells with diameter > 100 pc. Continuous curves give the model behavior of the shell magnetic field with shell gas density n, of the form $B \sim n^k$, for $0 \leq k \leq 2$. See Vallée (1993d) for details. The observed data show a

better fit to the behavior of the magnetic field given by the relation $B \sim n^{1.0}$.

The early theories of *thin* shells around superbubbles from combined stellar winds were adequate for explaining the primary observational features (defined as: shell age, outer shell radius, shell speed, shell mass, shell energy), but they were not adequate to explain some secondary features (defined as: shell thickness, shell magnetic field, shell gas density). More recently published theories for a stellar-wind superbubble predict a range of *thick* shells (e.g., Mineshige et al. 1993; Slavin and Cox 1993; Ferrière 1993a, 1993b, 1993c; Tomisaka 1992; Jun and Norman 1996; Shull 1995; Stone and Norman 1992). These later theories have been found more adequate when compared with the observations (Vallée, 1994d), showing for 9 such shells with a measured magnetic field value the presence of thick shells (mean shell thickness = 16% of outer shell radius), low shell magnetic fields (mean shell magnetic field strengths = 8μgauss), and low shell gas density (mean gas shell density = 2.4 cm^{-3}).

Verschuur (1993) has provided some evidence for a much bigger supershell, formed by high-velocity clouds towards l = 231° above the Perseus spiral arm, with thickness/radius of 55 pc / 1900 pc = 2.9% and a magnetic field value above 15 μGauss. If confirmed, this data point (not shown here) with such a lower B limit would not contradict the $B \sim n^1$ law.

2.4. Magnetic fields and Supernovae ($B \sim n^1$)

There is some nonthermal polarized emission from supernovae, due to synchrotron radiation from relativistic electrons moving in the magnetic fields (located in supernovae shells). Thin shells have been studied at centimetric wavelengths; but thick shells require shorter wavelengths (e.g., Weiler and Sramek 1988; Mineshige et al. 1993).

Theoretically, hot gas escaping from older superbubbles around supernovae and breaking into the galactic halo are said to form a 'galactic fountain' or 'chimney' (e.g., fig. 10 in Kahn & Brett 1993), complete with magnetic reconnections along adjacent galactic fountains. In the shell of a galactic fountain, the magnetic field strength is predicted to be proportional to the shell gas density, i.e., $B \sim n^{1.0}$, preventing the thickness of the shell to become too small as the shell cools with time.

2.5. The Center of the Milky Way Galaxy's disk (~ 8 kpc away)

The center of the Milky Way is roughly 8 kpc away from the Sun. Within 500 pc of the galactic center (i.e., within an angular radius of about 3.6 degrees), Spergel & Blitz (1992) predicted that there exist a *large* volume of space with high gas pressure, and a magnetic field strength close to 130 μGauss (magnetic pressure in equilibrium with the gas pressure).

Within 100 pc of the galactic center (i.e., within a radius of about 40 arc min), large and highly organized radio *filaments* or 'arcs' are found (Yusef-Zadeh et al., 1984; Yusef-Zadeh & Wardle, 1993; Tsuboi et al., 1995). The radio emission shows that the nonthermal emitting gas is arranged along magnetic filaments (poloidal component). The magnetic field lines are *parallel* to the long axis of the vertical filaments, and perpendicular to the circumnuclear disk, with a strength of order 1 mG (i.e., 1000 μGauss). Morris (1996) argued that the magnetic field of about 1000 μGauss cannot be localized to the filaments unless it can be confined by external pressure, and prefers a model where the filamentary structure is caused by a locally intermittent population of relativistic electrons in a *large* volume filled with a strong magnetic field.

An alternative model for the filaments is that the magnetic field is localized near the filaments over a *small* volume of space, and B is negligible outside. Uchida & Güsten (1995) have also studied several molecular clouds within 100 pc of the Galactic center, using the Zeeman effect in the OH line. They put an upper limit (rms) of 100 μGauss (outside of the filaments). They then argue that the magnetized filaments are lo calized and contained in bundles of magnetic fields over a small volume of space, and that the rest of the volume is at best pervaded by a diffuse magnetic field below 100 μGauss within 100 pc of the galactic center. A third model is where the filaments lie in a compressed, cylindrical ring surrouunding the galactic center over a *small* volume of space (e.g., Davidson 1996). Future trends: Clearly more data, not more theories, are most needed at this point, to find out if strong B values are found in a large or a small volume of space.

A similar magnetized filament or giant lobe has been discovered in the nucleus of the galaxy M 81, using the Very Large Array in New Mexico to observe the Stokes parameter at wavelengths of 6 cm and 20 cm. Kaufman et al. (1996) found a highly polarized non-thermal arc with a length of about 1 kpc and a width of about 0.2 kpc, located about 0.8 kpc northeast of the galactic center. Its minimum-energy magnetic field strength is 10-20 μGauss, and the magnetic field lines are aligned along the arc, It may be a large scale version of the filament or giant lobe found in our Milky Way galaxy.

Within 3 pc of the galactic center, there is a 2'-diameter circumstellar molecular ring around the center of the galaxy. Using Far IR dust polarimetry, Hildebrand et al. (1990; 1993) have found a magnetic field running *along* the circular ring, or at some small angle, drawn in the azimuthal/toroidal direction by differential rotation. HI Zeeman observations of this 2' ring have given conflicting results: less than 500 μGauss in both the South and North parts (Marshall et al., 1995); less than 1500 μGauss in the S but 500 μGauss in the N (Schwarz & Lasenby, 1990); ~ 600 μGauss in the N (Plante et al., 1995), ~ 2000 μGauss in maser spots (Yusef-Zadeh et al., 1996). In addition, some infalling gas (ionized streamers) seen near the N part of the circumnuclear ring has a magnetic field strength ~ 3 mGauss (Plante et al., 1995).

Within 1 pc of the galactic center, there is a 0.5' *mini-spiral* of gas with several arms, close to Sagittarius A*. Upper limits of 8 mGauss have been put on the magnetic field strength in the mini-spiral's northern area (e.g., Roberts & Goss 1993; Roberts et al. 1991). For a recent review of the galactic center environment, see Morris & Serabyn (1996).

3. THE MILKY WAY AS A WHOLE

3.1. Magnetic fields and Interstellar Superbubbles

In addition to the large-scale (regular and random) components of the galactic magnetic field, there are *localized deviations* (or detours) of the magnetic field, occasioned by interstellar magnetized superbubbles around OB associations and supernovae, with typical superbubble diameters of ≈ 200 - 250 pc.

Figure 6 shows the local deviations of the regular large scale magnetic field lines due to the presence of local superbubbles with a known supershell magnetic field.

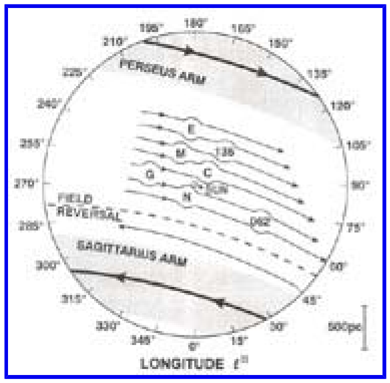

Figure 6. Face-on view of the local area of the Milky Way disk, showing the nearby superbubbles with a detected shell magnetic field. Arrows show the direction of the local galactic magnetic field lines. The expansion of the superbubbles caused local deviations or detours of the regular component of the galactic magnetic field. Two nearby spiral arms of stars are shown (Perseus arm, Sagittarius arm). The Sun's location is shown (circled dot). The location of the nearest magnetic field reversal is shown (dashes). See Vallée (1996) for more details.

The pioneering theories of galactic dynamos were made by Parker, 1971a; Parker, 1971b; Parker, 1973; Parker, 1976, Parker, 1979, and by others since (e.g., Ruzmaikin et al. 1985; Ruzmaikin et al. 1988). These early theories proved exciting and of great potential. They already could explain many diverse features in the Milky Way (e.g., Vallée 1991b).

Large interstellar magnetic bubbles are becoming *necessary* ingredients in the theories of galactic dynamos. More recent theories of galactic dynamos use cosmic-ray-driven dynamos (e.g., Parker 1992). Cosmic-ray-driven dynamos are dynamos powered by cosmic rays which originate in fast stellar winds of O-type stars inside interstellar bubbles, and in exploding supernovae (inside or outside interstellar bubbles).

The observations of the properties of large interstellar magnetic bubbles are compatible with the recent predictions of galactic dynamos (Vallée, 1993e), notably the mean shell magnetic field strength, the mean $k = 1$ exponent in the shell, and the mean shell expansion speed.

Zweibel (1996) also studied large scale fluctuations of the magnetic fields for the equilibrium and stability of the interstellar medium. The local magnetic field direction within 1000 pc was found some 30 years ago to differ according to the method used, and that difference was elucidated first by Vallée (1973) and Vallée and Kronberg (1973) as being almost entirely due to the effect of the nearby North Polar Spur a.k.a. Loop I. Others since, notably Heiles (1996a), have confirmed the strong effect of Loop I. Simonetti and Cordes (1986) and Simonetti et al. (1984) have studied enhanced magnetic turbulences along lines of sight going through various superbubbles. The HI shell is outside the synchrotron shell in Loop I (Heiles et al., 1980), both contributing to the rotation measure.

3.2. Magnetic fields and Spiral Arms (~ 15 kpc)

A quick survey of the literature from 1980 to 1995 shows the following: Of a dozen papers found on this subject, about 75% derived a spiral-type Milky Way with 4 spiral arms, and about 25% derived a spiral-type Milky Way with 2 spiral arms.

There is substantial non-thermal polarized emission from synchrotron radiating relativistic electrons trapped in the general interstellar magnetic field threading all spiral galaxies. Can the large scale magnetic field cross spiral arms in our Galaxy ? An early study of four nearby spiral arms suggested that the median pitch angle of the stellar arms (from O-type stars, and from HII regions there) was around 16° (rms = 6°), and the median pitch angle of the magnetic field lines in these arms (from quasars RM and radio galaxies RM, and from pulsars RM) was around 10° (rms = 6°) away inward from the circular tangent (e.g., Vallée 1988b). Both the magnetic field lines and the stellar arms follow a very similar spiral shape. Recent optical observations of nearby galaxies show that the magnetic field lines follow broadly the spiral arms, althought not exactly everywhere, such as in NGC1808 (Scarrott et al., 1993). Thus the determination of the magnetic field lines and directions should also give a determination of the spiral arms.

Many studies use *only one type of spiral tracers*. One such one-tracer study, by Beuermann et al. (1985), uses the galactic radio synchrotron emission at 408 MHz, with a spiral structure (4 arms, arm pitch angle taken as 13°). Another such one-tracer study, by Heiles (1996a), proposed a two-dimensional model of the stellar optical polarization data (data from stars not far from the sun), excluding stellar data in many regions (North Polar Spur; stars toward the galactic interior; Perseus and Taurus regions of star formation), and concluded that in the local neighbourhood of the sun the pitch angle was around -7° ± 4°. There are *different bias* in different spiral tracers.

A more recent study using *all types of spiral tracers* in the Milky Way (such as the dust, molecular gas, atomic gas, ionized gas, synchrotron gas, stars, and magnetic field), and weighting each result according to each tracer's limitations, found that the available evidence over the last 15 years indicated a mean spiral arm pitch angle of -12° ± 1° (radially inward), and that there are 4 main spiral arms (Vallée, 1995c).

Figure 7 shows the most likely locations of the spiral arms in the Milky Way, according to several different observational tests. The direction of the magnetic field lines is likely to follow the spiral arms, to a good approximation. The Sun is located in the local 'Orion spur', about halfway between the Perseus arm and the Sagittarius arm. A 12° pitch angle has been used (inward, starting from the circumference).

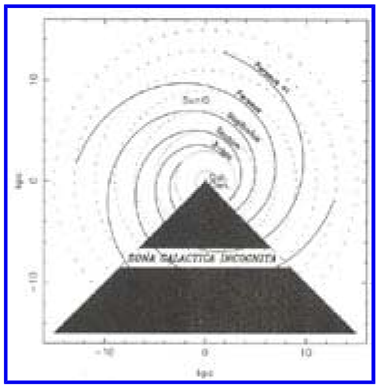

Figure 7. Face-on sketch of the Milky Way, showing 4 spiral arms drawn in logarithmic shapes. The pitch angle (12° inward) is obtained from a variety of different observational tests. Here all 4 arms start at a minimum r_g = 3 kpc from the galactic center. Circular orbits around the galactic center are shown by dots at galactic radii r_g = 1, 3, 5,..., 15 kpc. The position of the Sun at r_g = 8 kpc is shown (circled dot) - the Sun is located in a local Orion spur (not shown). Little or nothing is known of the area behind the Galactic Center refered to here as our modern-times "Zona Galactica Incognita". See Vallée (1995c) for more details.

Historically, the observational search for the magnetic field strength and direction in and between various spiral arms in the Milky Way has progressed slowly, starting in 1949 via polarized dust observations at optical wavelengths. In more recent times, the most useful data are obtained at radio wavelengths, via Faraday rotation measure (RM) values (e.g., a review is given in Vallée 1983d).

3.3. Distribution of B_{reg}, with galactic radius

The use of synchrotron radiation is often employed to get the total magnetic field strength. The average 'equipartition'-derived magnetic field strength follows from the assumption of energy-density equipartition between cosmic-ray particles and magnetic fields, the assumption or knowledge of the ratio between cosmic-ray electrons and protons (and its variation with particle energy), the synchrotron spectral index α, the extent of the radio emission along the line of sight, and the volume filling factor. Still, large uncertainties in these factors lead to only *moderate* errors in the total magnetic field strengths (e.g., Beck 1996; Heiles 1996b; Fitt & Alexander 1993).

The use of the Faraday rotation is often employed to get the uniform component of the magnetic field strength. The average 'Faraday'- derived magnetic field component follows from the assumption or knowledge of the density distribution of the thermal (non-synchrotron) electrons in the Galaxy. Since pulsars are often near the galactic plane, their emitted light often travels through the spiral arms. A distribution model for thermal electrons is thus used to analyse pulsar dispersion measures DM and pulsar rotation measures RM. The recent model of Taylor and Cordes (1993) for the distribution of thermal electrons in the galactic disk, employing 4 spiral arms, has been often employed, and its accuracy has been confirmed by Weisberg et al. (1995), and very slightly modified by Heiles et al. (1996) in the innermost areas. The use of this model allows small distance errors to pulsars, with a relative random error $\Delta r / r = 0.20$ (e.g., Fig. 7 in Taylor and Cordes 1993). In this case, after looking through 4 spiral arms, one has an error $\Delta r = 0.2 \times 4$ arm widths = 0.8 arm, enabling a proper study to be done all the way to the region of the galactic center (e.g., Vallée 1996b).

3.3.1. *Direction of B_{reg}*

The local galactic magnetic field near the Sun at galactic radius r_g = 8 kpc points toward $l \approx 80° \pm 15°$, i.e., clockwise as seen from the North Galactic Pole, and with the regular component strength $\approx 2\ \mu$gauss. There is a somewhat larger random component, as derived from radio RM observations of QSOs and galaxies (first reported in Fig. 1 of Morris & Berge, 1964; confirmed later in Fig. 3 of Gardner et al., 1969).

In the Scutum arm, the first detection of an excess rotation measure of $\approx$ 75 radians/m^2 was found, and the magnetic field was found to be directed clockwise as viewed from the north pole of our Galaxy (Fig. 1 in Vallée et al., 1988b).

In the Perseus arm, the first detection of an excess rotation measure of $\approx$ 30 radians/m^2 was found (Fig. 2 in Vallée, 1983d), with the magnetic field directed clockwise as viewed from the north pole of our Galaxy.

Averaging over three spiral arms in our Galaxy (Sagittarius, Perseus, Scutum) plus the Orion spur, one finds a mean arm rotation measure of ≈ 85 radians/m^2 (e.g., Table 1 in Vallée 1984b), corresponding to a uniform component of 3 μGauss for the magnetic field.

Going radially inward toward the Galactic center, one encounters a *first magnetic field reversal* near r_g = 7 kpc - the magnetic field direction at r_g < 7 kpc goes counterclockwise as seen from the North Galactic Pole, as obtained by radio RM observations of QSO and galaxies (first reported in Fig. 3 in Simard-Normandin & Kronberg, 1979), and confirmed one year later by radio RM observations of pulsars in the Milky Way (reported in Fig. 5 in Thomson and Nelson, 1980). More pulsar data re-confirmed this first magnetic field reversal (Rand & Kulkarni, 1990). RM analysis of pulsar data have generally confirmed the RM analysis of QSO and galaxies data (e.g., Rand, 1994).

Continuing radially inward toward the Galactic center, a *second magnetic field reversal* is observed near the Scutum arm at r_g = 5.5 kpc - the magnetic field direction at r_g < 5.5 kpc goes clockwise as seen from the North Galactic Pole, as obtained by radio RM observations of QSO and galaxies (first reported in Fig. 1 of Vallée et al., 1988b), and confirmed 6 years later by radio RM observations of pulsars in the Milky Way (reported in Fig. 5 of Rand & Lyne, 1994).

Going radially outward toward the galactic anticenter, *no magnetic field reversal* is encountered in the Perseus arm and "Perseus + I" arm at r_g > 10 kpc - the magnetic field there follows the clockwise direction as seen from the North Galactic Pole, with a strength of ~ 2 μGauss near the Perseus arm obtained by radio RM observations of QSO and galaxies (first reported in Fig. 2 of Vallée, 1983d; see also Vallée 1983c), and confirmed by radio RM observations of pulsars in the Milky Way (e.g., Fig. 3 in Lyne & Smith 1989). The lack of any radial reversal of the magnetic field in the outer Galaxy has been suggested by Simard-Normandin & Kronberg (1980), from early RM data.

Clegg et al. (1992) obtained the Rotation Measures of 56 sources in a selected part of the sky, mostly bounded by 45° < l < 93° and -5° < b < + 5° . The small RM increase in their Fig. 9 for the pulsar data near a distance of 4 kpc from the sun is *localized* to a small angular distance in longitude (between 70° and 90°), to a small radial distance range (between 4 and 5 kpc from the sun), and to a small angular area in latitude (between -10° and +10°) since it is not seen in the RM of quasars well above and well below the galactic plane. This resembles the effects of a *local* interstellar magnetic superbubble/shell there (not the effect of a large scale spiral arm magnetic field - i.e., Feature D in their Fig. 12 could be a superbubble). Thus the reality of a more distant large-scale magnetic field reversal is in doubt. Fig. 6d in Rand & Lyne (1994) corroborates Fig. 9 in Clegg et al. (1992), in showing a *localized*, not a large-scale, feature D. Clegg et al. (1992) also showed a large negative RM for extragalactic sources near l = 70° and l = 88° (their Fig. 9), which indicate a large scale magnetic field going away from the sun at > 20 kpc (not plotted in their Fig. 12 beyond Feature D, at > 20 kpc).

The combined effects of weaker, more distant superbubbles will average out, and only the effects from the most nearby superbubbles will stand out in the RM sky distribution.

3.3.2. *Location of zero B_{reg}*

Where does the magnetic field reverse, i.e., where can one find the field strength $B_{\rm reg}$ close to zero ? The radio observations of synchrotron emission (~ $B_{\rm tot}$) from nearby spiral galaxies at radio frequencies (100 MHz to 1 GHz, say) show a stronger radio emission *within* the arms, than in the interarm regions (e.g., Fig. 4 in Segalovitz 1977). Thus $B_{\rm tot}$ is maximum within the spiral arms.

The thermal electron density is observed to be strongest *within* the spiral arms, not in the interarm regions (e.g., Fig. 4 in Taylor & Cordes 1993). For thermal densities n > 100 cm^{-3}, the observed magnetic field is tied to the observed thermal electron density by the statistical relation $B_{\rm tot} \sim n^{0.5}$, supported by many observations (e.g., Troland and Heiles 1986; Heiles 1987; Fig. 4 in Vallée 1990b; Fig. 1 here), and both $B_{\rm tot}$ and n are thus found to be strongest in the spiral arms.

In nearby spiral galaxies, $B_{\rm reg}$ is highly tangled in the arms (yielding a low degree of polarization there), and $B_{\rm reg}$ is strongest in the interarm regions (yielding B lines parallel to the optical arms, yet offset by a distance from the arms) (e.g., Beck 1991a; Beck 1991b).

The observed magnetic field reversal $B_{\rm reg}$ nearest to the Sun occurs about 600 pc radially inwards toward the galactic center (e.g., Fig. 5 in Thomson & Nelson 1980; Fig. 6 here). This field reversal occurs at a location within an *interarm* region (about halfway between the Sagittarius arm and the Perseus arm). This large-scale magnetic field reversal near r_g = 7.5 kpc has been observed through the RM data from QSOs and galaxies, as well as from the RM data of pulsars - it is not limited to the local Orion spur in which the Sun is placed.

Also in the Milky Way, the second nearest observed magnetic field reversal occurs near r_g = 5.5 kpc (with the Sun at r_g = 8.0 kpc), i.e., located about 2.5 kpc from the Sun toward the galactic center (e.g., Fig. 1 of Vallée et al. 1988b; Fig. 5 of Rand and Lyne 1994; Fig. 9 here). This magnetic field reversal also occurs *within an interarm* region, about halfway *between* the Scutum arm and the Sagittarius arm (e.g., not within a spiral arm). This large scale magnetic field reversal has been observed through the RM data of QSO and galaxies, and independently from the RM data of pulsars.

Table 2 summarizes what we know and when we first detected the various orientations of the magnetic field in the Milky Way. In our Milky Way, the regular galactic magnetic field seems to follow the spiral arms, and to have the axisymmetric magnetic field shape $m_{\rm azim}$ = 0. Between galactic radii 5.5 and 7.5 kpc from the galactic center, the regular magnetic field reverses in direction (going anticlockwise) compared to the rest of the Galaxy (where it goes clockwise). Future trends: more observations are needed in the Perseus + II spiral arm, and more external spiral arms, to test more possible magnetic field reversals, as well as toward the center of the Galaxy (from the Galactic center up to the Scutum spiral arm).

Table 2: Chronology of observational mapping of the magnetism in the Milky Way

Object	B	Method	Discocerer(s) and Date	Telescope used
General:				
ISM Dust	-	Opt. stars	Hiltner (1949)	McDonald-82"
"	-	Opt. stars	Hall (1949)	Wash.-40"
Thermal electr.	-	QSO RM	Gardner and Whiteoak (1963)	Parkes-64m
Crab Neb.	-	Radio Polar	Mayer et al. (1962)	NRL-50'
Orion spur	3 μG	Synchr. RM	Muller et al. (1963)	Dwingeloo-25m
Spiral Arms:				
Sagittanus arm	5 μG	QSO RM	Simard-N. and Kronberg (1979)	Green Bank-2km
"		pulsars	Thompson and Nelson (1980)	re-analysis
Perseus arm	2.5 μG	QSO RM	Vallée (1983d)	Algonquin-46m
"		pulsars	Lyne and Smith (1989)	re-analysis
Scutum arm	4 μG	QSO RM	Vallée et al. (1988b)	Alg.46m; VLA-27km
"		pulsars	Rand and Lyne(1994)	Jodrell-76m
Superbubbles:				
Loop I bubble	6 μG	QSO RM	Garduer et al. (1969)	Parkes-64m
"	-	QSO RM	Vallée and Kronberg (1973)	Algouquin-46m
Cetus Arc	17 μG	QSO RM	Simard-N. and Kronberg (1979)	Green Bank-2km
Eridanus shell	8 μG	Hl Zeeman	Troland and Heiles (1982)	Hat Creek-26m
Gum Nebula	2 μG	QSO RM	Vallée and Bignell (1983)	Alg.46m; VLA-27km
Monogem Ring	4 μG	QSO RM	Vallée et al. (1984)	Alg.46m, VLA-27km
G135-40-10	11 μG	Hl Zeeman	Heiles (1989)	Hat Creek-26m
GO62-23+13	10 μG	Hl Zeeman	Heiles (1989)	Hat Creek-26m
Feature D	-	pulsar RM	Clegg et al. (1992)	VLA-27km

N.B.: See Vallée (1993d) for *B* field values in superbubbles; see Vallée (1996) for *B* field values in spiral arms.

The dynamo theories show that the location of a magnetic field reversal ($B_{\rm reg} = 0$) can *move* slowly in radial direction with time (e.g., Fig. 1a-1f in Beck et al. 1994; Fig. 4a in Poezd et al. 1993).

3.3.3. *Strength of B_{reg}*

How strong is the galactic magnetic field, and how does it change with increasing galactic radius ? Observations of $B(r)$ already exist, and can be compared with magnetic field models. The observational data from the radio RM observations of QSO and galaxies (e.g., Vallée 1991b) and those from the RM observations of pulsars (e.g., Rand & Lyne 1994) show a non-periodic, non-cosine variation of $B(r)$ with radius, between 5 and 10 kpc.

Figure 8 here shows the run of $B(r)$ versus the galactic radius. The radio RM observations are shown by open squares (from QSO & galaxies) and stars (from pulsars). The dynamo theories adapted to the Milky Way (e.g., Fig. 4a in Poezd et al. 1993) confirm a non-periodic variation of $B(r)$ with radius, similar to the observations. As can be seen, there is a clear agreement from the two sets of data (QSO and pulsars). Rand (1994) has shown that RM analysis of pulsar data have confirmed well (but later on) many of the results of the RM analyses of QSO and galaxies data. There have been recent claims that the pulsar RM data are not the best indicator for the large-scale galactic magnetic field (Heiles, 1996b; Heiles, 1995).

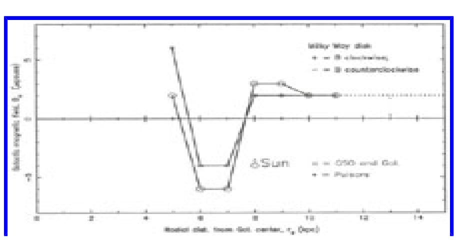

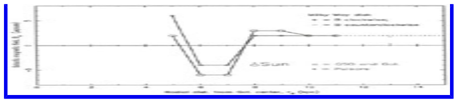

Figure 8. The run of $B_u(r)$, the uniform component of the galactic magnetic field, as a function of the galactic radius r_{gal}, in the Milky Way. The Sun is shown at r_{gal} = 8 kpc. Open circles: B from RM of quasars and galaxies (from Vallée, 1991b). Stars: B from RM of pulsars (from Rand & Lyne, 1994).

Recent claims were made by Nelson (1988), Battaner et al. (1992), Battaner (1993), and Binney (1992) that there exists a strong magnetic field which could speed up the interstellar gas (but not the stars), to the point of reproducing the flat curve of rotational velocity against galactic radius. These claims were investigated and found unsupportable. Observationally, Vallée (1994c) found that in the Milky Way (and in M31) the required magnetic field strength for magnetic support of the gas was too high by at least a factor 2, as compared to the weaker observed magnetic field strengths. Also, when the newly-born stars have formed from the interstellar gas and clouds (moving at 260 km/s), they will magnetically decouple from the interstellar medium and clouds, and will behave balistically with their initial input velocities (= cloud velocities). These initial balistic velocities of newly-formed stars (about 260 km/s) are thus much higher than those of the older stars (alleged to be moving at 160 km/s, following a Keplerian curve). Such a 100 km/s deceleration has not been properly worked out, via stellar encounters on a short time scale or otherwise, in the magnetic-support theory. Other investigators also found problems for the magnetic-support theory, as pointed out by Melrose (1995), Katz (1994), and Jokipii & Levy (1993).

Figure 9 shows the directions of the regular magnetic field over the Milky Way. For simplicity, the magnetic field deviations due to the superbubbles have been omitted.

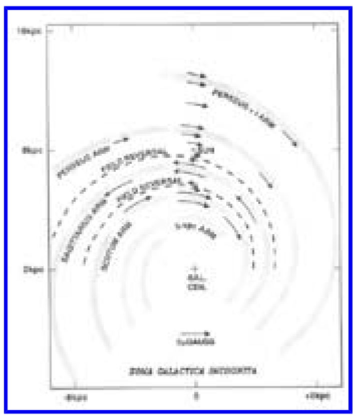

Figure 9. Face-on view of the whole area of the Milky Way disk. Arrows show the direction of the galactic magnetic field lines. For simplicity, the nearby superbubbles have been omitted. Four spiral arms of stars are shown. The Sun is shown (circled dot). Going radially inward from the Sun to the Galactic Centre, one encompasses two magnetic field reversals (shown with dashes). Little or nothing is known of the area behind the Galactic Center ("Zona Galactica Incognita"). See Vallée (1996) for more details.

3.4. Distribution of B_{ran}, and strength

Ohno & Shibata (1993) have studied the random component of the galactic magnetic field, using pairs of pulsar RM seen in almost the same directions in the sky. They found that $B_{ran} \approx 5$ μGauss, within cell sizes $\approx$ 50 pc.

Equipartition has occured, and the total magnetic energy density in the interstellar medium is now roughly equal to the energy densities found in other components of the interstellar medium (interstellar turbulence; cosmic rays; thermal pressure of a hot medium).

3.5. Larger scale view - ASS or BSS

Large-scale magnetic field orientations in the disk a spiral galaxy can follow either an AxiSymmetric (ASS) shape or a BiSymmetric (BSS) shape, or a mixture of both with a preponderance of one of the two shapes. If one travels along a 360° circle at a constant radius from the galactic center, an ASS magnetic field points in the same direction (clockwise and inward for 360°, say), while a BSS magnetic field points in one direction in half of the circular orbit (clockwise and inward for 180°, say) then points in the opposite direction in the second half of the orbit (counterclockwise and outward for 180°, say) - (e.g., Fig. 1 in Vallée 1992).

Figure 10 shows the two main shapes observed for the distribution of the global magnetic field lines. Each arrow indicates the local direction of the global magnetic field, following the prediction of theoretical models at each map point (e.g., Fig. 5 in Ruzmaikin et al. 1988; Fig. 1 in Moss 1995). In actuality, the magnetic field lines are continuous, going inward or outward all the way from or to the proximity of the galactic center (there are no magnetic monopoles).

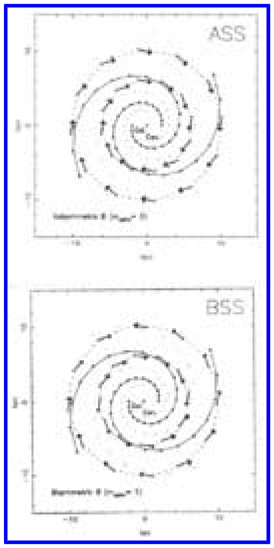

Figure 10. Two sketches show the global magnetic field lines (arrows) as observed in nearby spiral galaxies, along two concentric circles (dashes) aroud the galactic nucleus. Two spiral arms of stars are shown (continuous curves with stars). The spiral-type loci of the middle interarm areas ars shown (dots). (a) ASS magnetic field shape. (b) BSS magnetic field shape.

3.5.1. *ASS for the Milky Way*

Observations show that the large scale magnetic field in the Milky Way can be matched by predictions of the turbulent dynamo theory. The dynamo theory predicts, in cylindrical coordinates, an *azimuthal mode* m_{azim} predominantly of an axisymmetric shape ($m_{\mathrm{azim}} = 0$), a *radial mode* n that ensures a few reversals (n = 0, 1, 2) of the azimuthal mode with increasing galactic radius, and a vertical mode p (perpendicular to the galactic disk) with the magnetic field structure being symmetric above and below the galactic plane ($p = 0$). The limited knowledge of the radial gravitational potential of the Milky Way can theoretically allow two or three magnetic field reversals with galactic radius, and 2 are observed (Vallée, 1991b).

As viewed from the top of the Galaxy (North Galactic Pole), the magnetic field lines run clockwise near the Sun (r_{gal} = 8 kpc), near the Perseus arm (r_{gal} = 10 kpc), and near the Scutum arm (near r_{gal} = 5.5 kpc), but they run counterclockwise near the Sagittarius arm (near r_{gal} = 6.5 kpc). Going out from the galactic nucleus, a total of 2 magnetic field reversals have thus been seen, near r_{g} of 5.5 kpc and 7.5 kpc.

When it comes to the magnetic field in the Milky Way galaxy, our position in the Milky Way's galactic disk hinders our attempts at interpreting the observational data. Some recent papers have attempted to fit magnetic field models to spiral galaxies, and in particular to the Milky Way galaxy. *Magnetic field reversals* in the Milky Way are crucial to all interpretations, be they axisymmetric (ASS) or bisymmetric (BSS) global magnetic field models. Only a few magnetic field reversals can be found in ASS models, but 4 or more radial field reversals can only be found in tightly-wound BSS models.

Magnetic field observations in the Milky Way have already been fitted to an ASS model with a few radial reversals (Fig. 3 in Vallée, 1991b; Fig. 4a in Poezd et al., 1993). Dynamo theories already predict an ASS magnetic field model with 2 or 3 radial reversals (e.g., Fig. 1f in Beck et al. 1994a; Fig. 4a in Poezd et al. 1993; Fig. 5 in Ruzmaikin et al. 1985). Thus there is no need for a BSS model a priori for the Milky Way.

Statistics of the observed magnetic fields in a dozen nearby spiral galaxies indicate a net preference for the ASS model (about 3/5, including the Milky Way galaxy), a minority of cases with the BSS mode (about 2/5 of cases), and no galaxy with a quadrisymmetric spiral magnetic field QSS mode (e.g., Wielebinski & Krause 1993; Vallée 1994a).

3.5.2. Pitfalls of the BSS model

The *bisymmetric* magnetic field models as applied to the pulsar RM data and to the QSO and galaxies data have many problems in trying to explain the Milky Way galaxy. These are due to the many pitfalls in model fitting the magnetic field reversals observed in the Milky Way (e.g., Vallée 1996b; Sofue & Fujimoto 1983). The magnetic field strength does not go to zero in a spiral arm, as predicted there. Magnetic field reversals in BSS models are numerous but are not periodic. Magnetic field reversals are not due to the twisting of a primordial extragalactic magnetic field. Magnetic field reversals cannot be masked effectively by local interstellar magnetized shells. The prediction of a large number ($N \gg 4$) of magnetic field reversals by the bisymmetric magnetic field models, for spiral arms with pitch angles < 20°, is incompatible with the observations in the Milky Way of at most a small number ($N \leq 3$) of magnetic field reversals. Thus the strength and sense of the magnetic field with galactic radius (Fig. 8) show that bisymmetric magnetic field models are less suitable to explain the RM data in the Milky Way (e.g., Vallée

1996b).

3.6. Seeds of galactic magnetism

A few possible seeds for galactic magnetism have been proposed, from primordial cosmological origins to recent local origins.

3.6.1. *Primordial cosmological magnetic seeds in galaxies*

The original strength of such a primordial cosmical magnetic field is unknown, but weak. No observational evidence has been found for an uniform primordial field in intergalactic space (e.g., a review in Vallée 1990b), with upper limits of 10^{-10} gauss being set. This primordial hypothesis has already been shown elsewhere to be difficult, because the primordial magnetic field may diffuse out of the disk through the halo and out into the intergalactic medium. This diffusion arises on a short time scale (~ 10^8 yrs), shorter than the time scale of the galaxy (Parker, 1971; Parker, 1976), or not quite that short (e.g., Kulsrud and Howard 1997).

Ratra (1992) has argued for a very weak cosmological seed magnetic field, originating in quantum mechanical irregularities at an early epoch. The following rapid expansion of the Universe during the *inflation* era would stretch this early magnetic seed to reach between 10^{-60} Gauss and 10^{-10} Gauss nowadays over a length scale of ~ 20 Mpc (i.e., typical of a supercluster of galaxies).

The initial amplification of such a primordial seed is under debate: inflation, gravitation, and/or dynamo are proposed. Zweibel (1993) showed a picture with a primordial magnetic field being wound up by a rotating galaxy: "This winding up of the field into a bisymmetric spiral leads to reversals in direction on progressively smaller scales over time..." (p.591). Twisting and amplification of this primordial magnetic field, by galactic differential rotation under *gravitational forces*, is thought to produce a bisymmetric magnetic field distribution. This may not be the only way to produce a bisymmetric distribution.

In complex dynamo models, a weak primordial magnetic field may be necessary (e.g., Kulsrud & Anderson 1992) or may not be necessary (e.g., Field 1995) in the galactic disk. This area of research is being pursued with vigor.

3.6.2. *Battery origin for magnetic seeds in galaxies*

The original strength of such a battery-type magnetic seed is very small. In a moving ionized gas, there are thermal and inertial battery effects, capable of creating a weak magnetic field - this is now referred to as the Biermann battery (e.g., Biermann 1950; Kempt 1982). Battery effects in a protogalaxy could create a seed protogalactic magnetic field B ~ 10 - 20 Gauss.

The initial amplification of such a battery-type seed field is under debate: gravitational collapse, strong flows, or dynamos. In one model, the seed field of $\approx 10^{-20}$ Gauss could then be enhanced by a factor ~ 10^4 due to galactic collapse under gravitational forces, and it could be subsequently amplified by a factor ~ 10^8 in strong non-axisymmetric flows from bars and spirals (e.g., Lesch & Chiba 1995). Dynamo amplification would then follow. Unfortunately, these very weak magnetic fields are difficult to amplify and to order by a dynamo *alone* over a time scale ~ 10^8 years (e.g., Kulsrud and Anderson, 1992; Balbus, 1993).

Battery effects around a central massive black hole (~ 10^6 $M_\odot$) in the galactic center could also create a seed field by the rotation of an aspherical cloud of ionized gas. It is envisioned to be transported out to the galactic disk by jets, twin outflows, slow winds (e.g., Chakrabarti et al. 1994; Daly & Loeb 1990; Akasofu & Hakamada 1982). This magnetic field transport in the galactic disk could have occurred in an initial burst a long time ago, but would be unlikely to occur routinely now under current galactic disk conditions. For ejection along the galactic plane, radial *resistance* may be encountered in the spiral arms and the denser parts of the interstellar medium, stopping the ejections from the galactic nucleus at a radius r_{stop}. Within the distance r_{stop}, any previously ordered magnetic field distribution will be removed (e.g., Vallée 1982a). Beyond the distance r_{stop}, cosmic-ray particles may not move rapidly across pre-existing horizontal, azimuthal magnetic field lines, possibly drawn there by differential rotation (e.g., Vallée 1995a).

3.6.3. *Recent local origins for the magnetic seeds in galaxies*

Many chaotic magnetic fields are ejected by supernovae and by the stellar winds of young stars. These local stellar seed fields are plausibly created at various times within a galaxy by cosmic rays and/or interstellar turbulence (e.g., Poezd et al. 1993). They may be the best to create the real galactic seed fields. The original strengths of such stellar-ejected fields is under debate. Stellar magnetic fields are generated first, then deposited into the interstellar medium by stellar winds and supernovae, yielding a local magnetic field strength $\approx 10^{-9}$ Gauss.

The initial amplification of such stellar-ejected magnetic fields is under debate: interstellar turbulences, dynamos, or both. Stellar-ejected fields in turn can be amplified by the random motions of the interstellar turbulence, over a time scale of 10^7 years and a linear scale of 100 pc. The galactic dynamo would then easily and quickly amplify this seed field to the current values near a few μGauss.

3.7. Galactic Magnetic field Interpretations - dynamos or not ?

While the results of polarization observations are secure, repeatable, and do not vary with time, their interpretation has evolved for the better with time.

In the late 1970s, an interpretation in terms of *magnetic control* of gas and stellar systems by strong helicoidal magnetic fields was fashionable (e.g., Piddington 1981a; Piddington 1981b). Large-scale magnetic fields in this theory would be the result of twisting of a *primordial* cosmological universal magnetic field, in some ways (a gravitationnally contracting protogalaxy amplifies it by 2000; differential rotations in a galactic lifetime amplifies it by 30 (e.g. Beck et al. 1996). Strong magnetic fields used to be invoked only when there was a gap in our knowledge, rather like a strong 'magnetic field of the gaps' (Kahn and Brett, 1993). More data have been acquired since, revealing a weak galactic magnetic field, and an upper limit to a much weaker cosmological universal magnetic field.

In the late 1980s, an interpretation in terms of *galactic dynamos* (e.g., Parker 1976; Parker 1992) with weak azimuthal magnetic fields was preferred by most. The magnetic field structures 'preferred' by dynamo theory usually correspond to the most unstable linear eigenmodes of the system. Still, One can find occasionally a strong 'magnetic control' model in the litterature (e.g., Battaner & Florido 1995; Sánchez-Salcedo, 1996), despite the problem that the large magnetic field strength required would unacceptably expand the HI disk vertically (e.g., Melrose 1995).

In the 1990s, 'galactic dynamos' are currently preferred by most, but some authors have questioned its long-term ability and sustainability (see Sect. 3.7.2), and some others have proposed a non-dynamo theory of '*galactic fountains*' based on MHD winds driven by cosmic rays (e.g., Kahn and Brett 1993; Kahn 1992; Zirakashvili et al. 1996).

3.7.1. *Basic Notions*

The subject of galactic dynamo theory is still in a state of flux. Here is a short description of the basics of galactic dynamos.

The basic impetus for galactic dynamos has been made by Parker (1971a; Parker (1971b), and by followers since. Dynamo theories predict a *large* predominance of the $m_{\mathrm{azim}} = 0$ shape for the galactic magnetic field, but the observations show only a small predominance of that shape (due to a non-negligible number of galaxies with $m_{\mathrm{azim}} = 1$). Why ?

Turbulent dynamo theories formulate the problem of the large-scale magnetic field in a spiral galaxy with the general equation (e.g., Parker 1971a; Parker 1971b, Ruzmaikin et al. 1985; Ruzmaikin et al. 1988; Rádler, 1995):

$$\frac{\partial B}{\partial t} = \nabla \times (\mathbf{V} \times B) + \nabla \times (\alpha B) + \beta \nabla^2 B$$

where ∂ signifies a partial differential operator, t is the time, B is the global magnetic field, $\mathbf{V}$ is the regular velocity field (mainly due to differential rotation as a function of radius), α is the mean helicity of interstellar turbulences, and β is the turbulent diffusivity which represents the effect of the small scale magnetic field on the mean magnetic field.

As mentioned briefly in Section 3.5.1, the usual simple solution of this equation is achieved by separating it into 3 components in cylindrical coordinates (r, ϕ, z), and then using the WKB asymptotic method for differential equations. For B_ϕ this gives a solution proportional to cos ($m_{\mathrm{azim}}\ \phi$ +...), where the azimuthal angle is ϕ and the azimuthal modes $m_{\mathrm{azim}} = 0, 1, 2,$.... For B_z this gives a dynamo-type equation with a spectrum of eigenvalues with the vertical modes $p = 0, 1, 2,$ .... For B_r this gives a Schrödinger-type equation for the function $Q(r)$ with the radial potential $\gamma(r)$, where B_ϕ and B_r are proportional to $Q(r)$, and where $Q(r)$ can be approximated by various cosine functions with the radial modes $n = 0, 1, 2,$ ... (e.g., Fig. 5 in Ruzmaikin et al. 1985). The quasi-stationary but small number of radial reversals ($n < 3$) and their positions are controlled by the radial profiles of some parameters: the galactic rotation velocity, the disk thickness, and the gas density (e.g., Poezd et al. 1993).

With many galactic physical and dynamical conditions, the preferred modes are: $m_{\mathrm{azim}} = 0$ (axisymmetric azimuthal magnetic field lines as one goes along a circle at a fixed radius) or $m_{\mathrm{azim}} = 1$ (bisymmetric) in that order; $p = 0$ (same direction of magnetic field lines as one goes from below to above the galactic plane); and $n = 0$ (no radial reversal of the magnetic field lines as one goes from the galactic center radially outward) or $n = 1$ (first radial magnetic field reversal) or $n = 2$ (second radial magnetic field reversal) in that order. Thus for the Milky Way we have $m = 0$, $p = 0$, $n = 0, 1, 2$, whereas for M31 we have $m = 0$, $p = 0$, $n = 0$ (Poezd et al., 1993; Vallée 1991b; Vallée, 1996). There is ample evidence for an even parity across the galactic plane ($p = 0$) for the Milky Way, for M31, and for NGC 253 (e.g., Beck et al. 1996).

3.7.2. *Future trends in Galactic Dynamos*

Some criticism of the current dynamo theories has been voiced (e.g., Kim et al. 1996; Subramanian 1995; Kulsrud & Anderson 1992; Schramlowski & Achtenberg 1993) over some aspects of dynamo theory. Will the galactic dynamos survive the test of time ? Supporters of the galactic dynamos have started to look more closely at persistent problems (e.g., Parker 1981; Parker 1987, Field 1995; Subramanian, 1998). This subject is currently in a state of intense scrutiny, and improvements are needed in many areas. More complete theoretical treatments can be found in Cattaneo and Vashtein (1991), Vainshtein and Cattaneo (1992), Kulsrud and Anderson (1992), Tao et al. (1993), Kim et al. (1996), among others. More details on recent dynamo theories are reviewed in Wielebinski & Krause (1993), Kronberg (1994), and Beck et al. (1996).

As stated above, any primordial magnetic field may diffuse out of the disk through the halo and out into the intergalactic medium on a short time scale (~ 10^8 yrs), perhaps shorter than the time scale of the galaxy (Parker, 1971; Parker, 1976), or perhaps not that short (e.g., Kulsrud and Howard 1997). In more complex dynamo models, a weak primordial magnetic field may be found (e.g., Kulsrud & Anderson 1992) or may not be found (e.g., Field 1995) in the galactic disk.

Current dynamo models cannot yet explain the presence of strong regular interarm magnetic fields (e.g., Moss 1996a). Dobler et al. (1996) studied dynamo systems in which the thickness of the galactic disk grows with time, becoming so large as to suppress the dynamo action. A theoretical study by Fan and Lou (1996), about the locations of magnetic arms with respect to the locations of the stellar arms, used fast MHD density waves to give a coincidence of magnetic arms with stellar arms in disks with differential rotation, and used slow MHD density waves to give magnetic arms interlaced with stellar arms.

More recent developments include *non-linear* terms, which take account of the back reaction of the magnetic field on the motions. The full non-linear dynamo problem requires the solution of a complex non-linear system of partial differential equations, which is still beyond the access of even the best computers (e.g., Schultz et al. 1994). The magnetic field strength of the dynamo eventually exceeds the equipartition magnetic field by about a factor 2 (Rüdiger et al., 1993). Cross-helicity dynamos are being explored (Yokoi, 1996).

Thus to obviate the long length of time needed to activate the dynamo. Parker (1992) and others have since suggested a cosmic-ray driven galactic dynamo, requiring only minor changes to the basic equations for galactic dynamos as used to date. This suggestion needs to be followed up with numerical calculations. This model would replace the 'slow-acting' mean field dynamo driven by interstellar turbulence over a time scale of 3×10^9 years or so (e.g., Equ. 9 in Lesch 1993). The cosmic-ray-driven dynamo would operate over a shorter time scale of 3×10^7 years (e.g., Parker 1992). Parker (1992) used cosmic rays going out of the galactic plane to inflate the magnetic field lines into loops (cosmic-ray driven dynamo), providing a natural way for rapid reconnection between opposite vertically oriented magnetic field lines. Near the center of a loop one can expect a stellar association with stellar winds and supernovae that would generate the cosmic rays. The importance of cosmic-ray-driven dynamos comes from the discovery of strong galactic magnetic fields in quasars at an earlier epoch, requiring the need to build up quickly the galactic magnetic field there (Perry et al., 1993).

An important but perhaps not quite the same type of cosmic-ray-driven dynamo is pursued by Ferriére (1993a), Ferriére (1993b), and Ferriére (1993c).

There is a bit of confusion since Parker (1992) refered to his cosmic-ray-driven dynamo as 'fast-acting' dynamo, yet the term 'fast-acting' has been used with another meaning elsewhere, namely 'a dynamo in which the magnetic field is amplified exponentially in the limit that the plasma resistivity goes to zero' (e.g., Childress, Gilbert, and Ott 1996).

Using a global smoothing, Han and Qiao (1994) suggested a S1 dynamo ($m_{azim} = 1$; $p = 0$) in the Milky Way, while Han et al. (1997) suggested an A0 dynamo ($m_{azim} = 0$; $p = 1$) in the Milky Way halo, inside the solar orbit. In both studies, they neglected the strong RM of nearby superbubbles ($\approx$ 90 rad./m^2) and the huge size of Loop I in HI (Heiles et al., 1980; Heiles, 1996a). In Figure 3 of Han et al. (1997), the pulsar RM does not increase with distance from the sun (above 1 kpc), and pulsar RM are not the best indicator of B (Heiles, 1996b).

4. NEARBY SPIRAL GALAXIES

A method to distinguish between ASS and BSS magnetic fields based on a small amount of data has been proposed by Sofue et al. (1985). Basically, the RM distribution seen along the major axis of the galaxy can be symmetric with respect to the galaxy nucleus for BSS fields, and antisymmetric for ASS fields. A second method to distinguish between ASS and BSS magnetic fields, by analysing the polarization position angle as a function of azimuth angle, has been proposed by Sokoloff et al. (1992).

A small majority of spiral galaxies hosts an ASS magnetic field pattern, while a sizeable minority of spiral galaxies has a BSS magnetic field pattern (e.g., Ruzmaikin et al. 1985). Five examples of a unique or a predominant ASS magnetic fields in galaxies are: IC342 (e.g., Krause et al. 1989a), M31 (e.g., Beck et al. 1989), NGC253 (e.g., Beck et al. 1994b), NGC6946 (e.g., Ehle and Beck, 1993), the Milky Way (e.g., Vallée 1991b; Vallée 1996). Examples of probable or possible BSS magnetic fields in galaxies are: M81 (e.g., Krause et al., 1989b), M33 (e.g., Buczilowski & Beck 1991), M51 (e.g., Neininger 1992; Berkhuijsen et al. 1997), M83 (e.g., Neininger et al., 1993), NGC2903 (e.g., Sofue et al., 1986). More examples of ASS and BSS magnetic fields can be found in the Tables 2 and 3 of the review by Beck et al. (1996).

4.1. Methodology - different methods to obtain the magnetic field strength

Most of the galaxies studied here are located nearby, well within 20 Mpc of the Milky Way. Many claims have been made to show that the magnetic field strength in late-type galaxies is close to the "equipartition magnetic field" value B_{eq}, but one recent claim (Chi and Wolfendale, 1993) suggested otherwise. Vallée (1995a) carried out a statistical study of the three methods often employed to give magnetic field strengths, namely (i) the Faraday rotation method, (ii) the Equipartition method, and (iii) the Cosmic-ray-particle method.

4.1.1. *Faraday Method*

A first method to determine the strength of a galactic magnetic field is through the linear polarization (Stokes Q and U) observations of the radio synchrotron emission from electrons trapped in the magnetic fields, with observations at several radio frequencies between 1 and 5 GHz. The observed Faraday rotation (ΔPA) of the position angle PA of the electric (E) vector of the radiation varies as the square of the wavelength λ of observation (ie: ΔPA ~ RM λ^2), where RM is the rotation measure which is proportional to the uniform component of the total magnetic field strength along the line of sight B_I , the thermal electron density n, and the path length L (i.e., RM ~ nB_IL). The fractional linear polarization of the radiation is a function of a beam depolarization (e.g., Equ. 6 and 7 in Ehle & Beck 1993) and of a wavelength-dependent Faraday dispersion measure (e.g., Equ. 11 in Ehle & Beck 1993), both occasioned by a random component of the total magnetic field. The total magnetic field strength B_{tot} is the quadratic sum of the random component B_{ran} and the uniform or regular component B_{reg} (often using $B_{reg} \approx 1.6\ B_I$). Here we call B_{fa} the results obtained by this Faraday method. More details on the derivation of B_{fa} can be found in Ehle & Beck (1993), Vallée (1980), and depolarization in Chi et al. (1997), etc.

4.1.2. *Equipartition Method*

A *second* method to determine the strength of a galactic magnetic field is through the total continuum (Stokes I) observation of the radio synchrotron flux density S_ν from relativistic electrons over the whole galactic disk of size Θ_{gal}, often made near a radio frequency between 1 and 3 GHz to cover the whole galaxy (i.e.,: $B_{tot} \sim S_\nu^{2/7}\ \Theta_{gal}^{-4/7}$). The equipartition assumption postulates equal energy densities in the magnetic field and in cosmic-ray particles, very close to that of minimum energy conditions in a synchrotron plasma. For an energy index of -1, minimum energy estimates are equal to equipartition estimates. Here we call B_{eq} the results obtained by this equipartition method. More details on the derivation of B_{eq} can be found in Fitt & Alexander (1993). Models showed that the equipartition assumption is likely to be fulfilled *eventually* in time, because galaxies are approaching a form of steady-state while remaining a dynamic system, through normal redistribution of energy by known interactions among magnetic fields and cosmic-ray particles. Thus some atypical galaxies may currently have values of B different to what equipartition would predict, althought they may later reach the equipartition value. The equipartition assumption avoids unrealistic conditions in galaxies (e.g., Duric 1990), and such unrealistic conditions are seldom observed in nearby galaxies.

4.1.3. *Cosmic-ray Method*

A *third* method to determine the galactic magnetic field strength is through the gamma-ray emission (2.5×10^{-5} Å) by collisions of cosmic-ray protons and cosmic-ray electrons with the interstellar matter, as well as collisions of cosmic-ray electrons with optical interstellar photons (inverse-Compton), or else through the x-ray emission (12 Å) by collisions of cosmic-ray electrons with infrared interstellar photons (inverse-Compton). The derivation of cosmic-ray particle densities K in starforming sites of size P is made first, and the diffusion assumption that these cosmic-ray particles can expand from size P to cover the whole galactic disk of size L is then made to explain the radio synchrotron emission I from relativistic electrons over the whole galactic size L, finally enabling the final derivation of the total galactic magnetic field strength, i.e.,: $B_{tot} \sim I_v^{s} K^{-s} L^{-s}$, where $s = 2 / [\gamma + 1]$ and γ is the cosmic ray electron energy index ($\approx$ 2.5). Here we call B_{cr} the results obtained by this cosmic-ray particle method. Cosmic-ray electrons from a galactic nucleus (i.e., P) can find it difficult to diffuse quickly over a whole galactic disk (i.e., L). More details on the derivation of B_{cr} can be found in Chi & Wolfendale (1993), etc. The basic diffusion assumption of the cosmic ray method, i.e., that cosmic rays, gas, and magnetic fields are "well mixed" in the galaxy, has been questioned in the cases of the galaxies M82 and of the Large Magellanic Cloud (e.g., Table 2 in Vallée 1995a). In the Milky Way, most cosmic rays seem to come from SNR in the galactic disk (e.g., see Völk et al. 1984; Völk et al. 1989), and the basic diffusion assumption seems to work. Also, the wide use of a negligible cosmic-ray e/p flux ratio, in the cosmic-ray method, has been challenged recently (Pohl, 1993).

4.1.4. *Comparisons*

Vallée (1995a) found that two independent methods (Faraday rotation B_{fa} and Equipartition B_{eq}) are *converging* on similar values of the magnetic field strength. Observations show that B_{eq} agrees with B_{fa} to within the errors involved, and B_{fa} and B_{eq} are derived independently of each other since different Stokes parameters are involved (Stokes Q and U for B_{fa} ; Stokes I for B_{eq}). For the available observational data, he found on average that $1.0\ B_{eq} < B_{fa} < 1.2\ B_{eq}$. This convergent result, by two independent methods, strongly suggests that the real magnetic field $B \approx B_{fa} \approx B_{eq}$.

Figure 11 shows a plot of the magnetic field values, with B_{eq} on the x-axis, and B_{fa} on the y-axis (open squares) and also B_{cr} on the y-axis (open circles). A dashed line shows the equality $B_{eq} = B_{fa}$. The cosmic-ray particle B_{cr} appears in some cases to predict magnetic field strengths different than those of the other two methods, since the basic diffusion assumption ("well mixed" cosmic rays, gas, and magnetic fields) may not apply; cosmic-ray electrons from a galactic nucleus can find it difficult to diffuse quickly over a whole galactic disk. The value of $B_{cr} = 120 \mu$G in Fig. 8 belongs to a *part* of the galaxy M82, as derived by Chi and Wolfendale (1993).

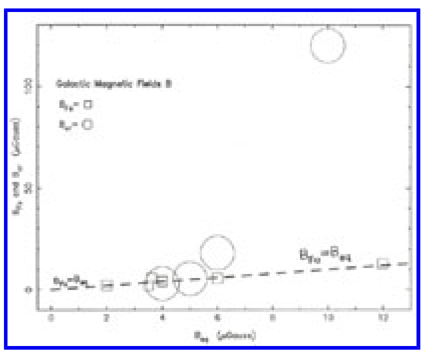

Figure 11. Plot showing the magnetic field values from the equipartition method B_{eq} on x-axis versus that from the Faraday method B_{fa} on y-axis (open squares) and from the cosmic-ray method B_{cr} on y-axis (open circles). A dashed line shows the equality $B_{fa} = B_{eq}$. The value of B_{cr} = 120 μG for M82 was derived by Chi & Wolfendale (1993). Caution is needed in interpreting the larger Bcr values (open circles), as some inherent assumptions in that method may not be valid. Each symbol (open square or open circle) stands for a different galaxy. See Vallée (1995a) for more details.

4.2. Galactic magnetic field *B* and star formation SF

There is a body of literature connecting the radio synchrotron emission from spiral galaxies with their Far Infrared emission, i.e., Niklas et al. (1995), Hummel et al. (1988), Dickey and Salpeter (1984). The interpretation of this narrow relation often involves star formation (e.g., dust emission in Far Infrared near newly-born stars) and cosmic rays (e.g., radio synchrotron electrons near supernovae and in the general interstellar medium).

The presence of a magnetic field is *indirectly* assumed, being necessary for synchrotron emission, and being capable to align dust particles emitting at Far Infrared. But is there a *direct* relation between star formation (SF) and magnetic field B ?

4.2.1. *Observed weak relationship of B with SF*

On the observational side, early statistics done for 8 spiral galaxies with an observed *galactic* Star Formation Efficiency (SFE) and an observed *galactic* magnetic field strength (B_{reg}) obtained via Faraday Rotation, indicated that an increase in SFE value did not result in a noticeable increase or decrease in B value (e.g., Table 3 in Vallée 1992). Rather, B^2 remained roughly constant with SFE, within the errors involved.

Later, published *homogeneously-calibrated* magnetic field data obtained from a *complete sample* of galaxies were used. The complete sample refers to all the late-type galaxies which are optically brighter than B_T = 12 mag and whose Declination is above +10° (Flett & Alexander, 1993). The homogeneous calibration refers to observations with the same telescope and data reduction procedure (VLA-C/D at 1.49 GHz). Recent statistics on these data showed a possible link between B and star formation SF. For 33 nearby galaxies, with both a measured equipartition magnetic field (= B_{tot}, from synchrotron emission) and an observed star formation rate (SFR), Vallée (1994b) found a law of the form: $B_{tot} = B_{eq} = 2.6\ \mu\text{Gauss}\ (\text{SFR}_{\text{solar mass / year}})^j$, with $j = 0.13 \pm 0.04$.

Figure 12 shows the run of B_{eq} as a function of SFR, in 33 nearby normal spiral galaxies. The correlation is weak but real at the 3 r.m.s. level, with a linear correlation coefficient $r = 0.55$. Here the SFR was defined by Kennicutt (1983; 1998) as the ratio: Hα luminosity (at 0.66 μm) / 1.2×10^{41} erg s^{-1}, and expressed in units of $M_{\odot}$ yr^{-1}. Also, B_{eq} was determined by Flett and Alexander (1993), using minimum energy conditions in a synchrotron plasma in a thin disk (0.6 kpc), emitting between 10 MHz and 100 GHz with a spectral index of -0.75, unity filling factor, and $k = 0$ for the electron/proton energy ratio.

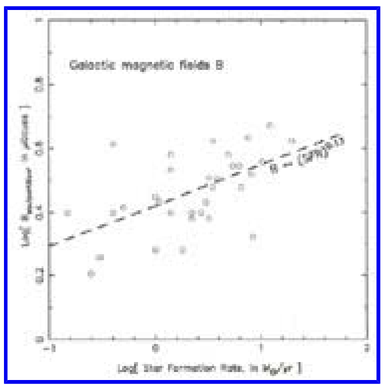

Figure 12. A correlation between the galactic magnetic field (B_{tot}) and the star formation rate (SFR), in 33 nearby spiral galaxies. The lsf line is shown, yielding the law: $B_{eq} = 2.6[\text{SFR}]^{0.13}$, where B_{eq} is in μG and SFR is in $M_{\odot}$/yr. See Vallée (1994b) for more details.

Such a *direct* relation is weak, not strong, contrary to some theoretical predictions. Thus Ko and Parker (1989) had predicted that, when the SFE is high, the interstellar medium is churned and in turns it amplifies the galactic magnetic field B. Chi and Wolfendale (1993) proposed a larger magnetic field strength B when the SFR is high.

For 48 nearby spiral galaxies in the complete sample, and both a measured equipartition magnetic field and an observed star formation efficiency (SFE), Vallée (1994b) found a relationship as follows: $B_{tot} = B_{eq} = 2.7\ \mu\text{Gauss}\ (\text{SFE}_{\text{solar lumin / solar mass}})^j$, with $j = 0.13 \pm 0.04$. Here the SFE was defined by Young et al. (1986) as the ratio: Infrared Luminosity (40 μm - 300 μm) / molecular hydrogen mass, and expressed in units of $L_{\odot} / M_{\odot}$.

These two findings indicate that there is a *weak* correlation between B and star formation SF, independently for 33 and for 48 nearby galaxies mostly located in the Virgo Supercluster of galaxies. Kameya (1996) has employed this *weak* correlation between interstellar magnetic fields and star formation rate. Future trends: it would be nice to study magnetic fields versus star formation in specific cases of late- type galaxies, notably in 'starburst' galaxies, as well as in 'disturbed' galaxies.

Some authors have predicted a stronger theoretical relation $B \sim SFR^j$, with $j \approx 3$, based on a derivation of a relation $B \sim n^k$ for intercloud B outside clouds and for thermal gas inside clouds - this is *not* appropriate for galactic-wide density and galactic-wide magnetic field values since B outside clouds and n outside clouds should be used (see e.g., Section 4.2.4).

4.2.2. *Expected weak relationship of B with SF*

Mestel and Paris (1984) have followed the galactic magnetic field as it becomes distorted by the contraction of a part of a molecular cloud, under flux-freezing conditions. In so doing, the growing self-gravity generates a magnetic force density opposing gravity.

Under practical conditions, the *radio* emission from a spiral galaxy includes two main components:

$$S_{\rm radio} = S_{\rm thermal\ gas} + S_{\rm sync\ gas}$$

where the $S_{\rm sync\ gas}$ is due to the cosmic ray electrons $N_{\rm e\ sync\ gas}$ embedded in a general magnetic field B, and where $S_{\rm thermal\ gas}$ comes from local HII regions and has no dependence on B. From synchrotron equations, we have:

$$S_{\rm sync\ gas} = K \cdot B^2_{\rm sync\ gas} \cdot N_{\rm e\ sync\ gas}$$

Similarly, the *far infrared* emission from a spiral galaxy includes two main terms:

$$S_{\rm FIR} = S_{\rm warm\ dust} + S_{\rm cold\ dust}$$

where $S_{\rm warm\ dust}$ comes from warm dust at local star formation (SF) sites so:

$$S_{\rm warm\ dust} = A \cdot ({\rm SF})^p$$

where A and p are constants, and SF could be either SFR or SFE. $S_{\rm cold\ dust}$ comes from cold dust pervading most of the spiral galaxy and has no dependence on SF nor B. $S_{\rm cold\ dust}$ accounts for roughly half of the $S_{\rm FIR}$ emission observed (Persson & Helou, 1987). There is thus a rough non-linear relation between $S_{\rm radio}$ and $S_{\rm FIR}$, both values being large at the same time, or small at the same time. At very high SF values, $S_{\rm FIR}$ is large, thus $S_{\rm radio}$ becomes large, and B^2 is likely to become large; at very low SF values, $S_{\rm warm}$ is small, thus $S_{\rm radio}$ is small, and B^2 is likely to be small.

More refined predictions, using fully non-linear turbulent models, have been made elsewhere. Passot et al. (1995, their Fig. 8) thus predict that the SFR should first decrease with an increase of the galactic magnetic field B from 0 μGauss to 0.5 μGauss (due to disruptions preventing contraction), then SFR should increase with B increasing from 0.5 μGauss to 5 μGauss (due to gravitational collapse along B lines), and finally SFR should decrease with B increasing beyond 5 μGauss (due to filamentary formation).

4.2.3. *Magnetic fields versus Gas density, on large linear scales ($B \sim n^{0.2}$)*

Early results with limited data gave inconclusive relationships, spanning the whole range of exponent k, from $k = 0$ to $k = 2/3$. At low gas density, early observations were plagued by lack of data. Troland and Heiles (1986) and Heiles (1987) proposed that $B \sim n^0$ at low gas density $n < 100$ cm^{-3}, since gas density increases can occur through quiescent streaming of thermal gas going along magnetic field lines, without the need to increase the B strength. Models by Bertoldi and McKee (1992) suggested that non-self-gravitating clumps in a cloud were supported by the internal pressure of the cloud, so that there is no mass-dependent force to enhance the magnetic field, leading to $B \sim n^0$. Fleck (1988, his Equ. 24) also modeled a low density non-self-gravitating cloud with $B \sim n^0$. Kronberg (1994) proposed that since intergalactic magnetic field energy densities are close to the energy density of the Cosmic Microwave Background Radiation (CMBR = 2.7° K), this implied a CMBR-equivalent magnetic field strength of 3 μGauss which can be viewed as a saturation limit in absence of stronger amplification processes, i.e., $B \sim n^0$. Myers (1990) noted that the emitted line width from non-self-gravitating clouds at low gas density values was comparable to the Alfven speed and was almost constant, and he predicted that $B \sim n^{0.5}$ with a model having a strong magnetic field.

Caveat. At low gas density $n = 5$ cm^{-3}, an observational claim of a $B \sim n^{0.65}$ law in the galaxy M31 has been reported, where B values have been measured from one type i of objects (interstellar synchrotron electrons, scales of 1 kpc) located outside molecular clouds, and where the corresponding gas density values n were measured from *another* type j of objects (atomic and molecular gas, cloud scales of 1 pc) located inside molecular clouds (e.g., Berkhuijsen et al. 1993, their Fig. 11, with B from intercloud synchrotron electrons and n from CO molecular lines). As these are *different* objects, $i \neq j$, this data selection *invalidates* claims that $B_i \sim n_i^k$ for M31, since both B OUTSIDE clouds and n OUTSIDE clouds should be used, and not B OUTSIDE with gas density n INSIDE extrapolated to predict n OUTSIDE.

Since then, better and more numerous data allowed more conclusive relations.

$B \sim n^{0.2}$. With the availability of many more observations, better statistics have now come out. For each object, care must be taken that one measures the gas density n and the magnetic field B from the *same* object - i.e., a B value should not come from a different object than the object used to measure the gas density n value. At low gas density $n < 100$ cm^{-3} , the *first* detection of a non-zero relationship between the gas density n and the magnetic field B on cosmic scales (> 100 pc) was found by Vallée (1990b - see his Fig. 4), indicating a law of the form $B \sim n^k$, where the exponent $k = 0.2 \pm 0.05$. This indicated the prevalence of some types of turbulence on large scales.

More data became available, with which Vallée (1995d) since confirmed this trend with $B \sim n^{0.2}$.

Figure 13, from Vallée (1995d), shows a $B \sim n^k$ law, with an exponential value $k = 0.17 \pm 0.03$ for gas density values $n < 100$ cm^{-3} on cosmic scales (> 100 pc). Thus the k value is non-zero at the 5 rms level.

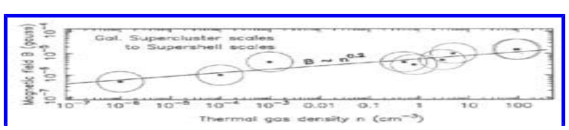

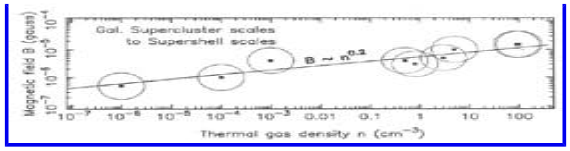

Figure 13. Observed behavior of the magnetic field B (in gauss) with the gas density n (in cm^{-3}), for objects with n < 100 cm^{-3}. The least-squares fitted line has $B \approx 6$ μGauss (n / cm^{-3})$^{0.2}$. A possible interpretation involves the free motion of matter along the magnetic field lines, accreting slowly at some points with little increase in B strength. See Vallée (1995d) for more details.

Theoretically, intermediate relations have been predicted. $B \sim n^{1/4}$ was used in the model of Henriksen (1991) with regions of little cooling and no shock, $B \sim n^{1/3}$ was used in the incompressible turbulence models (e.g., Myers 1983), as well as in MHD turbulent models (e.g., Pellegatti-Franco et al. 1985).

4.2.4. *Gas density versus Star Formation*

Galactic-wide values Star formation SF parameters have been determined for spiral galaxies, using the light integrated over the whole image of a galaxy. These published star formation rate parameters give galactic-wide SF_{gal} values, and they should be compared to galactic-wide gas density n_{gal} values and galactic-wide magnetic field B_{gal} values.

Caveat. At low gas density values $n \approx 1$ cm^{-3}, some authors used a relation $SFR_{gal} \sim n_{cloud}^{1.4}$ (e.g., Fig. 5 in Niklas & Beck 1997, with SFR from galactic-wide thermal radio emissivity and n from CO data from clouds) together with a relation $B_{gal} \sim n_{cloud}^{0.5}$ (e.g., Fig. 4 in Niklas & Beck 1997, with B from galactic-wide synchrotron electrons measured outside clouds and n from CO data from inside clouds) to eliminate n assuming $n_{gal} = n_{cloud}$ (however *only* the density from the interstellar intercloud gas n_{gal} should be used, not the cloud density), and thus they predict a relation $B \sim SFR^{2.9}$ (e.g., Section 4.5 in Niklas & Beck 1997). Since these are different objects, $n_{gal} \neq n_{cloud}$, then this data selection invalidates this claim, since both B OUTSIDE clouds and n OUTSIDE clouds should be used, and not B OUTSIDE with gas density n INSIDE extrapolated to predict n OUTSIDE.

The relationship $B \sim SFR^{j}$ (Section 4.2.1), and the other relationship $B \sim n^{k}$ for galactic wide gas density n < 100 cm^{-3} over large scales (Section 4.2.3) can be used together to eliminate B, yielding the galactic wide relation $SFR \sim n^{k/j}$. With $k = 0.17 \pm 0.03$ (Vallée, 1995d), and with $j = 0.13 \pm 0.04$ (Vallée, 1994b), then one computes that the exponent $k/j = 1.3 \pm 0.1$, i.e., one gets SFR $\sim n^{1.3}$ (Vallée, 1995d).

This exponent value 1.3 also agrees within the observational errors with the value of 1.5 ± 0.5 found elsewhere using the observed optical HII region emissivity measures (e.g., Shore and Ferrini 1995; Kennicutt 1992). It agrees with the value of 1.4 ± 0.3 found using the observed radio HII region emissivity (e.g., Niklas & Beck 1997). It also agrees within the errors with the rough value of 1.0 found in the galaxy NGC6946, and the favored value of 2 for the Milky Way galaxy (e.g., equation 3 in Young 1987). It agrees with the value < 2 for other spiral galaxies (e.g., Kamaya 1996). Such exponent values less than 2 are possibly indicative of a star formation process involving turbulences (e.g., Ikeuchi, 1988). Young et al. (1996) found that the SFE in interacting galaxies is 4 times the SFE in isolated galaxies.

4.2.5. *Magnetic fields in violent star-forming (starburst) galaxies*

A few galaxies exhibit violent star-forming activities. M82 is one such well-studied galaxy. Reuter et al. (1994) found that the origin of the galactic magnetic fields in M82 was unlikely to be due to a galactic dynamo, but more likely due to plasma streaming from the galactic center caused by a violent starforming activity. The center of M82 is completely depolarized, as expected from strong differential Faraday rotation within a dense medium. In the galactic halo but close to the minor axis of the galaxy, the magnetic field is poloidal or vertical, as expected for an outflowing plasma perpendicular to the disk of the galaxy. In the halo but away from the minor axis, not far from the galaxy's major axis, the magnetic field is found to be parallel to the disk of the galaxy, similar to what is seen in other nearby disk galaxies.

4.3. Magnetic field shape in Andromeda (M31) and other galaxies

An optical study of the magnetic field in M31 made by Martin & Shawl (1982) indicated a magnetic field aligned roughly in the plane of the disk, with more or less azimuthal field lines and along the spiral arms.

Only the first method, the Faraday rotation one, can give the magnetic field shape and direction. It does so through the variation of the position angle of maximum polarization value as a function of observed wavelength.

Figure 14 shows the run of the magnetic field B as a function of the galactic radius, in the Andromeda galaxy (= M31). Negative magnetic field values (opposite sense or direction, by convention) are not seen, implying no magnetic field reversal with increasing galactic radii.

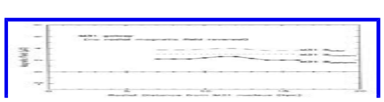

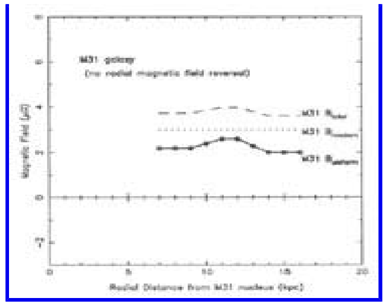

Figure 14. The run of the magnetic field value as a function of the galactic radius r_{gal}, in the Andromeda (M31) galaxy. The observed total magnetic field values (dashes), the uniform component values (open circles), and the random component values (dots) are shown.

As mentioned in Section 3.7.1, early solutions of the linear dynamo equations were done by splitting the dynamo equations into 3 independent axes. As mentioned in Section 3.5.1, observations of the global magnetism in nearby spiral galaxies have shown two shapes: ASS or BSS.

In M31, the azimuthal mode m_{azim} in the ϕ-axis is the lowest ($m_{azim} = 0$), i.e., the magnetic field is axisymmetric. In M31, the vertical mode p in the z-axis is the lowest ($p = 0$), i.e., the magnetic field is symmetric above and below the galactic plane. In M31, the radial mode n along the r-axis is the lowest ($n = 0$), i.e., there is no magnetic field reversal with radius. This radial mode n of the magnetic field is determined by the behavior of the combined radial potential $\gamma(r)$, and $\gamma(r)$ rises rapidly at a radius of 7 kpc (Fig. 4 in Ruzmaikin et al., 1985), contrary to the slow rise of $\gamma(r)$ in the Milky Way (Fig. 3 in Vallée, 1991b). So in M31 the ranges of dynamo solutions for the n modes start at the same inner radial boundary, not at different radii, and therefore the lowest n mode dominates ($n = 0$, no magnetic field reversal).

4.4. Magnetic field *B* in galactic disks and neutral hydrogen HI

4.4.1. *B shapes and HI masses*

The type of global magnetism (either ring/axisymmetric, or spiral/bisymmetric) has been studied as a function of 21 different physical parameters for 9 spiral galaxies (Vallée, 1986). The first type (ring/axisymmetric) of magnetism appears to occur more frequently in a spiral galaxy if that galaxy possesses a large amount of HI gas mass ($M_{HI} \approx$ a few $\times 10^9 M_\odot$). Conversely, the second type (spiral/bisymmetric) appears to occur more freqently in a spiral galaxy possessing a lesser amount of HI gas mass. On the theoretical side, nonlinear dynamo models predict a mixture of modes, usually with a predominent mode and a weaker secondary mode.

When looking at the suggested triggers for the appearance of the bisymmetric magnetic field in nearby galaxies, many suggested triggers (mostly from the dynamo theory) were: macroscopic shocks from density waves, or rotational shears in differential rotation, or half-thickness of the ionised gas layer, or the effects of a single warp in the outer galaxy. Again, the most likely trigger for bisymmetric magnetism, measured in terms of differences in average values for $m_{azim} = 0$ galaxies versus average values for $m_{azim} = 1$ galaxies, was the smaller amount of HI gas mass in a spiral galaxy (Vallée, 1993a).

What is the observational possibility of seeing another azimuthal mode, $m_{azim} = 2$ (quadrisymmetric magnetic field shape) ? A prediction was obtained (e.g., Equation 2 in Vallée 1992) that a lower HI gas mass in a spiral galaxy could allow for a higher magnetic field mode m_{azim}, i.e., the observation of a galaxy with $m_{azim} = 2$ would contain an amount of HI gas mass $< 10^8 M_\odot$.

A more recent study on the possible triggers of the global magnetic field shapes, using substantial corrections published on the galactic magnetic values, was made in Vallée (1993a). The updated data confirm the correlation between the HI gas mass and the azimuthal magnetic mode, i.e., the $m_{azim} = 0$ galaxies have more galactic HI mass (Vallée, 1993a). Yet the best dynamo theories to date still do not include the amount of *neutral* HI gas, preferring to use the amount of ionised HII gas. The best argument for theoreticians to include neutral HI gas parameters in future dynamo models is the confirmed observational link between HI shapes (MD, see below) and ASS or BSS magnetic field shapes (m_{azim}, see below).

Using the observed distribution of HI data in galaxies, and the critical HI mass separating $m_{azim} = 1$ galaxies from $m_{azim} = 0$ galaxies, a prediction of 1-to-1 equal predominance of $m_{azim} = 0$ galaxies versus and $m_{azim} = 1$ galaxies has been proposed (Vallée, 1993b).

4.4.2. *B shapes and HI shapes - companions or bars*

The second type of magnetism (spiral/bisymmetric) also occurs more frequently when there are strong effects from a close companion galaxy, or from a strong oval bar in the galactic nucleus (Vallée, 1988a). These results do not support the theory of a weak intergalactic magnetic field being amplified into a BSS shape by a large amount through gravitational contraction of a protogalaxy to give rise to the observed magnetic field strengths - rather, a leakage of galactic magnetic fields into the intergalactic space may be occurring.

The influence of the environment on the HI content of spiral galaxies has been reviewed previously (e.g., Haynes et al. 1984). The HI flux and distribution can be used to diagnose past dynamical traumas. Neutral hydrogen has proven to be a better tracer of past tidal disruption than does starlight data. Past descriptions of HI distributions have been morphological but loosely defined (e.g., "symmetric", "warped", "exhibiting appendages", "with an envelope", etc.). Such a morphological approach may appear somewhat mysterious to a physically oriented reader. Hence there was a need to order each morphology along a physical sequence.

A recent attempt has been made to set up a more rigorous morphological classification of HI distributions, ordered along a physical sequence of greater and greater complexities (Vallée, 1993c; Vallée, 1994a; Vallée, 1995b), based on *four basic HI shapes* in spiral galaxies, which are summarised briefly here:

- MD = 1, when the radio HI morphology is mostly symmetric and quiescent in a plane, with little or no morphological deformations (MD) to be seen above a HI level of 2% of the inner HI peak intensity levels located in the optical galaxy, with a linear resolution HPBW $\approx$ 2 kpc.
- MD = 2, when the radio HI morphology shows a moderate deformation, as seen at an HI level between 2% and 10% of the inner galactic peak HI levels, for a HPBW $\approx$ 2 kpc. Examples are warps, bumps, or spiral features at a larger pitch angle than that of the optical spiral arms.
- MD = 3, when the radio HI morphology shows a strong deformation *just outside* of the optical galaxy, as seen at an HI level between 5% and 30% of the inner galactic peak HI levels, for a HPBW $\approx$ 2 kpc. Examples are inverted *S*-shaped HI features (opposite to the *S*-shaped form of the inner optical stellar arms), or else spiral features at a much larger pitch angle (> 20°) than that of the optical spiral arms.
- MD = 4, when the radio HI morphology shows a more extreme deformation *far outside* of the optical galaxy, as seen at an HI level between 5% and 30% of the inner galactic peak HI levels, for a HPBW $\approx$ 2 kpc. Examples are spiral features at a much larger pitch angle (> 20°) than that of the optical spiral arms. This resembles MD = 3 except for the much larger distance involved.

Vallée (1993c) investigated the neutral hydrogen distributions (HI shapes) in 6 nearby spiral galaxies with known magnetism (M51, M63, M83, M106, NGC253, NGC2903). This was the first statistical evidence that a spiral galaxy with an apparently undisturbed (i.e., regularly shaped or slightly affected) HI shape seems to possess an axisymmetric magnetic field $m_{azim} = 0$, and that a spiral galaxy with a significantly disturbed (ie strongly arched or extremely perturbed) HI shape seems to possess a bisymmetric magnetic field $m_{azim} = 1$.

Vallée (1994a) pursued this matter, in 6 other spiral galaxies with a known magnetism (M31, M33, M81, IC342, NGC6946 and Milky Way), and found the same correlation between HI shape and magnetism: disturbed HI and $m_{azim} = 1$; undisturbed HI and $m_{azim} = 0$.

Figure 15 shows a sketch of four spiral galaxies with different HI distribution, from MD = 1 to MD = 4, to show how the HI shape (MD low to high) goes with the magnetism (m_{azim} low to high).

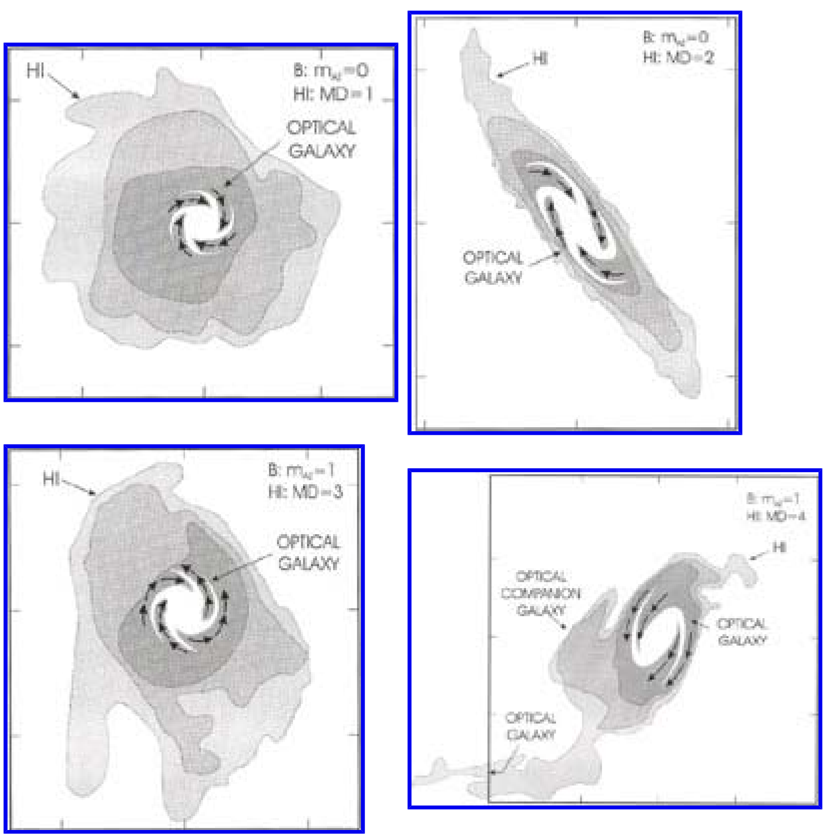

Figure 15. Model linking galactic dynamics with galactic dynamos. One sketch is shown of an optical galaxy with spiral arms (at center, in white), for each of the various MD shape for the HI gas (HI gas density in increasing shades of grey). The magnetic field directions are shown (arrows). (a) A simple undisturbed HI gas shape

MD = 1, with azimuthal ASS magnetic field *B* shape being m_{azim} = 0. (b) A HI gas shape MD = 2, with *B* shape m_{azim} = 0. (c) A disturbed HI gas shape MD = 3, with a complex azimuthal BSS magnetic field *B* shape m_{azim} = 1. (d) A complex HI gas shape MD = 4, with *B* shape m_{azim} = 1. See Vallée (1997) for more details.

Vallée (1995b) pursued the relationship between galactic dynamos and galactic dynamics, as evidenced by a link between the magnetic field shape and the neutral hydrogen shape, for 3 other galaxies (NGC891, NGC4631, and the LMC).

Thus the current list of 16 spiral galaxies with both observed m_{azim} and observed MD values are:

- MD = 1: M106, NGC253, NGC6946;
- MD = 2: IC342, M31, M63, Milky Way, NGC891;
- MD = 3: LMC, M33, M83, NGC2903;
- MD = 4: M51, M81, NGC2276, NGC4631.

All of these galaxies have a preliminary or definite m_{azim} value; in some cases, there is a predominant mazim value and a weaker secondary m_{azim} value, like a predominant m_{azim} = 0 and a secondary m_{azim} = 2 value in NGC6946 (e.g., Beck and Hoernes 1996).

Higher azimuthal Fourier modes m_{azim} could be expected by dynamo theory to be superimposed on the dominant lower mode, but these should have relatively small amplitudes (e.g., Beck et al. 1996).

Figure 16 shows the preliminary statistical link between HI shape and magnetic field shape. Only discrete numerical values can be observed in this Figure (m_{azim} = 0, 1, 2, ...; MD = 1, 2, 3, 4, ...) but the non-random locations of the data show a definite trend (bottom-left to top-right), suggesting that an increase in complexity in *B* goes along with an increase of complexity in HI. The statistical link points to a necessary *common cause* for creating complex HI fossils and complex magnetic field shapes.

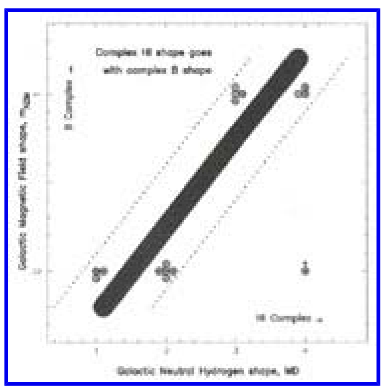

Figure 16. Plot of the observed HI gas shapes (MD parameter, on x-axis) versus the observed magnetic field shapes (mazim parameter, on y-axis) for 16 nearby galaxies with spiral structures (circled crosses, some shifted slightly to avoid overcrowding). Only discrete values of the parameters can be observed (m_{azim} = 0, 1, 2, ...; MD = 1, 2, 3, 4, ...), but the non-random locations of the data show a preliminary trend (bottom-left to top-right) as sketched by the broad line, implying that a more complex HI shape goes along with a more complex magnetic field configuration, while a simple HI shape goes along with a simple magnetic configuration. See Vallée (1995b) for more details.

In dealing with statistics of 'quantized' parameters (the MD classes use positive integer values; the m_{azim} classes use integer values and zero), then some *minimum* non-zero scatter is unavoidable even in a perfect relationship - much like the attempt to fit a straight linear diagonal to an ideal staircase.

Physical link. The most likely common cause would be a *deformed gravitational potential* around a spiral galaxy. Possible origins of such disturbances could be a tidal deformation caused by the passage of a nearby companion galaxy (e.g., NGC5086 is near NGC2903 and there is a large bar in NGC2903 as well as sizeable HI distortions; NGC5195 is very near M51 which has extreme HI distortions; M31 is near M33, and M33 has infalling HI companions and sizeable HI distortions; NGC3077 is very near M81 which has extreme HI distortions). It could also be caused by a large barred oval nucleus (e.g., M83 - see Zweibel 1991). Hummel & Beck (1995) also concur that NGC2276, in gravitational interaction with NGC 2300, has a severely distorted shape and a non-axisymmetric magnetic field shape. Limited RM data on NGC 1566 (Ehle et al., 1996) and on NGC4254 (Soida et al., 1996) await further study.

The presence of a deformation of the galactic gravitational potential implies the concept of dynamical time scale, and the possibility that when the disturbing agent goes away, then the galactic system may revert to a more quiescent state.

On the theoretical side, Moss (1995) and Moss (1996b) have laid down the first equations pertinent to the generation of BSS magnetic field shape in a spiral galaxy, due to a tidal interaction by a companion galaxy.

4.5. Magnetic fields in Halos of spiral galaxies

Most normal galaxies have little or no radio halo, with the radio surface brightness perpendicular to the disk being best described by exponential functions with a median scale height of ~ 1 kpc (Beck, 1997b).

Bright, extended radio halos around spiral galaxies are very rare - exceptional, rather than normal. One of these rare galaxies with an extended halo is NGC 4631, with a scale height of ~ 2 kpc, magnetic field lines going vertically out of the galactic disk, possibly due to a galactic fountain or galactic wind (Hummel et al., 1991).

Future trends. Little is known for sure on magnetic field strengths and shapes in halos of spiral galaxies. Very preliminary data have been reviewed in Beck et al. (1996) and Beck (1997b), and some early comparisons were made with galactic disks (Beck, 1997a).

In the case of M51, Berkhuijsen et al. (1997) used a multi-layer 3-dimensional model for the position angles of the polarization at 4 different radio wavelengths, smoothed to a beam of 3.5 kpc. Their method involves the Fourier parameterization of the magnetic field structure into many radial, azimuthal, and vertical components inside each layer. They found a small predominence of the bisymmetric (BSS) global magnetic field shape in the galactic disk, notably for a radial distance < 6 kpc. They also found a predominence of the axisymmetric magnetic field shape in the galactic halo facing us, possibly due to a topological pumping of magnetic field by a galactic fountain flow. They could not say anything about the magnetic field in the side of the halo on the other side of the disk, since the nearly face-on galaxy is not transparent at λ20cm. The general features of the magnetic fields seem to be in general agreement with predictions from dynamo theory, but detailed dynamo modelling is required to reach definite conclusions.

5. ELLIPTICAL GALAXIES, DISTANT GALAXIES, CLUSTERS AND VOIDS, QUASARS AND COSMIC SCALES

Interstellar gas in nearby elliptical galaxies may be rare, but not unseen. Magnetic fields have not yet been detected there. On the theoretical side, a small scale dynamo may be the only way to maintain the magnetic field inside elliptical galaxies, resulting in a random magnetic field of strengths of a few μGauss and of a few hundred parsecs in scale (Moss and Shukurov, 1996).

5.1. Individual Galaxies and quasars (~ 200 kpc)

Most of the radio galaxies and radio quasars studied here are located beyond 20 Mpc. The polarization of distant radio elliptical galaxies (and of quasars) comes from synchrotron radiation from relativistic electrons moving in the magnetic fields located in the nucleus of these objects, and also in 2 polarized radio lobes (~ 200 kpc long), located on both sides of the optical elliptical galaxy or the optical quasar. The central optical nucleus of the galaxy or quasar exhibits linear polarization at submillimeter and millimeter wavelenghts, amounting to ~ 4% in several quasars (Flett & Murray, 1991). One-sided or two-sided jets connect the optical galaxy/quasar to the radio lobe(s). For a review, see Asseo & Sol (1987). A recent theoretical model of magnetic fields in decelerating relativistic radio jets is given in Laing (1996).

The Hubble diagram for the brightest optical galaxies in clusters, showing a good linear relation between the redshift z of the spectral lines and the apparent visual magnitude m_V, also works for a subset of quasars. Basu (1994) showed that polarized quasars, i.e., quasars with a detectable value of optical linear polarization or of radio linear polarization, obey the Hubble relation between z and m_V.

Some quasars seen through intervening halos of galaxies (i.e., damped Lyα absorption systems) show higher value of RM (e.g., Oren & Wolfe 1995; Kronberg 1994), suggesting that the extra RM may come from these intervening galaxies.

Kronberg et al. (1996) studied the difference along a jet between the position angle of the image of a radio jet and the position angle of linear polarization, for a line of sight going close to two intervening galaxies. While the PA of the image can be bent by an intervening mass, the polarization PA cannot be bent, yielding the mass of the intervening galaxies.

5.2. Clusters of galaxies as the largest magnets (~ 5 to 50 Mpc)

5.2.1. ***Several sources per individual cluster of galaxies***

The technique of choosing selected celestial zones (see Sect. 2.1.4), originally used to study extended objects in our Milky Way, has been applied to study the intracluster gas within an entire cluster of galaxies, using more distant background galaxies and quasars as probes. Thus Broten et al. (1986) first studied in this way the Abell 2319 cluster of galaxies at $z = 0.053$ ($\approx$ 320 Mpc), with a canonical Abell cluster diameter of 6 Mpc.

A large scale magnetic feature was found at a level of 120 radians/m^2 in the A 2319 cluster of galaxies (Table 2 in Vallée et al., 1986). This is compatible with a model of a magnetic field located in a few uniform cells, each cell being randomly oriented. This allowed the first detection of a magnetic field strength in the intracluster gas between the galaxies, with values of ≈ 2 μGauss in cells of about 20 kpc in A 2319 (Vallée et al., 1987).

This technique involved the transformation of the X-ray emission profile of the intracluster gas into a thermal electron density distribution, following the inversion method first adapted for X-ray astronomy in Vallée (1981).

In a similar search for magnetic features in the Great Attractor supercluster of galaxies, no excess of rotation measure could be found across it, with an upper limit of 8 radians/m^2 (Vallée, 1989). In turn, this implied an upper limit on the supercluster magnetic field of at most 0.1 μGauss for the ordered component B_{reg}.

Using this technique, a second example of a detected excess rotation measure from a cluster of galaxies was found in the Coma cluster, at a level of 40 radians/m^2 (Kim et al., 1990), implying a cluster magnetic field B_{reg} of 2 μGauss. Also, Vallée (1990a) found an excess rotation measure of 10 radians/m^2 and a possible large scale magnetic field in the Virgo supercluster of galaxies, with B_{reg} of about 2 μGauss.

The nearest large scale structure or arrangement of galaxies found is the Local Virgo Supercluster of galaxies, centered at $z = 0.004$ (≈ 24 Mpc) and extending all the way to us (overall size ~ 50 Mpc). To study the Virgo supercluster, a Virgo-centered supercluster coordinate system has been proposed (see Appendix in Vallée, 1991c), improving on the earlier system of de Vaucouleur.

A further analysis of a 'complete sample' of galaxies in the Virgo supercluster of galaxies was made by Vallée (1993b), using the well-calibrated minimum-energy magnetic field obtained from a consistent set of 1.4 GHz radio observations, and using the Virgo-centered supercluster coordinate system. A trend for a larger neutral hydrogen mass in spiral galaxies located farther from the plane of the Virgo Supercluster was found, but there was no change of the magnetic field value as one goes away from the supercluster center.

5.2.2. *One source per individual cluster of galaxies*

Several studies have used the presence of one central radio source per cluster, to establish statistically over many clusters that the rotation measure is intrinsically high near the centers of clusters of galaxies. Thus Taylor and Barton (1994) have found that high RM is produced by magnetic fields associated with the relatively dense hot x-ray spherical cores in cooling flow clusters of galaxies.

Taylor & Perley (1993) studied one radio source in the Hydra A cluster, and interpreted its RM distribution with the help of a cluster *disk* of diameter 150 kpc (larger than the radio source) with an uniform magnetic field of 6 μGauss, inclined 48° to the line of sight. There is no optical or X-ray evidence that such a large-scale disk might exist in this cluster.

Carvalho (1994) used the variance in RM towards different clusters of galaxies, and found a cluster magnetic field strength of 0.3 to 1 μGauss. Crusius-Wätzel et al. (1990) found a typical cluster field of 5 μGauss, based on a statistical study of 1 source in each of 5 clusters of galaxies.

On the theoretical side, it is argued but not proven that cluster magnetic fields are maintained by dynamos. Still, assuming that a dynamo operates in clusters, then Poezd & Sokoloff (1993) used the non-linear turbulent dynamo to estimate the intracluster magnetic field. Lacking a large scale body of matter, they found that no cluster-scale regular component of a magnetic field can exist. Thus their "cellular dynamo" predicted a *chaotic* magnetic field with a strength of a few μGauss in a cluster of galaxies, distributed in a medium of *cells*. Norman and Meiksin (1996) have proposed that cool magnetic flux loops can reconnect with hot magnetic flux loops, to effect a rapid recycling of mass between the hot and cool phases of an intracluster medium, and to significantly reduce the mass inflow rates in clusters of galaxies. Many details remain to be worked out. A recent short review is given in Böhringer (1995).

5.2.3. *Seeds for magnetic fields in clusters of galaxies*

First, a primordial cosmological magnetic field has been proposed, althought very small in strength to comply with its non-detection, and thus it may be unimportant when compared to the turbulent kinetic energy in clusters. It is by no means certain that extremely weak, random, primordial seed magnetic fields < 10^{-10} Gauss are sufficient to account for observed magnetic fields in clusters of galaxies and in galaxies (e.g., Kim et al. 1996).

A second potential seed field would be coming from the relics of extended double radio sources or radio trails in clusters, being shredded by the turbulent wakes of passing galaxies. However, not all clusters have one or more extended radio doubles or radio trails, and many clusters have none. This seed field may be limited in its application.

A third potential seed field model proposed uses the ejected magnetic field and gas from the interstellar medium of the galaxies in the cluster, which could diffuse out of the galaxies or else be blown out of the galaxies by stellar winds, supernovae, galactic fountains, tidal strippings, etc, at a rate of ~ $1 M_\odot$ per galaxy per year (e.g., Goldschmidt & Rephaeli 1993; De Young 1992). This process can be widely distributed and it has the advantage of transfering kinetic energy from the extracting process to the intracluster medium.

5.3. Large Scale Voids in space (~ 100 to 200 Mpc)

There exists a substantial decrease of galaxies toward the center of the Bootes Void, and an increase of galaxies in a shell around the Void, with a total Void diameter of 120 Mpc. The Bootes Void (center and shell) was searched for any excess magnetic effects, over the large scale background to the left and right. No excess rotation measure (< 10 rad/m^2) was found, implying a shell magnetic field to < 0.1 μGauss for the ordered component (Vallée, 1991a).

5.4. Cosmological scales

5.4.1. *Foreground Cosmological Screen (~ 20 Gigaparsecs)*

The physical conditions of the gas outside of clusters of galaxies are not well known. Forman et al. (1984) found values near $n \sim 2 \times 10^{-8}$ cm^{-3} and $T \sim 3 \times 10^{8}$ K, from X-ray data and analysis. Somewhat higher n values have been used elsewhere.

On the scale of the Universe, a study of RM of 309 distant quasars (and galaxies), with both a measured redshift z and an observed rotation measure RM, led to a search for a possible increase of RM with z. No such increase was found up to a redshift $z = 3.5$, e.g., Figure 2 in Vallée (1990c). An *observed* upper limit of extragalactic RM = 2 rad/m^2 for any cosmological contribution was deduced, which in turn corresponds to < 10^{-9} Gauss for a regular cosmic magnetic field $B_{\rm reg}$ (outside clusters of galaxies), and a mean particle density of 10^{-7} cm^{-3} (or < 10^{-10} Gauss for 10^{-6} cm^{-3}).

Thus there is no cosmological magnetized foreground screen, out to a redshift $z = 3.5$. For $H_0 = 50$ km/s/Mpc, $q_0 = 1$, then such a z corresponds to a distance of about 20 000 Mpc (= 20 Gpc).

Of course, the absence of a measurable value of $B_{\rm reg}$ does not rule out the presence of a possible random magnetic field $B_{\rm ran}$ throughout the Universe. Searches for such a $B_{\rm ran}$ component have been reviewed by Kronberg (1994), and an upper limit of 10^{-9} Gauss is also indicated out to a redshift of $z \sim 3.5$.

5.4.2. *Background Cosmological Surface (~ 8000 Gpc)*

Another method to detect an intergalactic magnetic field is based on the delay in arrival of secondary γ rays with respect to primary γ rays from QSO and galaxies undergoing outburts. The delay would be caused by the action of an intergalactic magnetic field on the electron cascades caused by the scattering of some γ rays (photon-photon collisions in the cosmic background radiation, enabling particle pair productions). The time delay is proportional to B^2. The question of whether such a proposed model is practical deserves further study. As an example, an intergalactic magnetic field of 10^{-16} Gauss might have been detected (Plaga, 1995), althought confirmation is needed (see Kronberg, 1995).

Is there a cosmological background screen ? A *predicted* value of RM = 280 rad/m^2 has come out of a recent model of Kosowsky and Loeb (1996), for a magnetic field of 10^{-9} Gauss, for emission totally generated within the redshift range $900 < z < 1400$, near the surface of last scattering for the 2.7° K Cosmic Microwave Background Radiation. Observations of the CMB Radiation at 30 GHz with a 30' beamwidth is proposed. For $H_0 = 50$ km/s/Mpc, $q_0 = 1$, then such a $z \approx 1400$ corresponds to a distance of about 8 400 Gpc (= 8.4 Teraparsecs).

6. SUMMARY AND FUTURE TRENDS

Polarimetry is a powerful tool for the study of magnetic fields on interstellar scales and larger scales (e.g., Table 2).

A review has been carried out of the polarimetric observations to date, and their deductions for the magnetic fields on large scales (1 pc and up), in the Milky Way galaxy and beyond. In this review, I have attempted to tie together the many observational pieces of the puzzle of the galactic magnetic fields in the Milky Way (e.g., Table 1). If at places it appears incomplete, it should be viewed as an incentive to continue to piece the puzzle together to the end, Future trends over the subject areas covered in this review have been indicated.

The pace of progress in observational polarimetry is hampered by the relative lack of polarimetric instruments, by the larger amount of time needed as compared to other observational searches, and possibly by the necessity to do a better job of educating fellow astronomers on Telescope Time Allocation Committees about the usefulness of polarimetry.

Narrow magnetized features are found in the interstellar medium of the Milky Way disk (filaments, outflow cavities, edges of molecular clouds), and in the Galactic Center.

A few magnetic field maps of dusty molecular clouds observed at Extreme-Infrared (λ800 μm) wavelengths have now been published in the 1990s, e.g., W75N-IRS1, M17-SW (e.g., Figure 3 here), Sagittarius B2, and MonR2 core. Preliminary resuls indicate that the magnetic field lines in MonR2 core and in M17-SW do bend, suggesting that there is some *evolution* of the magnetic field inside a molecular cloud, but without excessive tangling of the magnetic field lines. Future trends: Extreme Infrared polarimetric observations of the magnetic field distribution in molecular clouds are in their infancy. Air-borne Far-Infrared (e.g., ISO, SOFIA) and Ground-based Extreme-Infrared (e.g., JCMT, CSO) polarimetry of dust aligned by magnetic fields in molecular clouds is likely to better reveal the complete structure of molecular clouds, and their dynamical interactions with the interstellar medium gas and with other clouds. Classification systems of magnetic fields in molecular clouds have been discussed (e.g., Fig. 2 here).

Numerous interstellar superbubbles near the sun have been found to be magnetized, causing local deviations of the larger scale regular galactic magnetic field in the Milky Way (e.g., Fig. 6 here). The magnetic field in the shells of superbubbles follows the relation $B \sim n^k$ with $k \approx 1.0$, suggestive of shocked expanding gas (e.g., Figure 5 here). A similar exponent $B \sim n^{1.0}$ is expected in the shells of supernovae remnants. A similar $B \sim n^{1.0}$ is expected in the compressed edges of molecular clouds near HII regions. Future trends: as there are still less than a dozen shells with a measured magnetic field strength, more observations are needed for better statistical analyses, and to look for other predicted trends. The theories of magnetic fields in superbubbles are likewise evolving rapidly.

Outside of these shocked expanding shells, there is a $B \sim n^k$ relation for gas and magnetic field, and the data show $k = 0.5$ for objects from $n >$ 100 cm^{-3} up to $n > 10^{11}$ cm^{-3}, suggestive of an equilibrium between various energies (e.g., Figure 1 here). Future trends: observations of even more dense objects, nearer $n \approx 10^{20}$ cm^{-3}, are needed to test theories of star formation, and the predicted flattening of the $B \sim n^k$ curve.

Data also show a $B \sim n^k$ relation, but with $k \approx 0.2$ for objects with size > 100 pc and $n < 100$ cm^{-3}, suggestive of relatively free gas motions bunching up along magnetic field lines (e.g., Figure 13 here).

In the Galactic center, magnetic field strengths of . 1000 μGauss over small regions of dense gas have been measured. Future trends: the presence or absence of strong magnetic field over large scales in the galactic center region is still problematic, and in need of more observations. Much theoretical work and observational studies need to be done before the overall magnetic field structure within the central 200 parsecs of our Galaxy is understood. Certain elements of a dynamo may be present there, with gas motions changing vertical, poloidal magnetic fields into toroidal, azimuthal magnetic fields.

There is an observed relationship between the galactic magnetic field B and the star formation rate SFR, or star formation efficiency SFE, of the form $B \sim SFR^j$ and $B \sim SFE^j$, with $j \approx 0.13$ (e.g., Figure 12 here). In combination with the $B \sim n^k$ law with $k \approx 0.2$ over large scales, one finds that SF $\sim n^{1.3}$ for nearby spiral galaxies. Future trends: more observations are needed to ascertain the SFE and SFR over sub-galactic regions, such as inside a specific spiral arm within the Milky Way Galaxy or within another spiral galaxy.

The most likely seed for galactic magnetism could be recent local ejecta from stellar winds and supernovae. The most likely amplification and orientation mechanism could be the galactic dynamo. Future trends: theories of seed magnetic fields are evolving rapidly, and tests of their predictions should be amenable to observations soon.

Over a galactic scale, the observations indicate that the Milky Way probably has 4 main spiral arms (e.g., Figure 7 here), 2 magnetic field reversals (e.g., Figure 8 here), and a large scale azimuthal ASS magnetic field shape (e.g., Figure 9 here).

Of the three main methods used to derive galactic magnetic fields, the Faraday rotation method seems to be the most accurate for giving the galactic magnetic field strength, which is about the same as that obtained from the equipartition method (e.g., Figure 11 here). The Faraday rotation method is the only one capable of giving the galactic magnetic field direction. Future trends: There are hundreds of QSO and galaxies with a detected RM (e.g., Figure 4 here), but there are thousands of QSO and distant galaxies that lack a known RM, due to their faintness. Better sensitivity in Faraday observations should help extend the areas of coverage of this technique.

In the 1990s, most large scale magnetic fields in spiral galaxies seem amenable to interpretation with the currently favored dynamo theories. Future trends: while the dynamo theories can readily explain many features of the galactic magnetic fields, the question of the viability of the dynamos or its replacement by some galactic fountain theories has not been settled entirely.

A majority of spiral galaxies have the axisymmetric magnetic field shape $m_{azim} = 0$. A number of spiral galaxies have the bisymmetric magnetic field shape $m_{azim} = 1$ (e.g., Figure 10 here). In M31, the azimuthal ASS magnetic field shape prevails, without magnetic field reversal (e.g., Figure 14 here). The $m_{azim} = 1$ shape may be due to past tidal interactions with nearby companions (e.g., Figure 15 here), as evidenced by a distorted HI tail outside of the galaxy (MD = 4). Future trends: Statistics suggest that a simple B shape corresponds to a simple HI shape, and that a complex B shape corresponds to a complex HI shape (e.g., Figure 16). Less than 2 dozen galaxies have had their global magnetic field structure assessed, and more observations are needed to test more predictions of recent theories in these areas.

The intracluster gas inside clusters of galaxies contains an intergalactic intracluster magnetic field near 1 μGauss, as detected by its contribution to the rotation measure. The best seed for this intracluster intergalactic magnetic field appears to be the ejecta from the interstellar medium of galaxies in clusters, via stellar winds, supernovae, galactic fountains, tidal strippings, etc. Future trends: as less than a dozen clusters have had their magnetic field strengths measured, more observations are needed to better test the fitting of the recent theories of magnetic fields in clusters of galaxies.

Acknowledgments

I thank Ms. Lyne Séguin (NRCC-Ottawa) for help in drawing some of the figures (2, 3, 6, 9, 15); the PGPLOT software was employed for the others. I am grateful to many people who spent much of their scientific lives on researching mid-scale and large-scale magnetic fields.

REFERENCES

1. Adams, F.C., Freese, K., Laughlin, G., Schwadron, N., Tarlé, G. 1997, Ap. J., 491, 6-12.
2. Akasofu, S.-I., Hakamada, K. 1982, Ap.J., 253, 552-555.
3. Alcock, C., Ross, R.R. 1986, Ap. J., 310, 838-941.
4. Amaral, L.H., Lépine, J.R. 1997, Monthly Not. Roy. Astron. Soc., 286, 885-894.
5. Arons, J., Max, C.E. 1975, Astrophys. J., 196, L77-L81.

6. Asseo, E., Sol, H. 1987, Phys. Rep., 148, 307-436.
7. Athreya, R.M., Kapahi, V.K., McCarthy, P.J., van Breugel, W. 1998, A & A, 329, 809-820.
8. Bagchi, J., Pislar, V., Lima Neto, G.B. 1998, MNRAS, 296, L23-L28.
9. Balbus, S.A. 1993, Ap.J., 413, L137-L139.
10. Bally, J. 1989, in *Low-mass star formation and pre-main sequence objects*, ed. by B. Reipurth, ESO, Garching, Germany - Confer. & Workshop Proceed., 33, 1-32.
11. Barker, D.M., Mestel, L. 1996, Monthly Not. R. Astron. Soc., 282, 317-326.
12. Barvainis, R., Clemens, D.P., Leach, R. 1988, A. J., 95, 510.
13. Barvainis,R., McIntosh, G., Predmore, C.R. 1987, Nature, 329, 613-615.
14. Bastien, P., Ménard, F. 1988, Ap. J., 326, 334-338.
15. Bastien, P., Ménard, F. 1990, Ap. J., 364, 232-241.
16. Basu, D. 1994, Ap. Lett. & Comm., 29, 249-252.
17. Battaner, E. 1993, *Twenty-First Century Science and Technology*, 6, no. 4, 49.
18. Battaner, E., Florido, E. 1995, Monthly Not. Roy. Astron. Soc., 277, 1129-1133.
19. Battaner, E., Jiménez-Vicente, J. 1998, Astron. & Astrophys., 332, 809-813.
20. Battaner, E., Garrido, J.L., Membrado, M., Florido, E. 1992, Nature, 360, 652.
21. Battaner, E., Florido, E., Jimenez-Vicente, J. 1997, Astron. & Astrophys., 326, 13-22.
22. Beck, R. 1991a, Astron. & Astrophys., 251, 15.
23. Beck, R. 1991b, in *The Interpretation of Modern Synthesis Observations of Spiral Galaxies*, ed. Duric, N., Crane, P.C., Astron. Soc. Pacific, San Francisco, USA - ASP Conf. Ser., 18, 43.
24. Beck, R. 1996, in *Polarimetry of the interstellar Medium*, ed. by W.G. Roberge and D.C. Whittet, Astron. Soc. Pacific, San Francisco, USA - A.S.P. Conf. Ser., 97, 475-485.
25. Beck, R. 1997a, in *High-Sensitivity Radio Astronomy*, ed. N. Jackson & R. Davis, Cambridge Univ. Press, Cambridge, UK, in press.
26. Beck, R. 1997b, in *The Physics of Galactic Halos*, ed. by H.Lesch, R.-J. Dettmar, U.Mebold, R. Schlickeiser, Akademie Verlag, Berlin, in press
27. Beck, R., Hoernes, P. 1996, Nature, 379, 47-49.
28. Beck, R., Brandenburg, A., Moss, D., Shukurov, A., Sokoloff, D. 1996, Annual Rev. Astron. Astrophys., 34, 155-206.
29. Beck, R., Carilli, C.L., Holdaway, M.A., Klein, U. 1994b, Astron. & Astrophys., 292, 409.
30. Beck, R., Loiseau, N., Hummel, E., et al. 1989, Astron. & Astrophys., 222, 58.
31. Beck, R., Poezd, A.D., Shukurov, A., Sokoloff, D.D. 1994a, Astron. & Astrophys., 289, 94-100.
32. Beck, R., Berkhuijsen, E.M., Bajaja, E. 1991, in *Molecular Clouds*, ed. by R. A. James & T.J. Millar, Cambridge Univ. Press, Cambridge, UK, 179-182.
33. Berkhuijsen, E.M., Bajaja, E., Beck, R. 1993, Astron. & Astrophys., 279, 359-375.
34. Berkhuijsen, E.M., Horellou, C., Krause, M., Neininger, N., Poezd, A.D., Shukurov, A., Sokoloff, D.D. 1997, Astron. & Astrophys., 318, 700-720.
35. Bertoldi, F., McKee, C.F. 1992, Ap. J., 395, 140-157.
36. Beuermann, K., Kanbach, G., Berkhuijsen, E.M. 1985, Astron. and Astrophys., 153, 17-34.
37.

Bhatt, H.C., Jain, S.K. 1992, Monthly Not. Roy. Astron. Soc., 257, 57-61.

38.
Biermann, L. 1950, Zs. Naturforschung., 5a, 65-71.

39.
Bignell, R.C., Vallée, J.P. 1983, Astron. & Astrophys. Suppl., 53, 147-150.

40.
Bignell, R.C., Simard-Normandin, M., Vallée, J.P. 1988, Astrophys. J. Suppl., 67, 279-282.

41.
Binney, J. 1992, Nature, 360, 624.

42.
Binney, J., Gerhard, O., Stark, A., Bally, J., Uchida, K. 1991, M.N.R.A.S., 252, 210.

43.
Blackman, E.G. 1998, Ap. J., 496, L17-L20.

44.
Blitz, L. 1991, in *Molecular Clouds*, ed. by R.A. James & T.J. Millar, Cambridge Univ. Press, Cambridge, UK, 49-68.

45.
Bloemhof, E.E., Reid, M.J., Moran, J.M. 1992, Ap. J., 397, 500-519.

46.
Böhringer, H. 1995, Reviews in Modern Astronomy, 8, 259-276.

47.
Breger, M., Gehrz, R.D., Hackwell, J.A. 1981, Ap. J., 248, 963-976.

48.
Broten, N.W., MacLeod, J.M., Vallée, J.P. 1985, Astrophysical Letters, 24, 165-171.

49.
Broten, N.W., MacLeod, J.M., Vallée, J.P. 1988, Astrophys. & Space Sci., 141, 303-331.

50.
Broten, N.W., Vallée, J.P., MacLeod, J.M. 1986, Astron. & Astrophys. Suppl., 64, 499-501.

51.
Buczilowski, U.R., Beck, R. 1991, Astron. & Astrophys., 241, 47.

52.
Burn, B.J. 1966, Monthly Not. Roy. Astron. Soc., 133, 67-83.

53.
Carvalho, J.C. 1994, A & A, 281, 641-648.

54.
Cattaneo, F., Vainshtein, S.I. 1991, Ap. J. Lett., 376, L21-L24.

55.
Chaboyer, B., Henriksen, R.N. 1990, A & A, 236, 275-288.

56.
Chakrabarti, S.K., Rosner, R., Vainshtein, S.I. 1994, Nature, 368, 434-436.

57.
Chi, X., Wolfendale, A.W. 1993, Nature, 362, 610-611.

58.
Chi, X., Young, E.C., Beck, R. 1997, Astron. & Astrophys., 321, 71-80.

59.
Childress, S., Gilbert, A.D., Ott, E. 1996, Physics Today, 49, no. 7, 59.

60.
Cioffi, D.F., Jones, T.W. 1980, Astron. J., 85, 368-375.

61.
Ciolek, G.E., Mouschovias, T.C. 1994, Ap. J., 425, 142-160.

62.
Ciolek, G.E., Mouschovias, T.C. 1993, Ap. J., 418, 774-793.

63.
Clayton, G.C. 1996, in *Polarimetry of the Interstellar Medium*, ed. by W.G. Roberge and D.C. Whittet, Astron. Soc. Pacific, San Francisco, USA - A.S.P. Conf. Ser., 97,618-622.

64.
Clegg, A.W., Cordes, J.M., Simonetti, J.H., Kulkarni, S.R. 1992, Ap.J., 386, 143-157.

65.
Clifford, P., Elmegreen, B.G. 1983, Monthly Not. Roy. Astron. Soc., 202, 629-646.

66.
Cronin, J.W. 1996, "The Galaxy as a Magnet Spectrometer", priv. communic.

67.
Crusius-Wötzel, A.R., Biermann, P.L., Lerche, I., Schlickeiser, R. 1990, Ap.J., 360, 417-426.

68.
Crutcher, R.M. 1991, in *Fragmentation of molecular cloiuds and star formation*, ed. by E. Falgarone et al., Kluwer Acad. Publ., Dordrecht, Neth. - I.A.U. Symp. 147, 61-64.

69.
Crutcher, R.M. 1994, in *Clouds, Cores, and low mass stars*, ed. by D.P. Clemens and R. Barvainis, Astro. Soc. Pacific, San Francisco, USA - ASP Conf. Ser., 65, 87-96.

70.

Crutcher, R.M., Mouschovias, T.C., Troland, T.H., Ciolek, G.E. 1994, Ap. J., 427, 839-847.

71. Crutcher, R.M., Roberts, D.A., Mehringer, D.M., Troland, T.H. 1996a, Ap.J., 462, L79-L82.

72. Crutcher, R.M., Troland, T.H., Lazareff, B., Kazès, I. 1996b, Ap.J., 456, 217-224.

73. Cuddeford, P., Binney, J. 1993, Nature, 365, 20.

74. Daly, R.A., Loeb, A. 1990, Ap.J., 364, 451-455.

75. Davidson, J. A. 1996, Astron. Soc. Pacific Conf. Ser., 97, 504-521.

76. Davies, R.D. 1994, in *Cosmical Magnetism*, ed. by D. Lynden-Bell, Kluwer, Dordrecht, Neth. - NATO ASI Ser. C, 422, 131-141.

77. De Young, D.S. 1992, Ap.J., 386, 464-472.

78. Dickey, J.M., Salpeter, E.E. 1984, Ap. J., 284, 461.

79. Dobler, W., Poezd, A.D., Shukurov, A. 1996, Astron. and Astrophys., 312, 663-669.

80. Dotson, J.L. 1996a, in *Polarimetry of the Interstellar medium*, ed. by W.G. Roberge & D.C. Whittet, Astron. Soc. Pacific, San Francisco, USA - A.S.P. Conf. Ser., 97, 290-294.

81. Dotson, J.L. 1996b, Ap. J., 470, 566-576.

82. Dowell, C.D. 1997, Ap. J., 487, 237-247.

83. Draine, B.T., Roberge, W.G. 1982, Ap. J., 259, L91-L96.

84. Dudorov, A.E. 1991, Sov. Astron., 35, 342-348.

85. Duncan, A.R., Haynes, R.F., Jones, K.L., Stewart, R.T. 1997, Monthly Not. R. Astron. Soc., 291, 279-295.

86. Duric, N. 1990, I.A.U. Symp., 140, 235-236.

87. Efremov, Y. N. 1998, Astron. & Astrophys. Trans., 15, 3-17.

88. Ehle, M., Beck, R. 1993, A & Ap, 273, 45-64.

89. Ehle, M., Beck, R., Haynes, R.F., Vogler, A., Pietsch, W., Elmouttie, M., Ryder, S. 1996, Astron. & Astrophys., 306, 73-85.

90. Elitzur, M. 1992, Annual Rev. Astron. & Astrophys., 30, 75-112.

91. Elmegreem, B.G. 1988, Ap. J., 326, 616-638.

92. Elmegreen, B.G., Combes, F. 1992, A & A, 259, 232-240.

93. Elmegreen, B.G., Fiebig, D. 1993, A & A, 270, 397-400.

94. Elmouttie,M., Haynes, R.F., Jones, K.L., Sadler, E.M., Ehle, M. 1998, M.N.R.A.S., 297, 1202-1218.

95. Ensslin, T.A., Biermann, P.L., Klein, U., Kohle, S. 1998, Astron. & Astrophys., 332, 395-409.

96. Fan, Z., Lou, Yu-Q. 1996, Nature, 383, 800-802.

97. Fan, Z., Lou, Yu-Q. 1997, Monthly Not. R. Astron. Soc., 291, 91-109.

98. Fendt, C., Beck, R., Neininger, N. 1998, Astron. & Astrophys., 335, 123-133.

99. Ferrière, K. 1993a, Astrophys. J., 404, 162-184.

100. Ferrière, K. 1993b, Astrophys. J., 409, 248-261.

101. Ferrière, K. 1993c, IAU Symp., 157, 383-387.

102. Fiebig, D., Güsten, R. 1989, A & A, 214, 333-338.

103. Field, G.B. 1995, in *Physics of the interstellar medium and intergalactic medium*, Ferrara et al. (eds), Astr. Soc. Pacific, San Francisco, USA - Astr. Soc. Pacific Conf. Ser., 80, 1-14.

104.
Fitt, A.J., Alexander, P. 1993, Monthly Not. Roy. Astron. Soc., 261, 445-452.
105.
Fleck, R.C. 1988, Ap. J., 328, 299-303.
106.
Flett, A.M., Murray, A.G. 1991, M.N.R.A.S., 249, 4p-6p.
107.
Forman, W., Jones, C., Tucker, W. 1984, Ap.J., 277, 19-26.
108.
Frail, D.A., Vasisht, G., Kulkarni, S.R. 1997, Ap. J., 480, L129-L132.
109.
Freudenreich, H. T. 1998, Ap. J., 492, 495-510.
110.
Frisch, P.C. 1981, Nature, 293, 377.
111.
Gardner, F.F., Whiteoak, J.B. 1963, Nature, 197, 1162-1164.
112.
Gardner, F.F., Morris, D., Whiteoak, J.B. 1969, Austral. J. Phys., 22, 813-819.
113.
Gloeckler, G., Fisk, L.A., Geiss, J. 1997, Nature, 386, 374-377.
114.
Goldshmidt, O., Rephaeli, Y. 1993, Ap. J., 411, 518-528.
115.
Gomez de Castro, A.I., Pudritz, R.E., Bastien, P. 1997, Astrophys. J., 476, 717-729.
116.
Goodfrooij, P., de Jong, T. 1995, Astron. & Astrophys., 298, 784.
117.
Goodman, A.A. 1995, in *Airborne Astronomy Symposium on the Galactic Ecosystem*, ed. by M.R. Haas et al., Astron. Soc. Pacific, San Francisco, USA - ASP Conf. Ser., 73, 45-52.
118.
Goodman, A.A. 1996, in *Polarimetry of the interstellar medium*, ed. by W.C. Roberge & D.C. Whittet, Astron. Soc. Pacific, Ssan Francisco, 1996 - A.S.P. Conf. Ser., 97, 325-344.
119.
Goodman, A.A., Jones, T.J., Lada, E.A., Myers, P. C. 1995, Ap. J., 448, 748-765.
120.
Goodman, A.A., Heiles, C. 1994, Ap. J., 424, 208-211.
121.
Gopal-Krishna, Nath, B.B. 1997, Astronomy & Astrophysics, 326, 45-50.
122.
Gray, A.D., Landecker, T.L., Dewdney, P.E., Taylor, A.R. 1998, Nature, 393, 660-662.
123.
Greaves, J., Holland, W., Murray, S., Oldham, G. 1992, JCMT-UKIRT Newsletter, 4, 43-44.
124.
Greaves, J.S., Holland, W.S., Murray, A.G., Nartallo, R. 1995a, Monthly Not. Roy. Astron. Soc., 272, L1-L4.
125.
Greaves, J.S, Holland, W.S., Murray, A.G. 1995b, A & A, 297, L49-L52.
126.
Güsten, R., Fiebig, D. 1990, I.A.U. Symp., 140, 305.
127.
Güsten, R., Fiebig, D., Uchida, K.I. 1994, A & A, 286, L51-L54.
128.
Hall, J.S. 1949, Science, 109, 166-167.
129.
Han, J., Qiao, G. 1994, Astron. & Astrophys., 288, 759.
130.
Han, J.L., Beck, R., Berkhuijsen, E.M. 1998, Astron. & Astrophys., 335, 1117-1123.
131.
Han, J., Manchester, R., Berkhuijsen, E., Beck, R. 1997, Astron. & Astrophys., 322, 98-102.
132.
Hanawa, T., Nakamura, F., Matsumoto, F., Nakano, T., Tatematsu, K., Umemoto, T., Kameya, O., Hirano, N., Hasegawa, T., Kaifu, N., Yamamoto, S. 1993, Ap. J., 404, L83-L86.
133.
Hartquist, T.W., Dyson, J.E. 1997, Astron. & Astrophys., 319, 589-592.
134.
Haynes, M.P., Giovanelli, R., Chincarini, G.C. 1984, Annual Rev. Astron. & Astrophys., 22, 445-470.
135.
Heiles, C. 1987, in *Interstellar Processes*, ed. by D.J. Hollenbach & H.A. Thronson, reidel Publ., Dordrecht, Netherlands - Ap. & Space Sci. Lib., 134, 171-174.
136.

Heiles, C. 1988, Ap.J., 324. 301.

137. Heiles, C. 1988b, Ap.J., 324, 321-330.

138. Heiles, C. 1989, Ap.J., 336, 808-821.

139. Heiles, C. 1995, in *Physics of the Interstellar Medium and Intergalactic Medium*, ed. by A. Ferrara et al., Astron. Soc. Pacific, San Francisco, USA - A.S.P. Conf. Ser., 80, 507-523.

140. Heiles, C. 1996a, Ap. J., 462, 316-325.

141. Heiles, C. 1996b, in *Polarimetry of the Interstellar Medium*, ed. by W.G. Roberge and D.C. Whittet, Astron. Soc. Pacific, San Francisco, USA - ASP Conf. Ser., 97, 457-474.

142. Heiles, C. 1997, Astrophys. J. Suppl. Ser., 111, 245-288.

143. Heiles, C., Chu, Y.-H. 1980, Ap. J., 235, L105-L109.

144. Heiles, C., Chu, Y.-H., Reynolds, R., Yeginhil, I., Troland, T. 1980, Astrophys. J., 242, 533.

145. Heiles, C., Troland, T.H. 1982, Ap.J., 260, L23.

146. Heiles, C., Goodman, A.A., McKee, C.F., Zweibel, E.G. 1991, in *Fragmentation of molecular clouds and star formation*, ed. by E. Falgarone et al., Kluwer Acad. Publ., Dordrecht, Neth. - IAU Symp. 147, 43-60.

147. Heiles, C., Goodman, A.A., McKee, C.F., Zweibel, E.G. 1993, in *Protostars and Planets III*, ed. E.H. Levy and J.I. Lunine, Univ. Ariz. Press, Tucson, USA - page 279.

148. Heiles, C., Reach, W.T., Koo, B.-C. 1996, Ap.J., 466, 191-223.

149. Heithausen, A. 1996, Astron. & Astrophys., 314, 251-257.

150. Henriksen, R.N. 1991, Astrophys. J., 377, 500-509.

151. Hildebrand, R.H. 1987, Ap. Lett. and Comm., 26, 263-275.

152. Hildebrand, R.H. 1988, Q.J.R.A.S., 29, 327-351.

153. Hildebrand, R.H. 1989, in *Interstellar Dust*, ed. by L.J Allamandola and A.G. Thielens, Kluwer, Dordrecht, Neth. - IAU Symp., 135, 275-281.

154. Hildebrand, R.H. 1996, in *Polarimetry of the Interstellar Medium*, ed. by W.G. Roberge and D.C. Whittet, Astron. Soc. Pacific, San Francisco, USA - A.S.P. Conf. Ser., 97, 254-268.

155. Hildebrand, R.H., Gonatas, D.P., Platt, S.R., Wu, X.D., Davidson, J.A., Werner, M.W., Novak, G., Morris, M. 1990, Ap.J., 362, 114-119.

156. Hildebrand, R.H., Davidson, J.A., Dotson, J., Figer, D.F., Novak, G., Platt, S.R., Tao, L. 1993, Ap.J., 417, 565-571.

157. Hiltner, W.A. 1949, Science, 109, 165-165.

158. Hoernes, P., Berkhuijsen, E.M., Xu, C. 1998, Astron. & Astrophys., 334, 57-70.

159. Howard, A.M., Kulsrud, R.M. 1997, Astrophys. J., 483, 648-665.

160. Hummel, E., Beck, R. 1995, A & A, 303, 691-704.

161. Hummel, E., van Gorkum, J.H., Kotanyi, C.G. 1983, Ap. J., 267, L5-L9.

162. Hummel, E., Davies, R.D., Wolstencroft, R.D., van der Hulst, J.M., Pedlar, A. 1988, A & A,199, 91.

163. Hummel, E., Beck, R., Dahlem, M. 1991, A & A, 248, 23.

164. Ikeuchi, S. 1988, Fundamentals of Cosmic Physics, 12, 255-327.

165. Johnson, P.E. 1982, Nature, 295, 371-375.

166. Jokipii, J.R., Levy, E.H. 1993, Nature, 365, 19-20.

167. Jones, T.J., Klebe, D.I., Dickey, J.M,. 1992, Ap. J., 389, 602-615.

168.
Jun, B.-I., Norman, M.L. 1996, Ap. J., 465, 800.
169.
Just, A., Jacobi, S., Deiss, B.M. 1994, A & A, 289, 237-255.
170.
Kahn, F.D. 1992, Irish Astronomical J., 20, 278-282.
171.
Kahn, F.D., Brett, L. 1993, Mont. Not. R. Astron. Soc., 263, 37-48.
172.
Kamaya, H. 1996, Astrophys. J., 469, L125-L126.
173.
Kamaya, H. 1998, Ap. J., 493, L95-L96.
174.
Kane, B.D., Clemens, D.P. 1996, in *Polarimetry of the interstellar medium*, ed. by W.C. Roberge & D. Whittet, Astron. Soc. Pacific, San Francisco, USA - A.S.P. Conf. Ser., 97, 269-273.
175.
Katz, J.I. 1994, Ap. & Space Sci., 213, 155-156.
176.
Kaufman, M., Bash, F.N., Crane, P.C., Jacoby, G.H. 1996, Astron. J., 112, 1021-1034 (with Plate 40, p.1328).
177.
Kazès, I., Crutcher, R.M. 1986, A & A, 164, 328-336.
178.
Kazès, I., Troland, T., Crutcher, R., Heiles, C. 1988, Astrophys. J., 335, 263.
179.
Kemp, J.C. 1982, Publ. Astr. Soc. Pacific, 94, 627-633.
180.
Kennicutt, R.C. 1983, Astrophys. J., 272, 54.
181.
Kennicutt, R.C. 1992, in *Star Formation in Stellar Systems*, ed. Tenorio-Tagle, G., Prieto, M., Sánchez, F., Cambridge Univ. Press, Cambridge, UK, p. 191.
182.
Kennicutt, R.C. 1998, Ap. J., 498, 541-552.
183.
Kim, K.-T., Kronberg, P.P., Dewdney, P.E., Landecker, T.L. 1990, Astrophys. J., 355, 29-37.
184.
Kim, E.-J., Olinto, A.V., Rosner, R. 1996, Astrophysical J., 468, 28-50.
185.
Kneib, J.P., Mellier, Y., Pellö, R., Miralda-Escudé, J., Le Borgne, J.F., Böhringer, H., Picat, J.P. 1995, A & A, 303, 27.
186.
Ko, C.M., Parker, E.N. 1989, Ap.J., 341, 828-831.
187.
Kobulnicky, H.A., Molnar, L.A., Jones, T.J. 1994, Astron.J., 107, 1433-1443.
188.
Königl, A., Ruden, S.P. 1993, in *Protostars and Planets III*, ed. by H. Levy and J.I. Lumine, Univ. Ariz. Press, Tucson, USA, 641-687.
189.
Korsakov, B.G., Tokarev, Y.V., Fleischman, G.D. 1997, Astron. Lett., 23, 229-233.
190.
Kosowsky, A., Loeb, A. 1996, Ap. J., 469, 1-6.
191.
Krause, F., Beck, R. 1998, A & A, 335, 789-796.
192.
Krause, F., Hummel, E., Beck, R. 1989a, Astron. & Astrophys., 217, 4.
193.
Krause, F., Beck, R., Hummel, E. 1989b, Astron. & Astrophys., 217, 17.
194.
Kronberg, P.P. 1994, Rep. Prog. Physics, 57, 325-382.
195.
Kronberg, P.P. 1995, Nature, 374, 404-405.
196.
Kronberg, P.P., Dyer, C., Roser, H.-J. 1996, Astrophys. J., 472, 115-124.
197.
Kronberg, P.P., Lesch, H., Hopp, U. 1999, Ap. J., 511, 56-64.
198.
Kulsrud, R.M., Anderson, S.W. 1992, Ap.J., 396, 606-630.
199.
Kulsrud, R.M., Cen, R., Ostriker, J., Ryu, D. 1997, Ap. J., 480, 481-491.
200.
Kulsrud, R.M., Howard, A. 1997, Ap. J., 483, 648.
201.

Laing, R.A. 1996, in *Energy Transport in Radio Galaxies and Quasars*, ed. by P.E. Hardee et al., Astron. Soc. Pacific, San Francisco, USA - A.S.P. Conf. Ser., 100, 241.
202.
Lang, K.R. 1980, *Astrophysical Formulae*, 2nd ed., Springer-Verlag, Berlin, xxx + 786 p.
203.
Langer, W.D. 1978, Ap. J., 225, 95-106.
204.
Larson, R.B. 1979, Monthly Not. Roy. Astron. Soc., 186, 479-490.
205.
Leach, R.W., Clemens, D.P., Kane, R.D., Barvainis, R. 1991, Ap. J., 370, 257-262.
206.
Leahy, D.A., Roger, R.S., Ballantyne, D. 1997, Astron. J., 114, 2081-2094.
207.
Lesch, H. 1993, in *Cosmic Dynamo*, ed. by F. Krause et al., Kluwer Acad. Publ., Dordrecht, Netherlands - I.A.U. Symp. 157, 395-401.
208.
Lesch, H., Chiba, M. 1995, A & A, 297, 305-310.
209.
Lesch, H., Chiba, M. 1997, Fundamentals of Cosmic Physics, 18, 273-368.
210.
Lyne, A.G., Smith, F.G. 1989, Monthly Not. Roy. Astron. Soc., 237, 533-541.
211.
MacLeod, J.M., Vallée, J.P., Broten, N.W. 1984, Astron. & Astrophys. Suppl., 56, 283-287.
212.
MacLeod, J.M., Vallée, J.P., Broten, N.W. 1988, Astron. & Astrophys. Suppl., 74, 63-66.
213.
Makino, N. 1997, Ap. J., 490, 642-648.
214.
Marshall, J., Lasenby, A.N., Yusef-Zadeh, F. 1995, M.N.R.A.S., 274, 519-522.
215.
Martin, P.G., Shawl, S.J. 1982, Ap. J., 253, 86-90.
216.
Mathews, W.G., Brighenti, F. 1997, Ap. J., 488, 595-605.
217.
Mayer, C.H., McCullough, T.P., Sloanaker, R.M. 1962, Ap.J., 135, 656-658.
218.
McCutcheon, W.H., Vrba, F.J., Dickman, R.L., Clemens, D.P. 1986, Ap. J., 309, 619-627.
219.
McDavid, D. 1984, Ap. J., 284, 141-143.
220.
McGregor, P.J., Harrison, T.E., Hough, J.H., Bailey, J.A. 1994, Monthly Not. Roy. Astron. Soc., 267, 755.
221.
McLaughlin, D.E., Pudritz, R.E. 1996, Ap. J., 469, 194-198.
222.
Medina Tanco, G.A., de Gouveia Dal Pino, E.M., Horvath, J.E. 1998, Ap. J., 492, 200-204.
223.
Melatos, A., Johnston, S., Melrose, D.B. 1995, MNRAS, 275, 381-397.
224.
Melrose, D. 1995, Publ. Astron. Soc. Australia, 12, 137-138.
225.
Mestel, L. 1965, Quat. J. Roy. Astron. Soc., 6, 265-298.
226.
Mestel, L., Paris, R.B. 1984, A & A, 136, 98-120.
227.
Mezger, P.G., Duschl, W.J., Zylka, R. 1996, Astron. Astrophys. Rev., 7, 289-388.
228.
Miesch, M.S., Bally, J. 1994, Ap. J., 429, 645-671.
229.
Minchin, N.R., Murray, AG. 1994, A & A, 286, 579-587.
230.
Mineshige, S., Shibata, K., Shapiro, P.R. 1993, Astrophys. J., 409, 663-681.
231.
Moneti, A., Pipher, J.L., Helfer, H.L., McMillan, R.S., Perry, M.L. 1984, Ap. J., 282, 508-515.
232.
Morganti, R., Parma, P., Capetti, A., Fanti, R., de Ruiter, H., Prandoni, I. 1997, A & A Suppl. Ser., 126, 335-355.
233.
Morris, M. 1996, I.A.U. Symp., 169, 247-261.
234.
Morris, M., Davidson, J.A., Werner, M., Dotson, J., Figer, D.F., Hildebrand, R., Novak, G., Platt, S. 1992, Astrophys. J., 399, L63-L66.
235.

Morris, D., Berge, G.L. 1964, Astrophys. J., 139, 1388-1392.

236. Morris, M., Serabyn, G. 1996, Annual Rev. Astron. Astrophys., 34, 645-702.

237. Morton, S. A., Mouschovias, T.C., Ciolek, G.E. 1994, Ap. J., 421, 561-569.

238. Moss, D. 1995, Monthly Not. Roy. Astron. Soc., 275, 191-194.

239. Moss, D. 1996a, Observatory, 116, 142-144.

240. Moss, D. 1996b, Astron. & Astrophys., 315, 63-70.

241. Moss, D. 1997, Month. Not. Roy. Astron. Soc., 289, 554-558.

242. Moss, D. 1998, Month. Not. Roy. Astron. Soc., 297, 860-866.

243. Moss, D., Shukurov, A.M. 1996, Monthly Not. Roy. Astron. Soc., 279, 229-239.

244. Moss, D., Shukurov, A., Sokoloff, D.D., Berkhuijsen, E.M., Beck, R. 1998, Astron. & Astrophys., 335, 500-509.

245. Mouschovias, T.C., Paleologou, E.V., Fiedler, R.A. 1985, Ap. J., 291, 772-797.

246. Muller, C.A., Berkhuijsen, E.M., Brouw, W.N., Tinbergen, J. 1963, Nature, 200, 155-156.

247. Myers, P.C. 1983, Ap. J., 270, 105-118.

248. Myers, P.C. 1990, in *Galactic and Intergalactic Magnetic Fields*, ed. by R, Beck et al., Reidel, Dordrecht, Neth. - I.A.U. Symp., 140, 313.

249. Myers, P.C., Goodman, A.A. 1990, in *Galactic and Intergalactic magnetic fields*, ed. by R. Beck et al., Kluwer, Dordrecht, Neth. - I.A.U. Symp., 140, 309-311.

250. Myers, P.C., Goodman, A.A. 1991, Ap. J., 373, 509-524.

251. Nakajima, Y., Hanawa, T. 1996, Ap. J., 467, 321-333.

252. Nakano, T. 1997, in *Advances in Dusty Plasmas*, Proc. of Internat. Confer. on Physics of Dusty Plasmas, ed. Shukla, P.K., Mendis, D.A., Desai, T., World Scientific, Singapore, p. 336- 345.

253. Nakano, T., Tademaru, E. 1972, Ap. J., 173, 87-101.

254. Neininger, N. 1992, Astron. & Astrophys., 263, 30.

255. Neininger, N., Beck, R., Sukumar, S., Allen, R.J. 1993, Astron. & Astrophys., 274, 687.

256. Nelson, A.H. 1988, Monthly Not. Roy. Astron. Soc., 233, 115.

257. Niklas, S., Beck, R. 1997, Astron. & Astrophys., 320, 54-64.

258. Niklas, S., Klein, U., Wielebinski, R. 1995, Astron. & Astrophys., 293, 56-63.

259. Norman, C., Meiksin, A. 1996, Astrophys. J., 468, 97-101.

260. Novak, G., Dotson, J.L., Dowell, C.D., Goldsmith, P.F., Hildebrand, R.H., Platt, S.R., Schleuning. D.A. 1997, Ap. J., 487, 320-327.

261. Novak, G., Dotson, J.L., Dowell, C.D., Hildebrand, R.H., Renbarger, T., Schleuning, D.A. 1998, Ap. J., in press (Submm Polar. Observ. of the Gal. Center)

262. Ohno, H., Shibata, S. 1993, Monthly Not. R. Astron. Soc., 262, 953-962.

263. Oren, A.L., Wolfe, A.M. 1995, Ap.J., 445, 624-641.

264. Ossendrijver, A.J., Hoyng, P. 1997, Astron. & Astrophys., 324, 329-343.

265. Otmianowska-Mazur, K., von Linden, S., Lesch, H., Skupniewicz, G. 1997, Astron. & Astrophys., 323, 56-70.

266. Owen, F.N., Eilek, J.A. 1998, Ap. J., 493, 73-80.

267. Parker, E.N. 1971a, Astrophys. J., 163, 255-278.

268.
Parker, E.N. 1971b, Astrophys. J., 163, 279-285.
269.
Parker, E.N. 1973, Astrophys. Space Sci., 24, 279-288.
270.
Parker, E.N. 1976, in *Physics of non-thermal radio sources*, ed. by G. Setti, Reidel Publ. Co., Dordrecht, Holland, p. 169-178.
271.
Parker, E.N. 1979, *Cosmical magnetic Fields*, Clarendon Press, Oxford, UK - Chapter 22.
272.
Parker, E.N. 1981, Astrophys. J., 244, 644-652.
273.
Parker, E.N. 1987, Astrophys. J., 321, 349-354.
274.
Parker, E.N. 1992, Astrophys. J., 401, 137-145.
275.
Passot, T., Vazquez-Semadeni, E., Pouquet, A. 1995, Astrophys. J., 455, 536-555.
276.
Pellegatti-Franco, G.A., Tarsia, R.D., Quiroga, R.J. 1985, Ap. and Space Sci., 111, 343-354.
277.
Perry, J.J., Watson, A.M., Kronberg, P.P. 1993, Ap.J., 406, 407-419.
278.
Persson, C.J.L., Helou, G. 1987, Astrophys. J., 314, 513-524.
279.
Piddington, J.H. 1981a, Astrophys. & Space Sci., 80, 457-471.
280.
Piddington, J.H. 1981b, Astrophys. J., 247, 293-299.
281.
Plaga, R. 1995, Nature, 374, 430-432.
282.
Plante, R.L., Lo, K.Y., Crutcher, R.M. 1995, Ap.J., 445, L113-L116.
283.
Poezd, A.D., Sokoloff, D.D. 1993, Astron. Rep., 37, 197-202 (= 1993 Astron. Zh., 70, 381-391).
284.
Poezd, A., Shukurov, Sokoloff, D. 1993, Month. Not. Roy. Astron. Soc., 264, 285-297.
285.
Pohl, M. 1993, A & Ap, 279, L17-L20.
286.
Porro, I., Silvestro, G. 1993, A & A, 275, 563-572.
287.
Pudritz, R. E., Silk, J. 1987, Ap. J., 316, 213-226.
288.
Puget, J.J. 1991, in *Fragmentation of molecular clouds & star formation*, ed. by E. Falgarone et al., Kluwer Acad. Publ., Dordrecht, Neth. - I.A.U. Symp. 147, 75-81.
289.
Rádler, K.-H. 1995, Reviews in Modern Astronomy, 8, 295-321.
290.
Rand, R.J. 1994, in *Physics of the Gaseous and Stellar Disks of the Galaxy*, ed. by I.R. King, Astron. Soc. Pacific, San Francisco, USA - A.S.P. Conf. Ser., 66, 269-276.
291.
Rand, R.J., Kulkarni, S.R. 1990, in *Galactic & Extragalactic Magnetic Fields*, ed. by R. Beck et al., Kluwer Acad. Publ., Dordrecht, Netherlands - I.A.U. Symp. 140, 44-46.
292.
Rand, R.J., Lyne, A.G. 1994, Monthly Not. Roy. Astron. Soc., 268, 497-505.
293.
Ratra, B. 1992, Ap.J., 391, L1-L4.
294.
Reid, M.J., Silverstein, E.M. 1990, Ap. J., 361, 483-486.
295.
Reuter, H.-P., Klein, U., Lesch, H., Wielebinski, R., Kronberg, P.P. 1994, A & A, 282, 724-730.
296.
Roberts, D.A., Crutcher, R., Troland, T. 1995, Astrophys. J., 442, 208.
297.
Roberts, D.A., Crutcher, R.M., Troland, T.H. 1996, Astron. Soc. Pacific Conf. Ser., 97, 527-531.
298.
Roberts, D.A., Goss, W.M. 1993, Ap. J. Suppl. Ser., 86, 133-152.
299.
Roberts, D.A., Goss, W.M., van Gorkum, J.H., Leahy, J.P. 1991, Ap.J., 366, L15-L18.
300.
Rohde, R., Elstner, D., Rüdiger, G. 1998, A & A, 329, 911-919.

301. Rüdiger, G., Elstner, D., Schultz, M. 1993, in *The Cosmic Dynamo*, ed. by F. Krause et al., Kluwer Acad. Publ., Dordrecht, Netherlands - I.A.U. Symp. 157, 321-331.
302. Ruzmaikin, A.A., Sokoloff, D.D., Shukurov, A.M. 1985, Astron. & Astrophys., 148, 335-343.
303. Ruzmaikin, A.A., Sokoloff, D.D., Shukurov, A.M. 1988, Nature, 336, 341-347.
304. Ryu, D., Kang, H., Biermann, P.L. 1998, A & A, 335, 19-25.
305. Sánchez-Salcedo, F.J. 1997a, Ap. & Space Sci., 249, 223-226.
306. Sánchez-Salcedo, F.J. 1997b, Monthly Not. Roy. Astron. Soc., 289, 863-868.
307. Sánchez-Salcedo, F.J. 1996, Ap. J., 467, L21-L24.
308. Scarrott, S.M. 1996, Quarterly J. Roy. Astron. Soc., 37, 297-305.
309. Scarrott, S.M., Draper, P.W., Stockdale, D.P., Wolstencroft, R.D. 1993, M.N.R.A.S., 264, L7-L12.
310. Scarrott, S.M., Foley, N.B., Gledhill, T.M., Wolstencroft, R.D. 1996, Monthly Not. Roy. Astron. Soc., 282, 252-262.
311. Schleuning, D.A. 1998, Ap. J., 493, 811-825.
312. Schleuning, D.A., Dowell, C.D., Platt, S.R. 1996, in *Polarimetry of the Interstellar Medium*, ed. by W.G. Roberge and D.C. Whittet, Astron. Soc. Pacific, San Francisco, USA - A.S.P. Conf. Ser., 97, 285-289.
313. Schramkowski, G.P, Achtenberg, A. 1993, Astron. & Astrophys., 280, 313-323.
314. Schultz, M., Elstner, D., Rndiger, G. 1994, A & A, 286, 72-79.
315. Schwarz, U.J., Lasenby, J. 1990, in *Galactic & Intergalactic magnetic fields*, ed. by R. Beck et al., Kluwer Acad. Publ., Dordrecht, Netherlands - I.A.U. Symp. 140, 383-384.
316. Segalovitz, A. 1977, Astron. & Astrophys., 54, 703-711.
317. Shibata, K., Matsumoto, R. 1991, Nature, 353, 633-635.
318. Shore, S.N., Ferrini, F. 1995, Fundamentals of Cosmic Physics, 16, 1-110.
319. Shull, J.M. 1995, Astron. Soc. Pacific Conf Ser., 73, 365-385.
320. Sijbring, D., de Bruyn, A.G. 1998, Astron. Astrophys., 331, 901-915.
321. Simard-Normandin, M., Kronberg, P.P. 1979, Nature, 279, 115-118.
322. Simard-Normandin, M., Kronberg, P.P. 1980, Ap. J., 242, 74-94.
323. Simoneti, J.H., Cordes, J.M. 1986a, Ap. J., 303, 659-666
324. Simonetti, J.H., Cordes, J.M. 1986b, Astrophys. J., 310, 160-171.
325. Simonetti, J.H., Cordes, J.M., Spangler, S.R. 1984, Astrophys. J., 284, 126-134.
326. Slavin, J.D., Cox, D.P. 1993, Ap. J., 417, 187-195.
327. Smirnova, T.V., Boriakoff, V. 1997, Astron. & Astrophys., 321, 305-310.
328. Sofue, Y., Fujimoto, M. 1983, Ap.J., 265, 722-729.
329. Sofue, Y., Klein, U., Beck, R., Wielebinski, R. 1985, A & A, 144, 257-260.
330. Sofue, Y., Fujimoto, M., Wielebinski, R. 1986, Annual Rev. A & A, 24, 459-497.
331. Soida, M., Urbanik, M., Beck, R. 1996, Astron. & Astrophys., 312, 409-418.
332. Soker, N. 1997, Ap.J., 488, 572-578.
333. Sokoloff, D.D., Shukurov, A.M., Krause, M. 1992, A & A, 264, 396-405.

334.
Sokoloff, D.D., Bykov, A.A., Shukurov, A., Berkhuijsen, E.M., Beck, R., Poezd, A.D. 1998, M. N.R. A. S., 299, 189-206.
335.
Spergel, D.N., Blitz, L. 1992, Nature, 357, 665-667.
336.
Stanev. T. 1997, Ap. J., 479, 290-295.
337.
Stone, J.M., Norman, M.L. 1992, Ap. J. Suppl., 80, 753.
338.
Subramanian, K. 1995, Bull. Astron. Soc. India, 23, 481-488.
339.
Subramanian, K. 1996, J. Korean Astron. Soc., 29, S155-S158.
340.
Subramanian, K. 1998, M.N.R.A.S., 294, 718-728.
341.
Tao, L., Cattaneo, F., Vainshtein, S.I. 1993, in *Solar and Planetary Dynamos*, ed. by M.R. Proctor, P.C. Matthews, et al., Cambridge Univ. Press, Cambridge, UK - pages 303-310.
342.
Taylor, G.B., Barton, E.J. 1994, A.J., 107, 1942-1952.
343.
Taylor, J.H., Cordes, J.M. 1993, Astrophys. J., 411, 674-684.
344.
Taylor, G.B., Perley, R.A. 1993, Ap. J., 416, 554-562.
345.
Thompson, C., Duncan, R.C. 1996, Ap. J., 473, 322-342.
346.
Thomson, R.C., Nelson, A.H. 1980, Month. Not. Roy. Astron. Soc., 191, 863-870.
347.
Tomisaka, K. 1992, Pub. Astr. Soc. japan, 44, 177-191.
348.
Troland, T.H., Crutcher, R., Goodman, A., Heiles, C., Kazès, I., Myers, P.C. 1996, Astrophys. J., 471, 302-307.
349.
Troland, T.H., Heiles, C. 1982, Ap.J., 260, L19-L22.
350.
Troland, T.H., Heiles, C. 1986, Astrophys. J., 301, 339-345.
351.
Tsuboi, M., Kawabata, T., Kasuga, T., Handa, T., Kato, T. 1995, Publ. Astron. Soc. Japan, 47, 829-836.
352.
Uchida, K.I., Güsten, R. 1995, A & A, 298, 473-481.
353.
Udomprasert, P.S., Taylor, G.B., Pearson, T.J., Roberts, D.H. 1997, Astrophys. J., 483, L9-L12.
354.
Urbanik, M., Elstner, D., Beck, R. 1997, Astron. & Astrophys., 326, 465-476.
355.
Vainshtein, S.I., Cattaneo, F. 1992, Ap.J., 393, 165-171.
356.
Vallée, J.P. 1973, Ph.D. Thesis, University of Toronto, Toronto, Canada - Chapter 13.
357.
Vallée, J.P. 1980, Astron. & Astrophys, 86, 251-253.
358.
Vallée, J.P. 1981, Astrophysical Letters, 22, 63-68.
359.
Vallée, J.P. 1982a, Ap.J., 261, L55-L58.
360.
Vallée, J.P. 1982b, A.J., 87, 486-493.
361.
Vallée, J.P. 1983a, J. Roy. Astron. Soc. Canada, 77, 177-202.
362.
Vallée, J.P. 1983b, Astron. & Astrophys. Suppl., 52, 125-129.
363.
Vallée, J.P. 1983c, Astron. & Astrophys. Suppl., 51, 127-129.
364.
Vallée, J.P. 1983d, Astron. & Astrophys., 124, 147-150.
365.
Vallée, J.P. 1984a, J. Roy. Astron. Soc. Canada, 78, 57-74.
366.
Vallée, J.P. 1984b, Astron. & Astrophys., 136, 373-377.
367.
Vallée, J.P. 1986, Astron. J., 91, 541-545.

368. Vallée, J.P. 1988a, Astrophys. & Space Sci., 140, 119-123.
369. Vallée, J.P. 1988b, Astron. J., 95, 750-754.
370. Vallée, J.P. 1988c, Ap. And Space Sci., 149, 225-231.
371. Vallée, J.P. 1989a, Astron. & Astrophys., 224, 191-198.
372. Vallée, J.P. 1989b, Ap. J., 341, 238-245.
373. Vallée, J.P. 1989c, Astrophys. & Space Sci., 152, 9-13.
374. Vallée, J.P. 1990a, Astron. J., 99, 459-462.
375. Vallée, J.P. 1990b, Astron. & Astrophys., 239, 57-62.
376. Vallée, J.P. 1990c, Astrophys. J., 360, 1-6.
377. Vallée, J.P. 1990d, Astrophys. J., 361, 419-425.
378. Vallée, J.P. 1991a, Astrophys. & Space Sci., 178, 41-44.
379. Vallée, J.P. 1991b, Astrophys. J., 366, 450-454.
380. Vallée, J.P. 1991c, Astron. & Astrophys., 251, 411-416.
381. Vallée, J.P. 1992, Astron. & Astrophys., 255, 100-104.
382. Vallée, J.P. 1993a, Astrophys. & Space Sci., 200, 313-323.
383. Vallée, J.P. 1993b, Monthly Not. Roy. Astron. Soc., 264, 665-672.
384. Vallée, J.P. 1993c, Astrophys. & Space Sci., 206, 275-284.
385. Vallée, J.P. 1993d, Astrophys. J., 419, 670-673.
386. Vallée, J.P. 1993e, Astrophys. & Space Sci., 207, 109-117.
387. Vallée, J.P. 1994a, J. Roy. Astron. Soc. Canada, 88, 201-212.
388. Vallée, J.P. 1994b, Astrophys. J., 433, 778-779.
389. Vallée, J.P. 1994c, Astrophys. J., 437, 179-183.
390. Vallée, J.P. 1994d, Astrophys. & Space Sci., 220, 243-252.
391. Vallée, J.P. 1994e, Astrophys. & Space Sci., 220, 289-297.
392. Vallée, J.P. 1995a, Astron. & Astrophys., 296, 819-822.
393. Vallée, J.P. 1995b, Astron. & Astrophys., 301, 11-17.
394. Vallée, J.P. 1995c, Astrophys. J., 454, 119-124.
395. Vallée, J.P. 1995d, Astrophys. & Space Sci., 234, 1-10.
396. Vallée, J.P. 1996, Astron. & Astrophys., 308, 433-440.
397. Vallée, J.P. 1997a, Comments on Astrophysics, 18, 309-321.
398. Vallée, J.P. 1997b, Fundamentals of Cosmic Physics, 19, 1-89.
399. Vallée, J.P., Bastien, P. 1995, Astron. & Astrophys., 294, 831-834.
400. Vallée, J.P., Bastien, P. 1996, Astron. and Astrophys., 313, 255-268.
401. Vallée, J.P., Bignell, R.C. 1983, Astrophys. J., 272, 131-136.
402.

Vallée, J.P., Kronberg, P.P. 1973, Nature Phys. Sci., 246, 49-51.

403. Vallée, J.P., Broten, N.W., MacLeod, J.M. 1984, Astron. & Astrophys., 134, 199-203.

404. Vallée, J.P., MacLeod, J.M., Broten, N.W. 1986, Astron. & Astrophys., 156, 386-390.

405. Vallée, J.P., MacLeod, J.M., Broten, N.W. 1987, Astrophys. Letters, 25, 181-186.

406. Vallée, J.P., MacLeod, J.M., Broten, N.W. 1988a, Astron. & Astrophys., 196, 255-260.

407. Vallée, J.P., Simard-Normandin, M., Bignell, R.C. 1988b, Astrophys. J., 331, 321-324.

408. Vallée, J.P., Strom, R.G. 1988, A.J., 95, 1360-1362.

409. Vallée, J.P., Wilson, A.S., van der Laan, H. 1979, A & A, 77, 183-188.

410. van der Werf, P.P., Goss, W.M., Heiles, C., Crutcher, R.M., Troland, T.H. 1993, Ap. J., 411, 247-259.

411. Verschuur, G.L. 1970, in *Interstellar Gas Dynamics*, ed. by Habing, H.J., Reidel Publ. Co., Dordrecht, Netherlands - IAU Symp. 39, 150-167.

412. Verschuur, G.L. 1979, Fundamentals of Cosmic Physics, 5, 113-191.

413. Verschuur, G.L., 1993, Astrophys. J., 409, 205-233.

414. Verschuur, G.L. 1995a, Ap. J., 451, 624.

415. Verschuur, G.L. 1995b, Astrophys. J., 451, 645-659.

416. Verschuur, G.L. 1996, Astron. J., 112, 2718-2725.

417. Völk, H.J., Drury, L., McKenzie, J.F. 1984, A. & Ap, 130, 19-28.

418. Völk, H.J., Klein, U., Wielebinski, R. 1989, A. & Ap, 213, L12-L14.

419. von Linden, S., Otmianowska-Mazur, K., Lesch, H., Skupniewicz, G. 1998, Astron. & Astrophys., 333, 79-91.

420. Vrba, F.J., Strom, S.E., Strom, K.M. 1976, Astron. J., 81, 958-969 and 1021-1029.

421. Vrba, F.J., Coyne, G.V., Tapia, S. 1981, Ap. J., 243, 489-511.

422. Warren-Smith, R.F., Draper, P.W., Scarrott, S.M. 1987, Monthly Not. Roy. Astron. Soc., 227, 749-771.

423. Weiler, K.W., Sramek, R.A. 1988, Annual Rev. Astron. Astrophys., 26, 295-341.

424. Weisburg, J.M., Sieger, M.H., Frail, D.A., Johnson, S. 1995, Ap.J., 447, 204.

425. Whittet, D.C., Gerakines, P.A., Carkner, A.L. et al. 1994, Month. Not. Roy. Astron. Soc., 268, 1.

426. Whitworth, A. 1991, in *Fragmentation of molecular clouds & star formation*, ed. by E. Falgarone et al., Reidel, Dordrecht, Neth. - I.A.U. Symp., 147, 519-522.

427. Wielebinski, R. 1995, Reviews in Modern Astronomy, 8, 185-200.

428. Wielebinski, R., Krause, F. 1993, Astron. & Astrophys. Review, 4, 449-485.

429. Wieringa, M.H., de Bruyn, A.G., Jansen, D., Brouw, W.N., Katgert, P. 1993, A. & A., 268, 215-229.

430. Yokoi, N. 1996, Astron. and Astrophys., 311, 731-745.

431. Young, J.S., Allen, L., Kenney, J., Lesser, A., Rownd, B. 1996, Astron.J., 112, 1903-1927.

432. Young, J.S., Schloerb, F.P., Kenny, J.D., Lord, S.D. 1986, Astrophys. J., 304, 443.

433. Yusef-Zadeh, F., Morris, M., Chance, D. 1984, Nature, 310, 557-561.

434. Yusef-Zadeh, F., Roberts, D.A., Goss, W.M., Frail, D.A. 1996, Ap. J., 466, L25-L29.

435. Yusef-Zadeh, F., Wardle, M. 1993, Ap.J., 405, 584-590.

436.
Yusef-Zadeh, F., Wardle, M., Parastaran, P. 1997, Astrophys. J., 475, L119-L122.
437.
Zimmer, F., Lesch, H., Birk, G.T. 1997, Astron. & Astrophys., 320, 746-756.
438.
Zirakashvili, V.N., Breitschwerdt, D., Ptuskin, V.S., Vlk, H.J. 1996, A. & A., 311, 113-126.
439.
Zweibel, E. 1991, Nature, 352, 755-756.
440.
Zweibel, E. 1993, Nature, 362, 591-592.
441.
Zweibel, E. 1996, in *Polarimetry of the interstellar medium*, ed. by W.C. Roberge & D.C. Whittet, Astron. Soc. Pacific,, San Francisco, USA. - A.S.P. Conf. Ser., 97, 486-503.
442.
Zweibel, E.G., Heiles, C. 1997, Nature, 385, 131-136.